

Transition-Metal-Free Hydroxylation of Aryl Halides and Nitroarenes

Andrew Greener

MSc by Research

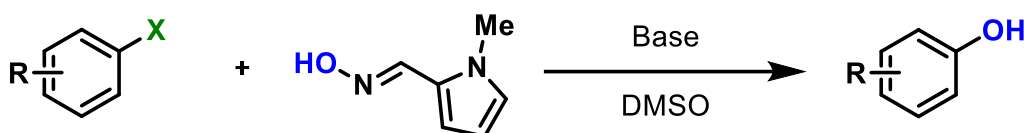
University of York
Chemistry

December 2021

Abstract

This thesis describes the development of two new methods for the synthesis of phenols. Chapter 1 provides an introduction into this area and sets out the aims of this project.

Chapter 2 describes a single-step reaction protocol for synthesising phenols from aryl halides using an oxime anion as a hydroxide surrogate. The synthesis of the oxime reagent could be achieved simply by condensing an aryl aldehyde with hydroxylamine. The reaction protocol could be applied to complex molecular structures alongside simple aryl halides. Many functional groups could be tolerated, however substrates generally required electron-withdrawing group substituents for a successful reaction. Some substituents did not promote the reaction if they were in the *meta*- or *ortho*- positions. Mechanistic studies suggested that a radical-nucleophilic substitution ($S_{RN}1$) mechanism was operative.



Chapter 3 describes a protocol for the conversion of nitroarenes into phenols using the same oxime reagent. This reaction showed similar trends in reactivity in regard to substituent effects. However, higher reaction temperatures were generally employed to promote this reaction.

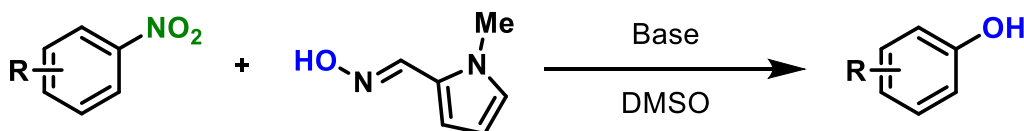


Table of Contents

Abstract	I
Table of Contents	II
Acknowledgments	IV
Declaration	V
Abbreviations	VI
Chapter 1. Introduction	1
Phenols in Organic Synthesis	1
Arene Oxidation	3
Functional Group Substitution	4
Radical-Nucleophilic Substitution ($S_{RN}1$).....	10
Initiation.....	11
Substitution and Propagation.....	17
Termination	18
Synthetic Applications and Limitations	19
Project Aims.....	21
Chapter 2. Hydroxylation of Aryl Halides.....	23
Oxime synthesis	23
Oxime comparison	25
Scoping studies.....	27
Hydroxylation of aryl halide drug molecules.....	31
Mechanistic studies	34
Summary	38
Chapter 3. Denitrative Hydroxylation of Nitroarenes.....	38
Introduction	38
Initial Scope.....	40

Chapter 1. Introduction

Mechanistic studies	45
Summary	52
Chapter 4. Experimental	53
General Information	53
General Procedures	54
References	71

Acknowledgments

I would like to acknowledge all the various people who made this year possible through their hard work and support. First, I would like to acknowledge all the people at the University of York Chemistry Department who worked behind the scenes to keep the labs open during the recent lockdowns which allowed me to do this research. I would like to thank all the PhD students in C/D/217 and C/D/216 for being willing to help me whenever a technical problem arose. I would like to thank Illya Zalessky for being a constantly cheerful lab companion during the hard months of lockdown in January and February.

I would also like to acknowledge the various members of the James group for creating an enjoyable working environment. Will Owens-Ward and George Smith for their contributions and, significantly, Patrycia Ubysz for being a great lab partner and for her support both in and out of work that helped me enormously.

Finally, I would like to give huge thanks to Dr Michael James for all the guidance he has given throughout this degree. His level of support has been great, and I would like to thank him for his advice, time and patience.

Declaration

The research presented in this Thesis was carried out at the University of York between September 2020 and September 2021. This work is, to the best of my knowledge, original except where due reference has been made to other workers.

This work has not previously been presented for an award at this, or any other, University. All sources are acknowledged as References.

Elements of this work have been reproduced in a recent publication:

Radical–Anion Coupling Through Reagent Design: Hydroxylation of Aryl Halides

A. J. Greener, P. Ubysz, W. Owens-Ward, G. Smith, I. Ocaña, A. C. Whitwood, V. Chechik, M. J. James, *Chem. Sci.* **2021**, *12*, 14641–14646

Abbreviations

°C	Degrees Centigrade
Ar	Aryl group
cS _n Ar	Concerted nucleophilic aromatic substitution
DCM	Dichloromethane
DFT	Density functional theory
DMSO	Dimethylsulfoxide
d	Doublet
EDG	Electron donating group
ESI	Electrospray ionisation
Eq.	Equivalent
EWG	Electron withdrawing group
h	Hour(s)
hν	Irradiation with light
<i>Ips</i> o-	<i>Ips</i> o position
KHMDS	Potassium hexamethyldisilazide
<i>Meta</i> -	<i>Meta</i> position
m	Multiplet
NMR	Nuclear magnetic resonance
Nu	Nucleophile
<i>Ortho</i> -	<i>Ortho</i> position
<i>Para</i> -	<i>Para</i> position
PEG-400	Polyethylene glycol
R	Group
rt	Room temperature
s	Singlet
S _N Ar	Nucleophilic aromatic substitution

$S_{RN}1/2$

Radical nucleophilic aromatic substitution

t

Triplet

TLC

Thin-layer chromatography

Chapter 1. Introduction

Phenols in Organic Synthesis

Phenols are one of the most common functional groups present in drug molecules.^[1] For example, the phenol functional group of paracetamol **1** is vital to its mode of action because of its ability to bind to specific proteins.^[2,3] Phenolic compounds have a large variety of biological activities and this can be seen with drugs such as: amodiaquine **2** (anti-malarial drug), oxymetazoline **3** (decongestant), eugenol **4** (perfume and antiseptic), propofol **5** (anaesthetic) and dronabinol **6** (appetite stimulant) (**Figure 1**).^[4-8] Phenols are able to interact with a number of enzymes and other biological molecules due to their ability to oxidise to quinones in a physiological environment.^[9] This oxidation can occur very quickly and hence most phenols do not simply act as H-bond donors. The quinone oxidation products are known to form strong interactions with H-bond donor amino acids, such as lysine **7** or tryptophan **8** (**Scheme 1**).^[10,11] Hence these metabolites are able to interact and inhibit specific enzymes. In addition to their redox activity, the mild acidic nature of phenols means they have an additional use as antiseptics, indeed the first commonly used antiseptic was phenol.^[12,13] This antiseptic activity is due to phenol being both non-polar enough to cross microbial plasma membranes, and Brønsted acidic enough to disrupt microbial metabolic pathways through the protonation of microbial proteins.^[14]

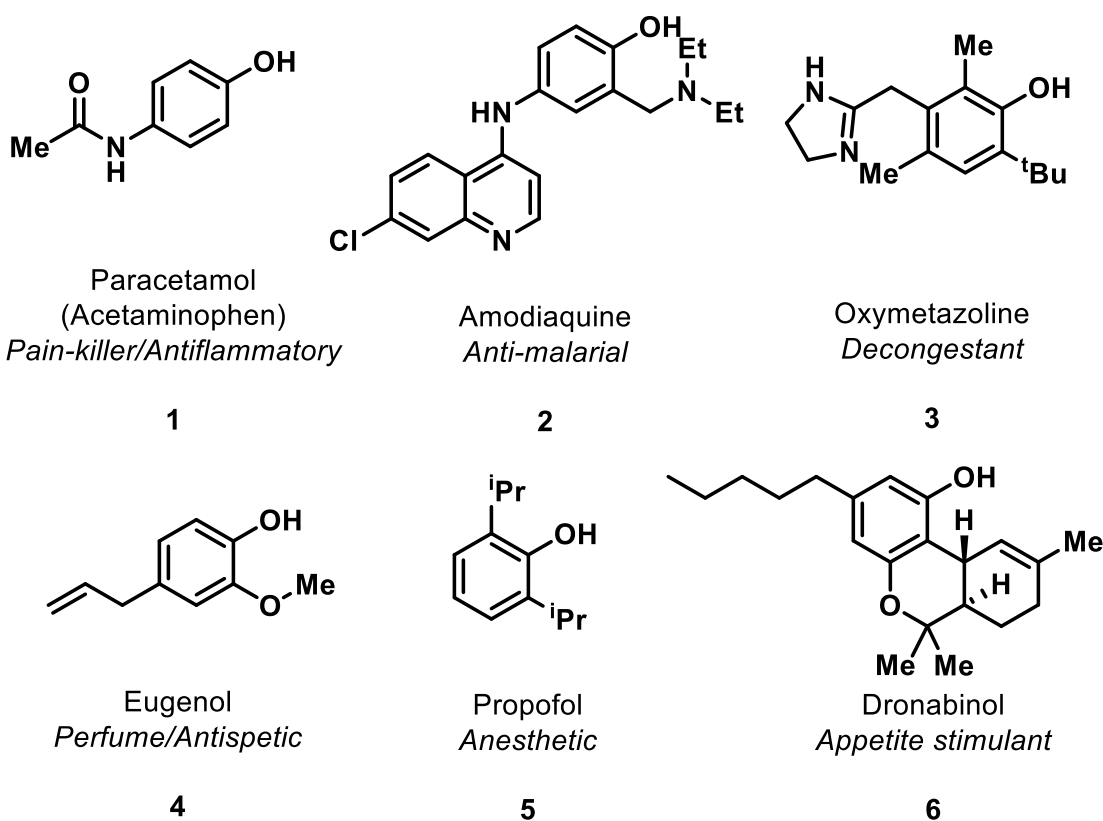
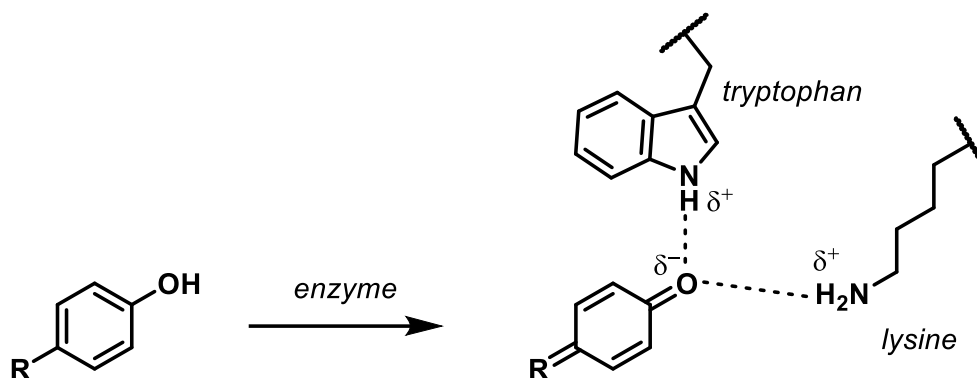


Figure 1: Structures of different phenolic pharmaceutical molecules

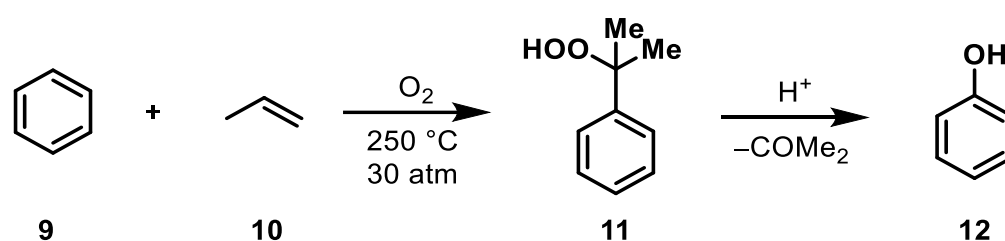


Scheme 1: Conversion of phenol to quinone and the interactions quinones can have with amino acid sides chains; tryptophan (top) and lysine (right)

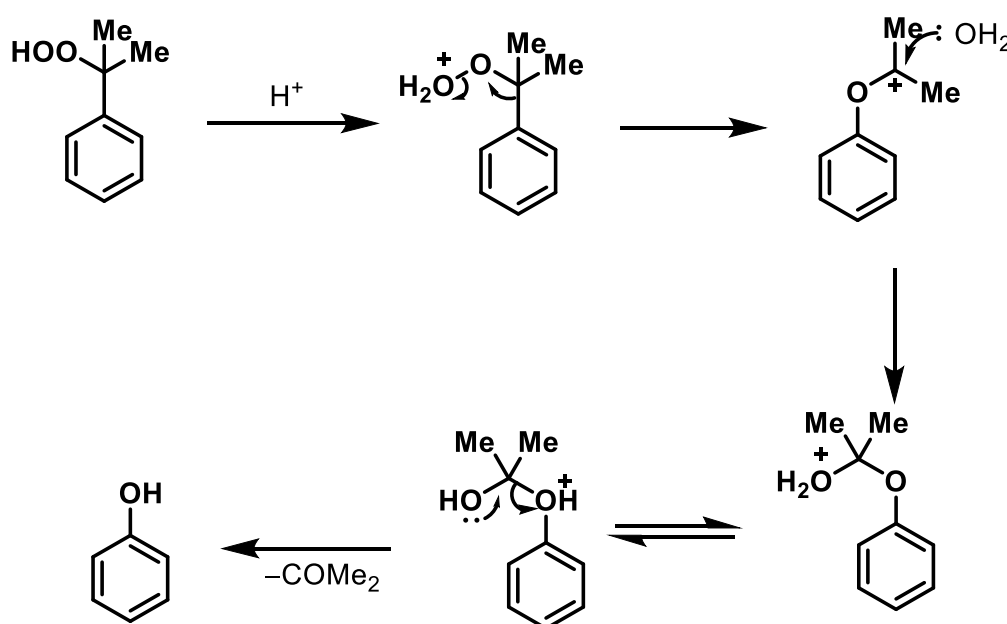
There are arguably two main strategies for synthesising phenols: 1) the oxidation of aromatic rings; and 2) the nucleophilic displacement of a functional group such as a halide. Selected illustrative examples of the two strategies are described in the following sections.

Arene Oxidation

One method that is commonly used in the chemical industry is the cumene-phenol process discovered by Hock (**Scheme 2**).^[15] In this process, benzene **9** is reacted with propene **10** and molecular oxygen to form cumene peroxide **11**. Phenol **12** and acetone can then be obtained by inducing a Hock rearrangement with an acid catalyst (**Scheme 3**).^[16] A significant limitation of this reaction is the high temperatures and pressures required to induce the formation of peroxide **11**. Therefore, it is largely unsuitable for laboratory scale synthesis and reactions involving complex organic molecules. However, it is a good representation of how phenols are synthesised in the chemical industry.

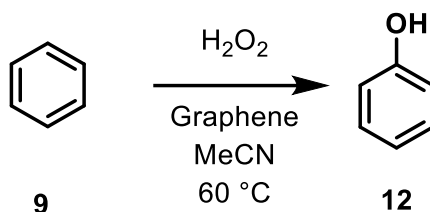


Scheme 2: Synthesis of phenol from benzene using cumene-phenol process.



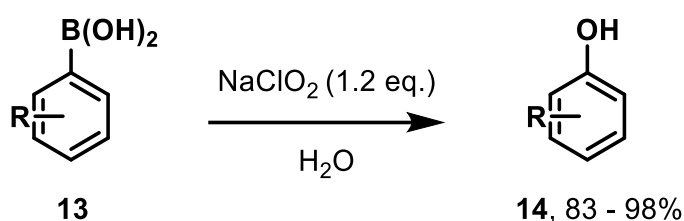
Scheme 3: Mechanism of the Hock rearrangement.

Alternatively, peroxides are often used to synthesise phenol via the oxidation of benzene. For example, Ma and co-workers used hydrogen peroxide and a graphene catalyst to prepare phenol **12** via the oxidation of benzene **9** (**Scheme 4**).^[17] Notably, these conditions improved the selectivity for the phenol product in comparison to the cumene-phenol synthesis.^[18]



Scheme 4: Method of synthesising phenol proposed by Ma and co-workers.

Phenols can also be prepared via the oxidation of arylboronic acids. For example, Boruah and co-workers showed that sodium chlorite can be used to oxidise phenylboronic acids **13** and form phenols **14** with good functional group tolerance (**Scheme 5**).^[19]



Scheme 5: Hydrolysis of boronic acid to phenol using sodium chlorite.

Functional Group Substitution

Nucleophilic aromatic substitution (S_NAr) is a reaction class that has been known to chemists for several decades and is one of the most common reactions employed in organic chemistry.^[20–23] This reaction class can be used to easily introduce functionality on to a variety of aromatic rings,^[24] S_NAr reactions are therefore a common and important class of reactions in the fields of medicinal and agro-chemistry.^{[25], [26]}

The direct substitution of an aryl halide by a hydroxide ion via a S_NAr mechanism is an attractive method for the synthesis of phenols. For example, 4-chloronitrobenzene **15** can be substituted using tetrabutylammonium hydroxide as shown by Mizuno and co-workers (**Scheme 6A**)^[27]. Here, as with most S_NAr reactions, a strong EWG is often necessary to activate the arene towards substitution. However, less activated arenes can be substituted by hydroxide at higher reaction temperature and pressures.^[28] Stridfeldt and coworkers showed that arenes bearing more easily substituted leaving groups such as diaryliodonium salts **17** can also be used to enable substitution to proceed under milder reaction conditions (**Scheme 6B**).^[29] However, a significant limitation of this method is that the phenol **18** product often reacts with the diaryliodonium salt, to yield an aryl ether by-product **19**.



Figure 2: Different approaches of orbital attack by a nucleophile, σ^* orbital is hindered by the benzene ring, whereas the π^* is not.

However, there still remains uncertainty over whether these reactions proceed via a step-wise or a concerted addition-elimination mechanism (**Figure 3**).^[22] Rather than there being a single answer for all substrates, it has been proposed that the selectivity between a step-wise or concerted mechanism is dependent on the relative stability of a Meisenheimer complex against the starting and product molecules.^[32] This can be dependent on a number of factors, such as the presence of one or multiple electron-withdrawing groups (EWGs) in the *ortho*- or *para*-positions of the arene, which can directly stabilise the anionic Meisenheimer complex and favour a step-wise mechanism.^[33] Notably, S_NAr reactions with less activated arenes bearing electron-donating groups (EDGs) do not appear to be common, as these groups can destabilise any anionic intermediates and transition states formed during the course of the reaction.^[34]

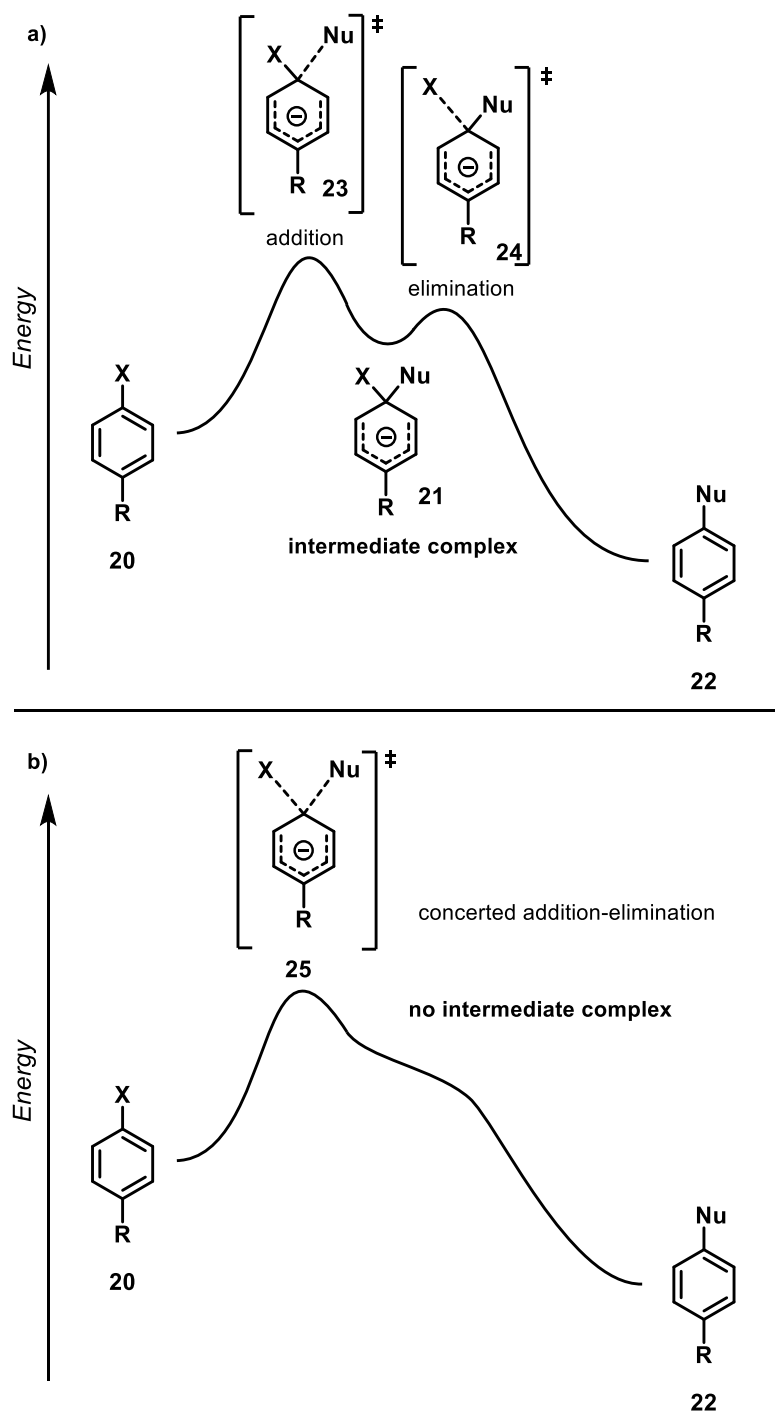
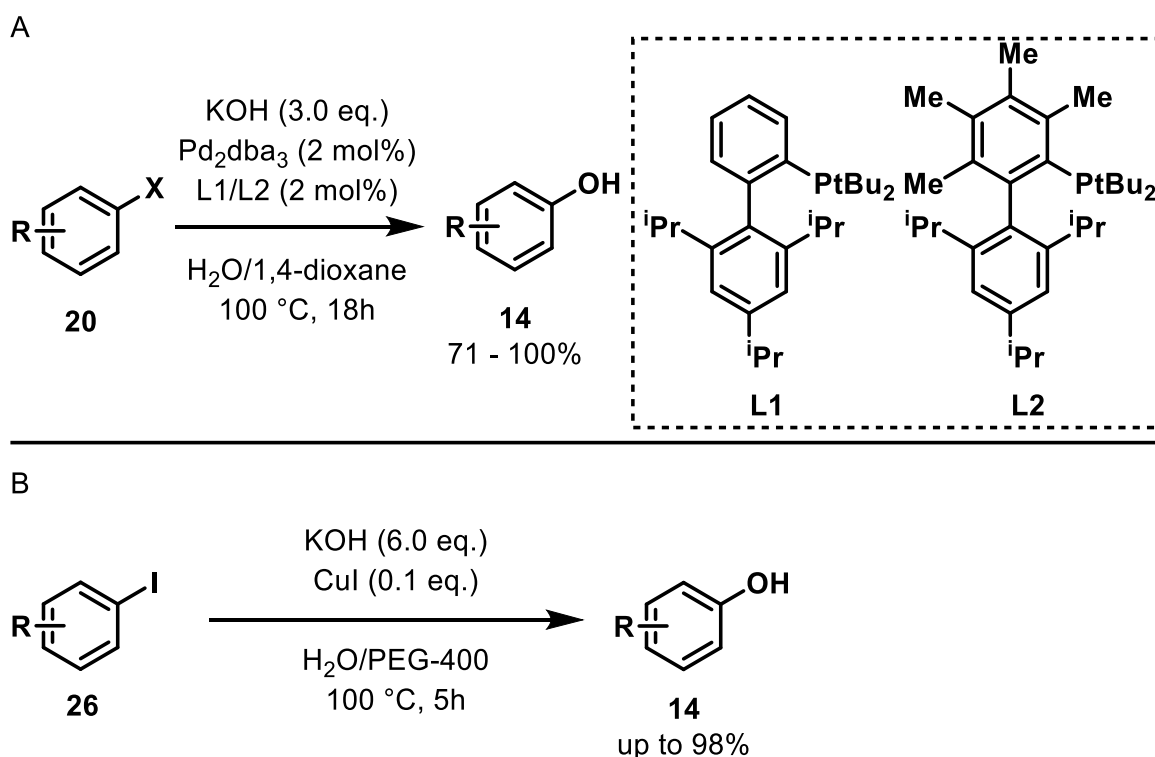


Figure 3: Energy surface diagrams for step-wise (a) and concerted (b) S_NAr reactions.

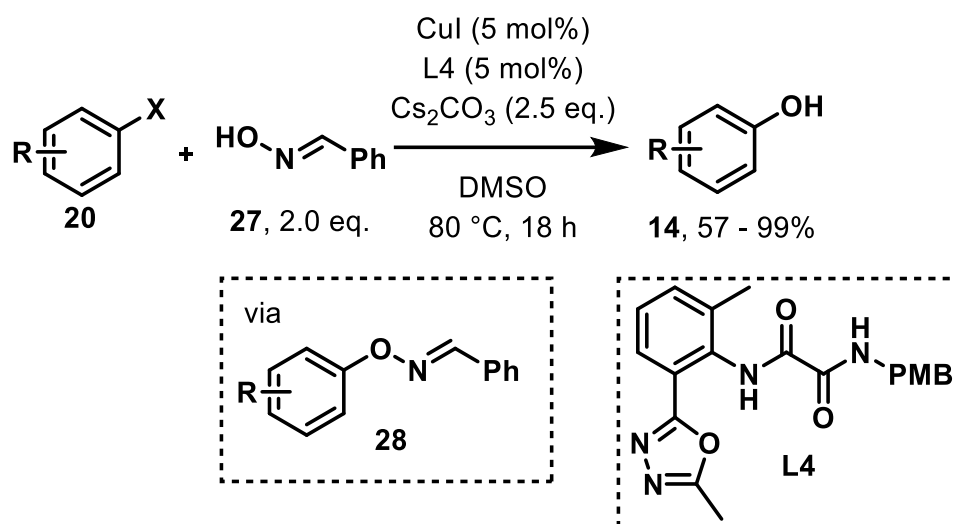
Alternative to direct substitution via an addition-elimination mechanism, transition-metal catalysis can also be readily utilised to substitute different functional groups with a hydroxide (or hydroxide surrogate) nucleophile. For example, Buchwald and co-workers demonstrated that aryl halides can be coupled with potassium hydroxide using palladium catalysis (**Scheme 8A**), this method gave greater substrate versatility than S_NAr reaction, as substrates with EDGs could be

used in this methodology.^[35] Later, Chen and co-workers showed that a cheaper copper catalyst system could also be used to promote this transformation (**Scheme 8B**).^[36]



Scheme 8: Synthetic routes for making phenols from simple aryl halides using transition metals. **A** – Method developed by Buchwald and co-workers.^[35] **B** – Method developed by Chen and co-workers.^[36]

The relatively harsh reaction conditions required to couple hydroxides with aryl halides may be attributed to the poor nucleophilicity of hydroxide anions. To circumvent this limitation, hydroxide surrogates may be used. For example, Fier and Maloney coupled aryl halides **20** with oxime **27** using copper catalysis to yield phenols **14** in high yield and under milder reaction conditions (**Scheme 9Scheme 6**).^[37] The oxime would act as the nucleophile to yield the intermediate **28**, which would then fragment in the presence of base to generate the desired phenol product **14**.

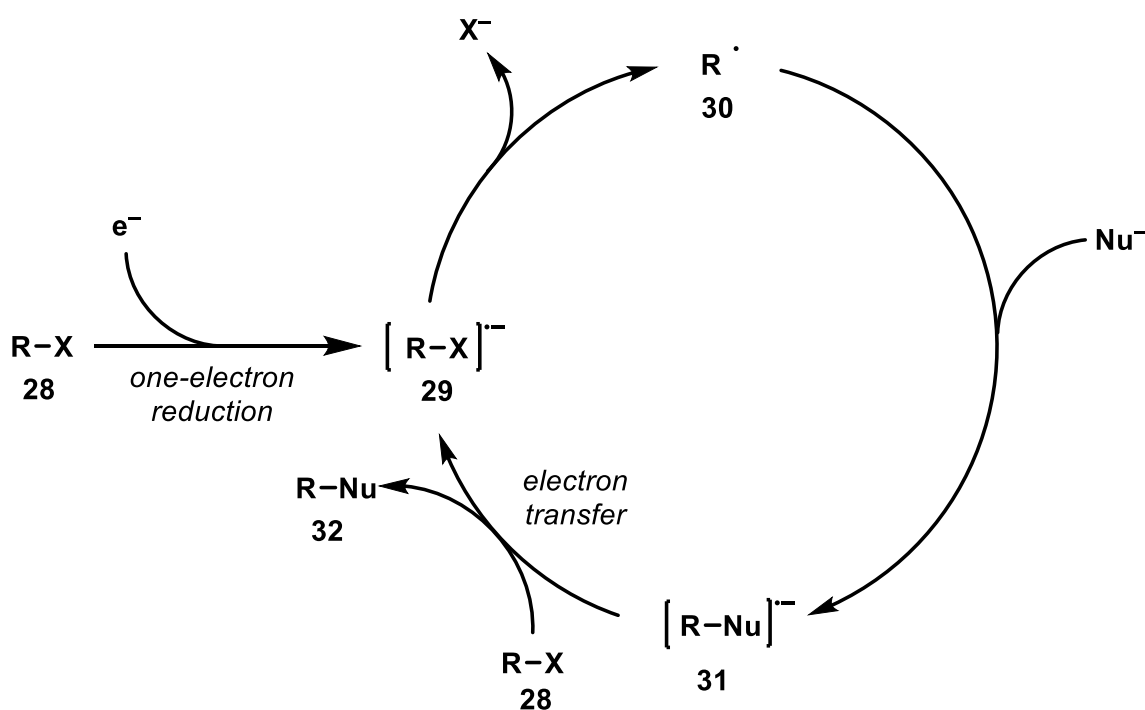


Scheme 9: Substitution of aryl halide with benzaldoxime to yield phenol.^[37]

Radical-Nucleophilic Substitution ($S_{RN}1$)

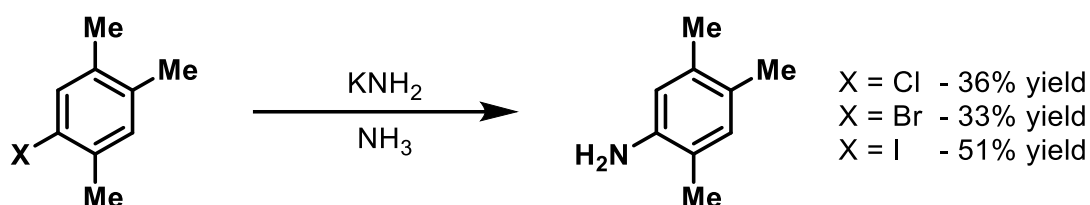
Another alternative to functional group displacement via the S_NAr mechanism is the radical-nucleophilic substitution ($S_{RN}1$) chain mechanism. Here, highly reactive radical intermediates are used which can obviate the need for high reaction temperatures. Additionally, no Meisenheimer intermediate is formed in this reaction, therefore no EWGs are needed to stabilise this intermediate. Hence, $S_{RN}1$ reactions are compatible with a broad range of substrates, including aliphatic systems, and are a very powerful synthetic tool.^[38] However, prior to the work described in this thesis, no general method had been described for the synthesis of phenols via an $S_{RN}1$ mechanism.

Generally, $S_{RN}1$ reactions are proposed to initiate via the one-electron reduction of the substrate **28**, which forms an aryl radical anion **29**. This is followed by a substitution by a nucleophile, forming a new radical aryl anion **31**, with fragmentation of **29** being the first step of the substitution. Finally, electron transfer from radical-anion **31** to another equivalent of the substrate **28** occurs to form the substituted product **32** and regenerate radical anion **29** (Scheme 10).^[39,40]



Scheme 10: Originally proposed general radical chain mechanism that occurs during an $S_{RN}1$ mechanism. Key steps being reduction of substrate by electron transfer (initiation), fragmentation of $R-X$ bond, nucleophilic addition to the substrate then electron transfer to a new molecule of substrate.

This reaction class was discovered when Bunnett and co-workers observed that aryl iodides exhibited a greater reactivity with respect to being substituted by NH_2 groups than their chloride and bromide counterparts (**Scheme 11**). This is contrary to expectations that the reverse reactivity trend would be observed should an $\text{S}_{\text{N}}\text{Ar}$ mechanism.^[41] They claimed this mechanism was radical in nature, due to observations of inhibition by radical scavengers (2-methyl-2-nitrosopropane and tetraphenyl hydrazine).

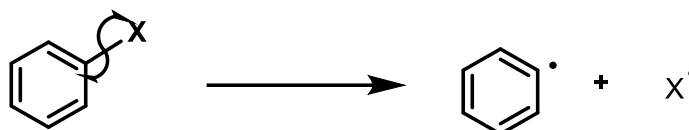


Scheme 11: Reaction performed by and co-workers, showing $\text{S}_{\text{RN}}1$ substitution of halides by an amide ion.^[41]

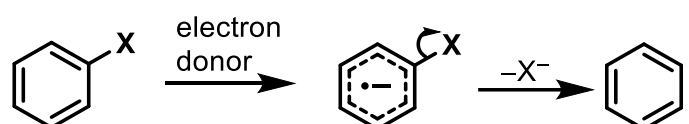
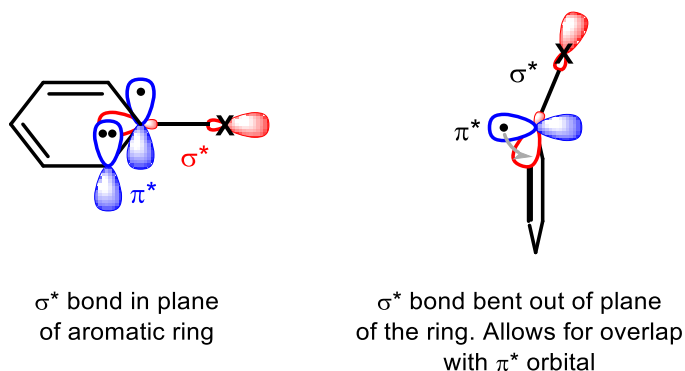
Initiation

As in all radical reactions, an $\text{S}_{\text{RN}}1$ reaction first requires some form of initiation. This is commonly achieved through either the homolytic cleavage of a C-X bond^[42] or as mentioned previously the one-electron reduction of or an R-X compound (**Scheme 12**). For aryl halides, this fragmentation of the radical anion C-X bond often proceeds via the transfer of an electron in the π^* system of the aromatic ring to the σ^* orbital of the C-X bond, which needs to bend out of plane to facilitate the orbital overlap needed for the electron transfer to occur between orbitals (**Figure 4**).^[43] However there are some arguments that can be made to negate this step being necessary, such as transfer of an electron directly into the σ^* orbital from another species, or multiple electron being transferred to the substrate, forming a dianion.^[44,45]

homolytic cleavage



one-electron reduction

**Scheme 12:** Methods of initiation for $S_{RN}1$ reactions.**Figure 4:** Diagram of electron transfer from π^* orbital to σ^* orbital. Likely to be bending of the C-X bond to allow for orbital overlap.

Traditionally, sacrificial electron donors, photochemistry or electrochemistry have been used to promote the one-electron reduction of R-X compounds (**Figure 5**).^{46, [47,48]} Each method of initiating a $S_{RN}1$ reaction has advantages and disadvantages. Thermal methods using sacrificial electron donors are limited as electron transfer is dependent on the reduction potential of the electron donor. In many cases the nucleophile itself plays the role of electron-donor, which presents the challenge of designing nucleophiles that are adequately electron-donating.^[49] Photochemical methods can be used to generate a photoexcited electron donor, from which electron transfer to another species is favourable (photoinduced electron-transfer). However, such photochemical processes are often limited by the frequently low quantum yield of said processes.^[50] Electrochemistry can be used to circumvent the need for a carefully designed homogenous electron donor or photochemistry. However, the radical species are often generated

at the site of the electrode and in high concentrations, which means the success of the reaction is dependent on the diffusion and mixing of radical species throughout the reaction medium.

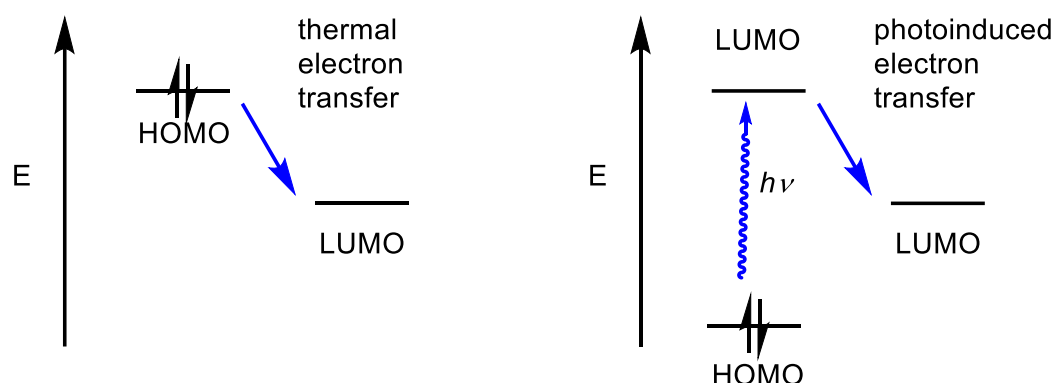


Figure 5: Energy level diagrams for thermal and photoinduced electron-transfers.

Charge transfer complexes (CTCs) are another chemical phenomenon which can be used to initiate $S_{RN}1$ reactions.^[51] A CTC can be interpreted as the interaction between the orbital wavefunctions of the HOMO of the donor and the LUMO of the acceptor (**Figure 6**).^[52] CTCs can be easily identified during UV-vis, IR or NMR spectroscopic analysis by the formation of new spectral peaks.^[53] Indeed, CTCs can often be observed by the naked eye as strong coloured reaction mixtures are formed once the donor and acceptor are mixed together, which corresponds to the CTC charge-transfer band.

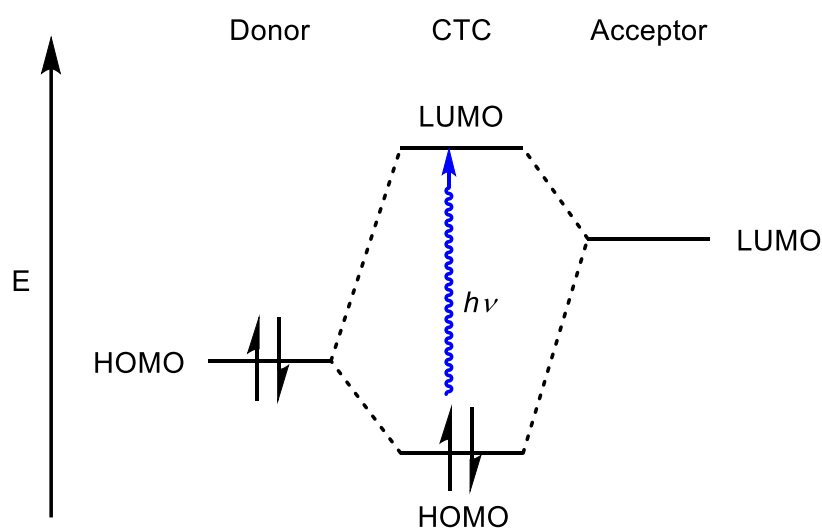


Figure 6: ET between HOMO of donor and LUMO of acceptor within a CTC

The strength of the interaction in a CTC is dependent on the electron affinities of the donor and the acceptor, which can be equated to their Lewis basicity and acidity respectively.^[54] It was also noted that the type of interaction i.e. π - π , n- π , etc. (**Figure 7**Error! Reference source not found.) plays little part in the strength of the interactions in a CTC.^[55] Instead, it is the extent of orbital overlap within the complex which is important.^[56] Hence, the HOMO of the donor and the LUMO of the acceptor need to be of a comparable energy level to facilitate this orbital overlap.

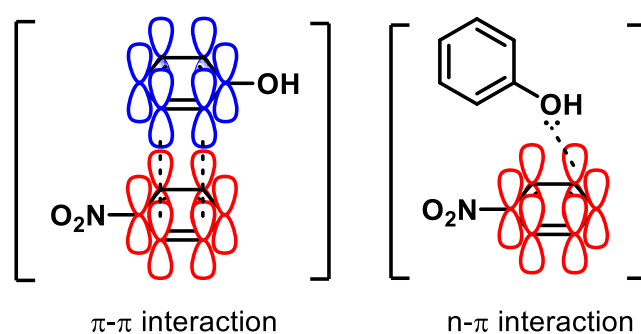
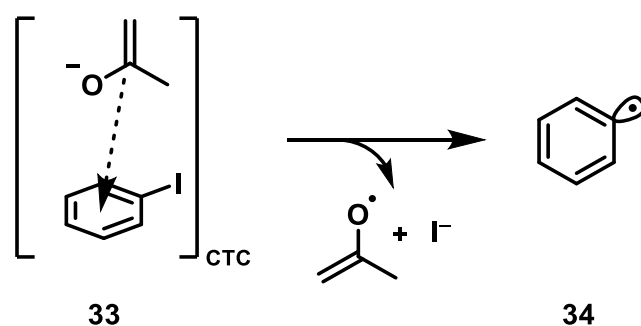


Figure 7: Diagram of different orbital interactions in CTCs

Importantly, the formation of a CTC can facilitate electron transfer between the donor and acceptor through an inner-sphere electron mechanism. Work by Kochi and co-workers suggests that an inner-sphere electron transfer can be far more favourable than outer-sphere, however the often-weak interactions in CTCs cannot always mediate such an inner-sphere mechanism.^[57]

The charge-transfer band of a CTC can also be photoexcited to promote electron transfer from the donor to the acceptor. For example, Fox and co-workers demonstrated that the CTC formed between phenyl iodide and acetone enolate can be photoexcited to yield an aryl radical (**Scheme 13**).^[58]



Scheme 13: Formation of an aryl radical from a radical aryl anion formed by an electron transfer in CTC between acetone enolate and phenyl iodide.

Chapter 1. Introduction

Interestingly, CTC-type interactions have also been proposed by Weaver and co-workers to facilitate S_NAr reactions (**Scheme 14**).^[59] Here, the addition of a chloride anion to polyfluoroarenes was proposed to be partially facilitated by the precomplexation of the polyfluoroarene **35** substrate with the aromatic catalyst **36**.

Substitution and Propagation

Following the generation of a radical species (R^\bullet) it can then be coupled with an anionic nucleophile (Nu^-). The rate and thermodynamic feasibility of radical-anion coupling is strongly influenced by the standard potential of the $RNu/RNu^{\bullet-}$ couple,^[60] as this potential directly reflects the stability of the coupled radical-anion product ($RNu^{\bullet-}$). Therefore, radical species (R^\bullet) bearing EWGs often couple with anions very quickly as the standard potential of the $RNu/RNu^{\bullet-}$ couple will be more positive. However, the rate of electron transfer between the coupled radical-anion product ($RNu^{\bullet-}$) and the substrate (RX) is then dependent on the relative standard potentials of the $RNu/RNu^{\bullet-}$ and $RX/RX^{\bullet-}$ couples, which is therefore favoured by less stable (more reducing) radical-anion products (**Figure 8**). This rate typically needs to be fast in order to achieve a reasonable rate of reaction, given the often-low number of radicals present in solution following initiation.^[60]

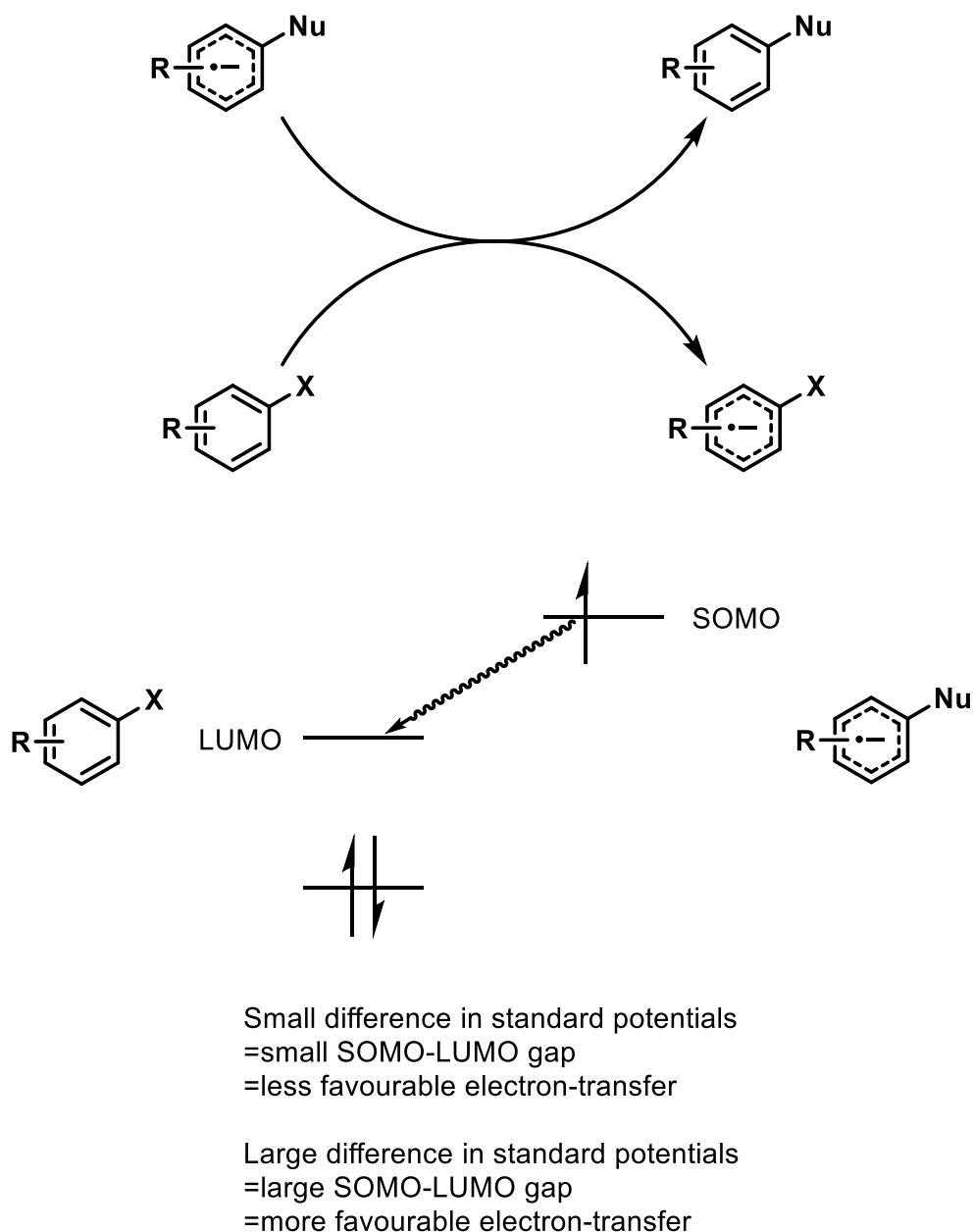
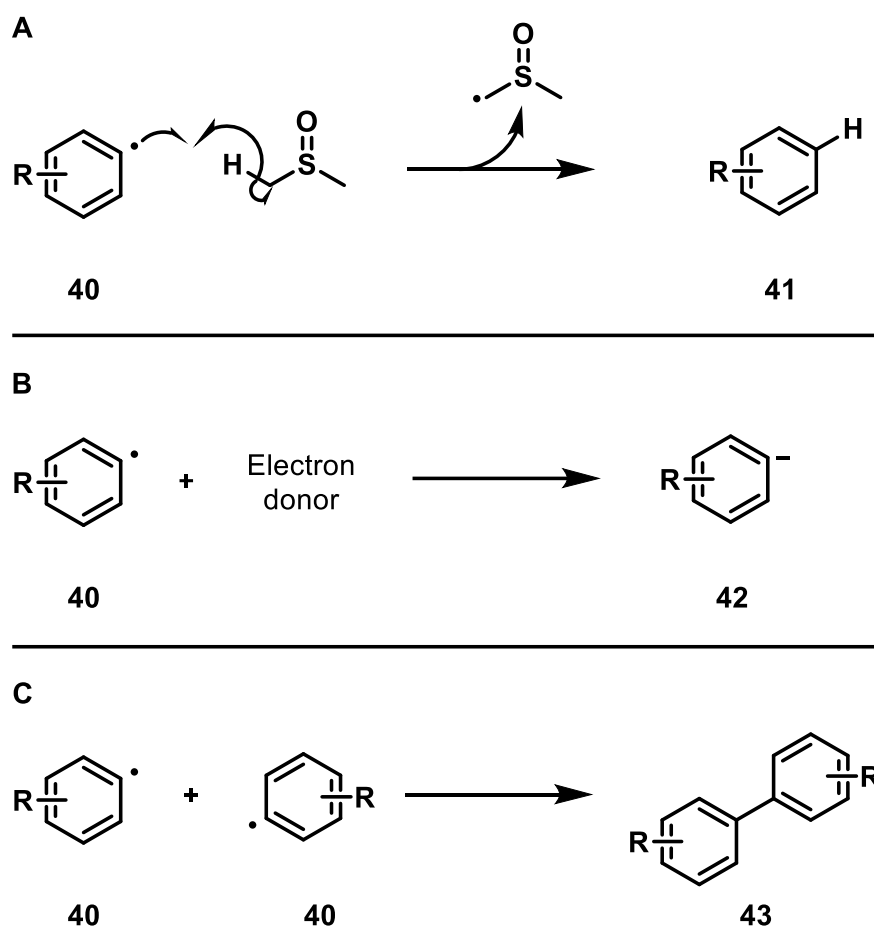


Figure 8: Energy levels of ET occurring in the propagation step of a $S_{RN}1$ reaction.

Termination

Termination of $S_{RN}1$ radicals chain may occur through a variety of reactions. (**Scheme 15A**).^[61] In solvents with weak C-H bonds, H-atom abstraction by the intermediate radical **40** can be facile. Alternatively, easily reduced radical species, such as aryl radicals, can be reduced to the corresponding anion **42** (**Scheme 15B**). Radical-radical coupling is also a viable means of terminating the radical chain if the concentration of radicals is sufficiently high (**Scheme 15C**).

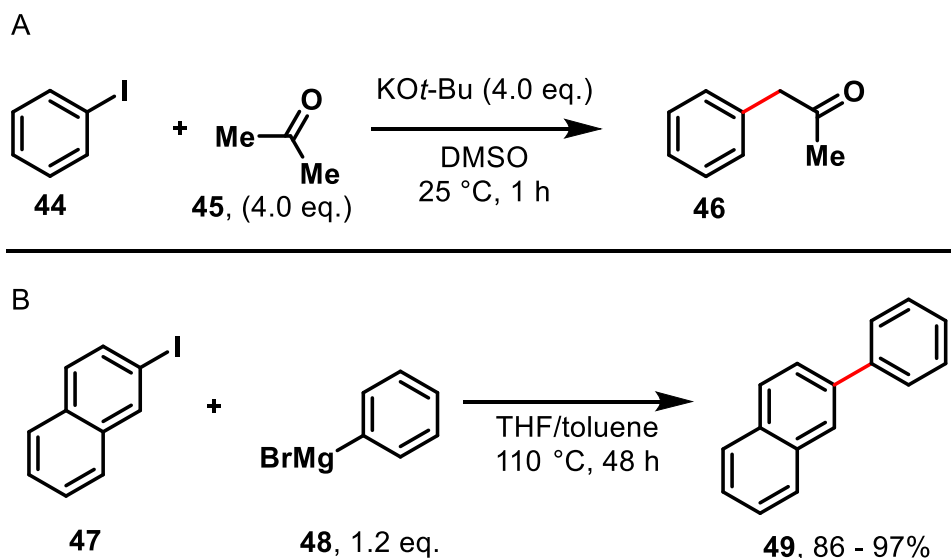
Ultimately the number of radicals present in $S_{RN}1$ processes are typically low, therefore there is unlikely to be a large number of termination products present at the conclusion of the reaction.



Scheme 15: Different mechanisms of termination for an $S_{RN}1$ mechanism. **A** – H-abstraction from solvent. **B** – Reduction of aryl radical. **C** – Radical-radical cross-coupling.

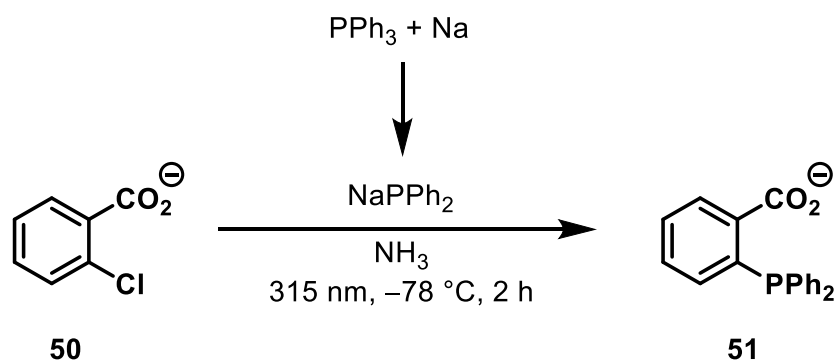
Synthetic Applications and Limitations

$S_{RN}1$ reactions are highly versatile and can be used to form challenging new bonds (e.g. C-C bonds). For example, Scamehorn and co-workers showed that the α -arylation of ketones can be readily achieved simply by reacting acetone enolate with phenyl iodide (**Scheme 16A**).^[62] This reaction was hindered by radical scavengers, strongly suggesting that an $S_{N}Ar$ mechanism was operative. More recently, Hayashi and co-workers coupled Grignard reagents **48** with aryl iodides **47** via a proposed thermally initiated $S_{RN}1$ mechanism (**Scheme 16B**).^[63,64]



Scheme 16: **A** – Aryl enolation via $S_{RN}1$ reaction as proposed by Scamehorn and co-workers. **B** – Arene cross-coupling via $S_{RN}1$ mechanism, as proposed by Hayashi and co-workers, further evidence of $S_{RN}1$ in this reaction published by Wiest and co-workers.^[49,62,64]

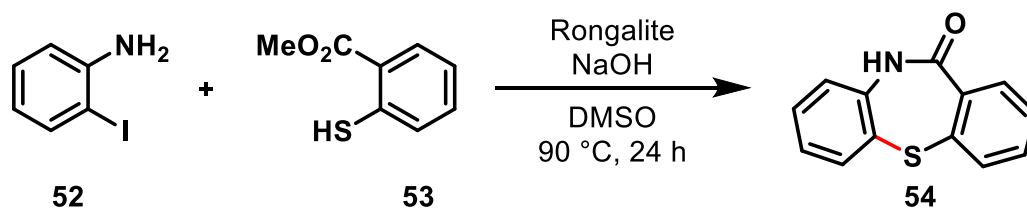
Reactions for forming other C-X bonds, such as C-P bonds, are also wide-spread. Rossi and co-workers showed how an $S_{RN}1$ reaction can be used to synthesise 2-(diphenyl-phosphino)benzoate **51** from 2-chlorobenzoate ion **50** (**Scheme 17**). This reaction could be completed at $-78\text{ }^{\circ}\text{C}$; a strong indicator that photoinduced electron transfer was occurring, rather than a thermal mechanism being involved.^[65] With the light being absorbed by the diphenylphosphide anion which allowed for a PET to the aromatic species to initiate the reaction.



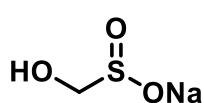
Scheme 17: Phosphonation of chlorobenzoic acid utilising a photochemically mediated $S_{RN}1$ reaction.^[65]

$S_{RN}1$ reactions have also been applied to the formation of carbon sulfur bonds. An example of this was reported by Wang and co-workers who were able to use $S_{RN}1$ methodology to synthesis a precursor to the antipsychotic drug Quetiapine (**Scheme 18**).^[48] This was achieved by the $S_{RN}1$ substitution of the iodoaniline **52** by thiol **53** followed or preceded by an amide coupling of the

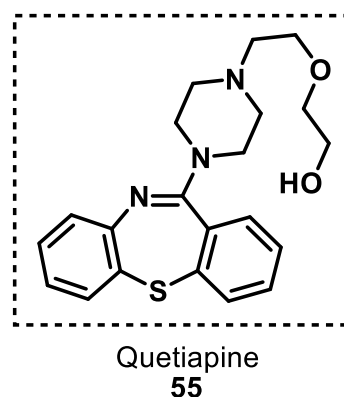
amine and ester groups. With the Rongalite acting as the electron donor for initiation of the reaction.



Rongalite



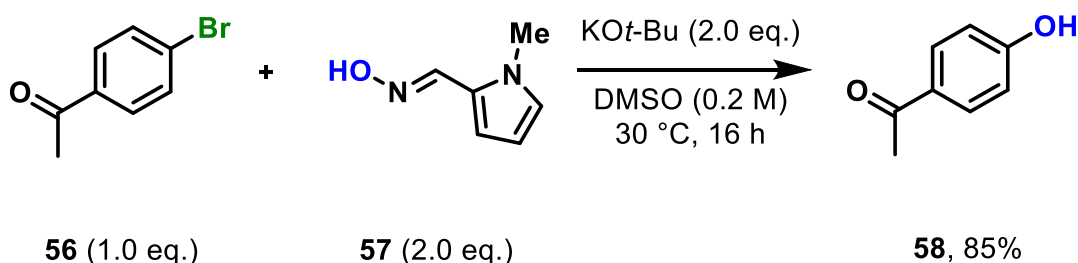
SO_2^{2-}
Reducing agent



Scheme 18: Synthesis of intermediate for Quetiapine synthesis utilising $\text{S}_{\text{RN}}1$ reaction.^[48]

Project Aims

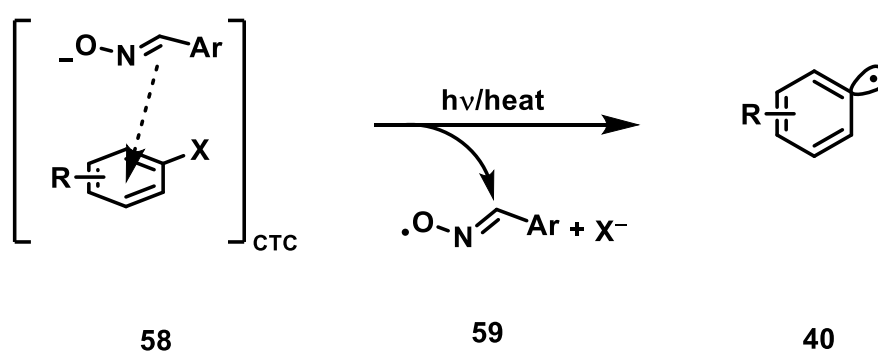
The aim of this project was to determine if a hydroxide surrogate could be used as means of introducing a hydroxyl functionality onto an aromatic ring via an $\text{S}_{\text{RN}}1$ mechanism. Preliminary studies conducted in the James group showed that aryl halide **56** could be coupled with an oxime-based hydroxide surrogate **57** to form phenol **58** in 85% yield (**Scheme 19**).



Scheme 19: Preliminary experiment completed by the James group using oxime **57** as a hydroxide surrogate in the substitution of bromine in 4'-bromoacetophenone.

The first objective was to establish optimal conditions for this hydroxylation protocol and determine its generality. The second objective was to determine the mechanism of substitution.

It was anticipated that an $S_{RN}1$ process could be initiated via the thermal or photochemical activation of a CTC formed between the oxime anion and aryl halide substrate (**Scheme 20**). It was hypothesised that by varying the aromatic substituent of the oxime, the electronic properties of the nucleophile could be tuned to favour this process. Since the oxime would need to act as both an electron-donor and a nucleophile. In addition, it was hoped that the π -system of the oxime would also provide greater stabilisation of the coupled radical-anion product in comparison to if the nucleophile was a hydroxide ion (**Figure 9**).



Scheme 20: Scheme depicting electron transfer in a CTC as a means of forming aryl radical anion **60**, an intermediate necessary for $S_{RN}1$ reactions.

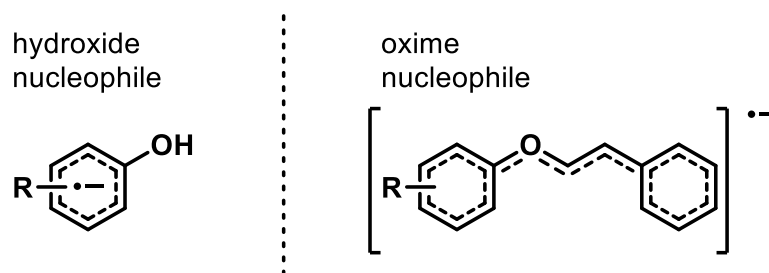
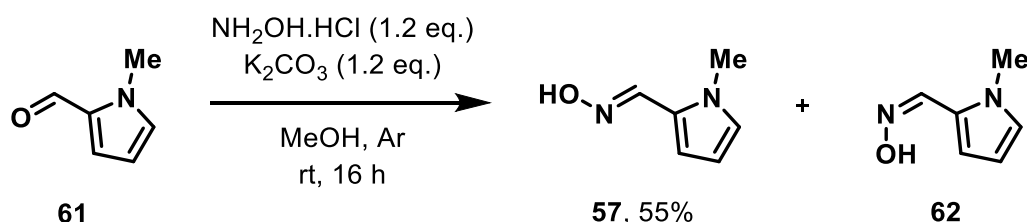


Figure 9: Different extents of negative charge delocalisation between if a hydroxide ion was the nucleophile in comparison to an oxime nucleophile.

Chapter 2. Hydroxylation of Aryl Halides.

Oxime synthesis

Studies building on this promising preliminary result began with optimising the synthesis of oxime **57**. The aim was to find optimal conditions which would allow oxime **57** to be quickly prepared and on large scale. Oxime **57** was first prepared by condensing aldehyde **61** with hydroxylamine hydrochloride in the presence of a base (**Scheme 21**).^[66] Both oxime isomers **57** and **62** could be separated by column chromatography and their stereochemistry confirmed by X-ray crystallography (**Figure 10**). The yield of the *Z*-isomer of oxime **62** was not determined as the *Z*-isomer **62** performed poorly in preliminary studies. Therefore, further optimisation was aimed at increasing the yield of the *E*-isomer **57** only.



Scheme 21. Reaction conditions for the initial synthesis of oxime **57** that were used in previous work by the James research group.

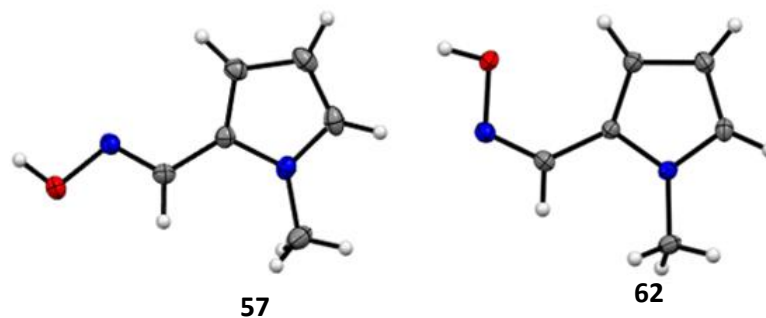
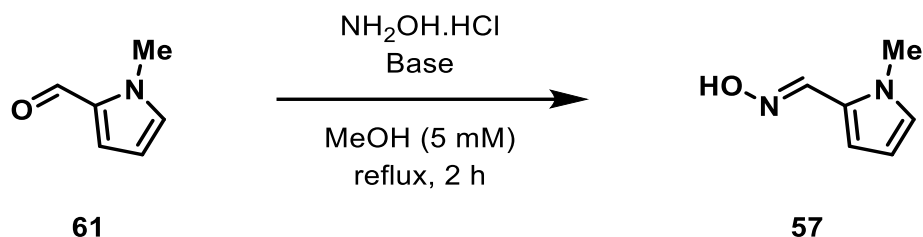


Figure 10. X-ray crystal structures of *E*-isomer of oxime **57** (Left, obtained by WOW) and *Z*-isomer of oxime **62** (Right, obtained by MJJ).

To improve the yield of oxime **57**, the reaction stoichiometry, base and temperature were varied (**Table 1**). Performing the reaction under reflux and increasing the equivalents of hydroxylamine hydrochloride (1.6 eq.) and potassium carbonate (2.0 eq.) afforded oxime **57** as a pale brown solid in 68% yield (Entry 1). It should be noted that this reaction was also conducted under air and so the use of an inert atmosphere was abandoned (compared to the initial conditions trialled in (**Scheme 21**)). Using weaker potassium and sodium acetate bases ($\text{p}K_{\text{a}} = 4.7\text{--}8$ ^[67] vs $\text{p}K_{\text{a}} = 10.3$ for carbonates)^[68] reduced the yield of oxime **57** to 39% and 37%, respectively (Entries 2 and

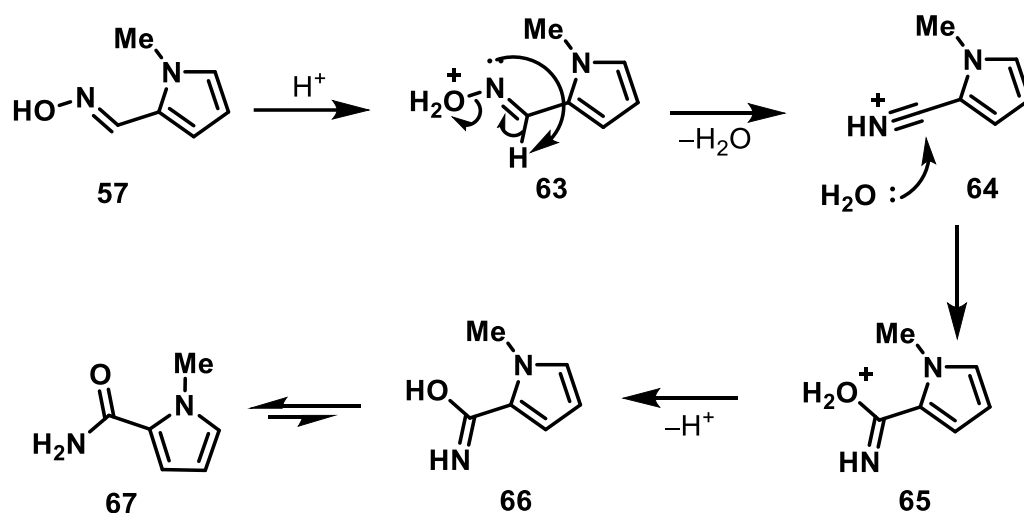
3). Sodium carbonate was then examined, which afforded oxime **57** in comparable yield to potassium carbonate, but as an easily handled crystalline white solid (Entry 4). Finally, a significant improvement in yield (89%) was observed when the quantity of hydroxylamine hydrochloride and sodium carbonate were decreased to 1.2 eq. (Entry 5).



Entry	NH ₂ OH·HCl (eq.)	Base	eq. Base	Yield / %
1	1.6	K ₂ CO ₃	2.0	68
2 ^a	1.6	NaOAc	2.0	39
3 ^a	1.6	KOAc	2.0	37
4	1.6	Na ₂ CO ₃	2.0	62
5	1.2	Na ₂ CO ₃	1.2	89

Table 1. Conditions trialed for the synthesis of oxime **57**. ^a reaction conducted by George Smith.

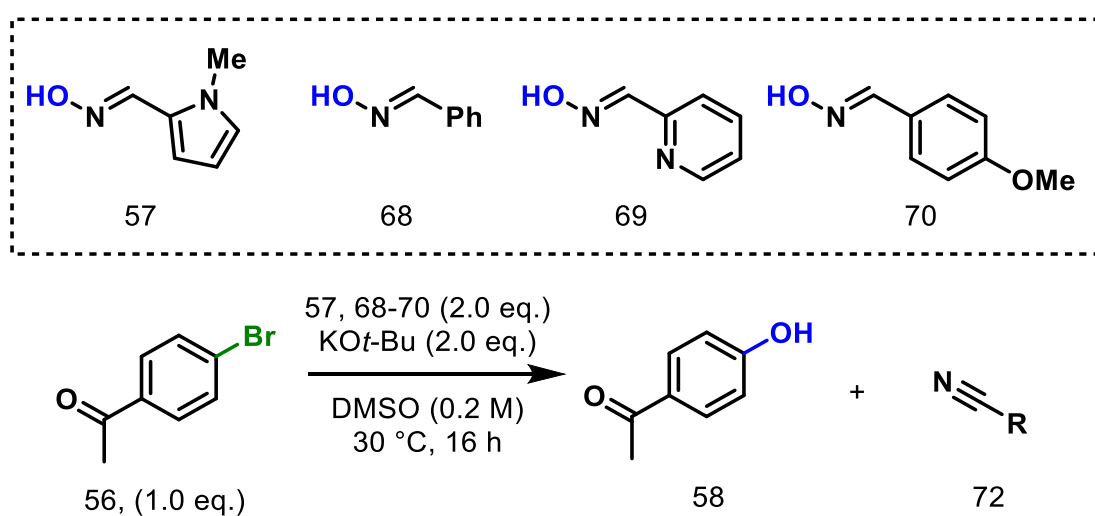
During these optimisation studies there was potential that the product was degrading during purification by column chromatography due to the acidic nature of silica gel. This was a believed to be a possibility for why the yield of oxime never exceeded 90%. It is known that oximes can be converted into amides under acidic conditions via a Beckmann rearrangement (**Scheme 22**).^[69] Thus to counter-act this potential degradation pathway, 1-3% of Et₃N was added as a basic additive to the eluent used in column chromatography.



Scheme 22. Reaction mechanism for the acid mediated degradation of oxime **57** via a Beckmann rearrangement, yielding amide **67**.

Oxime comparison

Using the optimised conditions developed in **Table 1**, a small selection of oximes; **57**, **68–70** was prepared (by other group members) and their reactivity was compared using the model reaction with aryl bromide **56** (**Table 2**). Pleasingly, the desired phenol **58** was obtained with every oxime, but the original pyrrole derivative **57** proved optimal (Entries 1–4). Nitrile by-products **71** were also observed in every entry, indicating that these reactions proceed via a common pathway, the base-mediated fragmentation of an intermediate *O*-aryl oxime **72**.



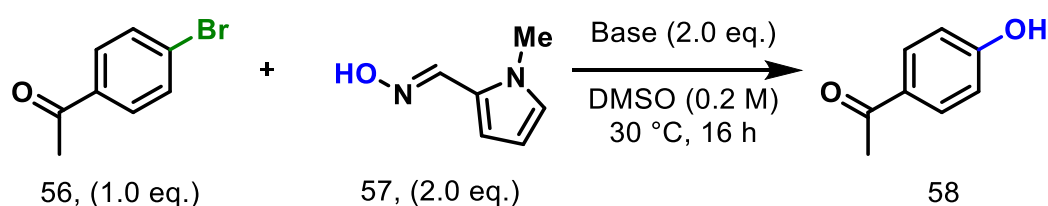
Entry	Oxime	Yield / %
1	57	75

2	68	52
3	69	38
4	70	41

Table 2. Oxime comparison for the synthesis of phenol **58**. Yields were determined by ^1H NMR spectroscopic analysis of the crude reaction mixture using CH_2Br_2 as an internal standard.

There was a loose link between the electronic properties of the oxime and the yield of phenol **58**, with more electron-rich oximes generally performing better (Note: the reactivity of methoxy derivative **70** may have been impacted by its poor solubility in DMSO). If this reaction proceeds via an $\text{S}_{\text{RN}}1$ mechanism, it was postulated that more electron-donating oximes might be able to initiate these reactions more effectively. Alternatively, the different aromatic systems could have affected the hardness of the nucleophile and hence its suitability for coupling with soft-electrophilic aryl radicals.^[70] Additionally, more electron-rich oximes could favour the polar $\text{S}_{\text{N}}\text{Ar}$ mechanism.

Next, to investigate the effect of the base on the yield of the reaction, alternative bases to potassium *tert*-butoxide were used in the reaction (**Table 3**).^[71] First, weaker bases caesium carbonate and potassium hydroxide were trialed (Entries 2–3), which afforded phenol **58** in diminished yields. Next, the stronger base KHMDS (1.0 M in THF) was used, which improved the yield of phenol **58** to 96% (Entry 5). All of these results indicated that potassium *tert*-butoxide was not essential to the reaction, but this base was retained for further studies as it was anticipated that stronger bases (e.g. KHMDS) may decrease the functional group tolerance of this reaction protocol.

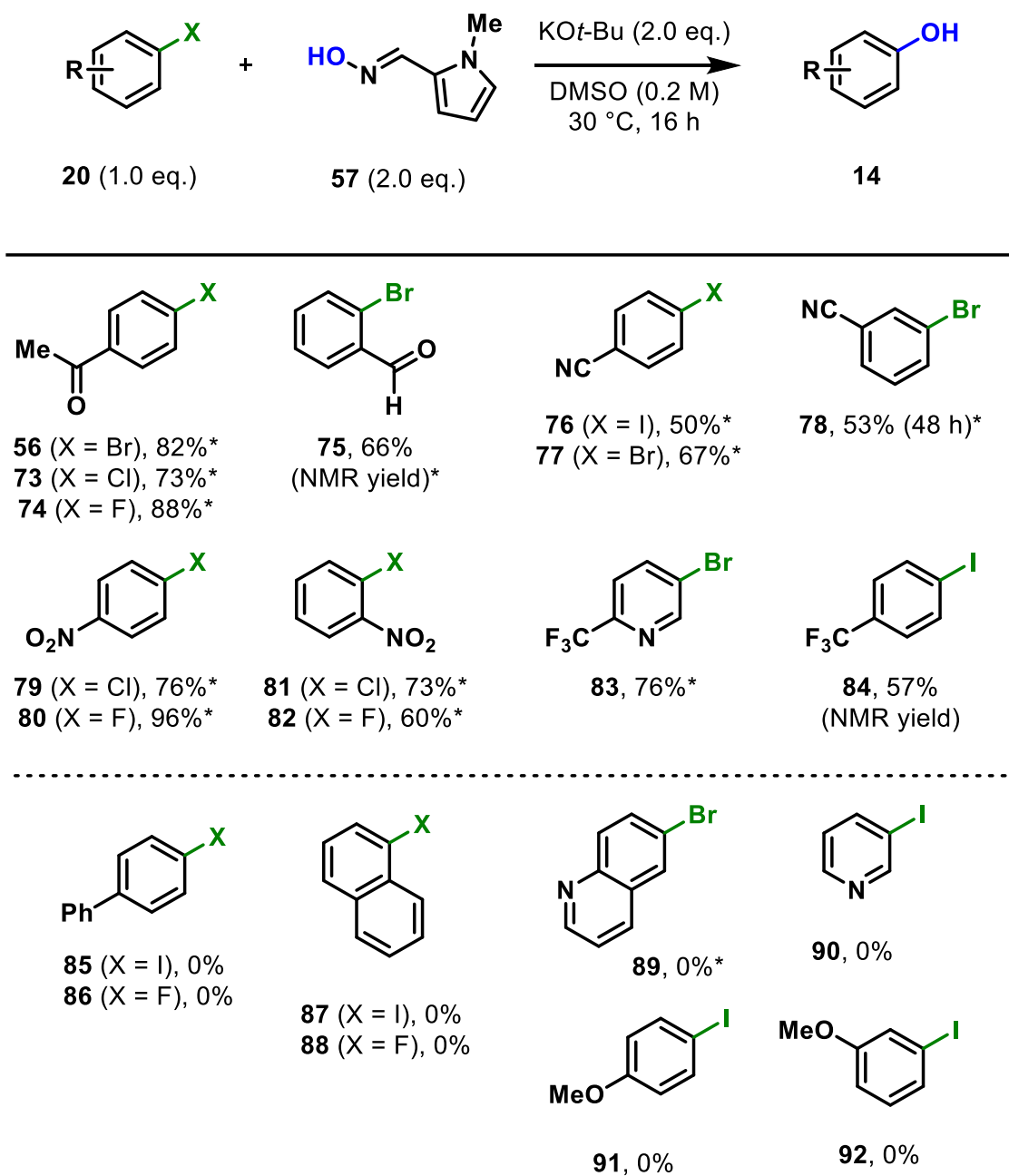


Entry	Base	Yield / %
1	$\text{KO}t\text{-Bu}$	75
2	Cs_2CO_3	25
4	KOH	38
4	KHMDS in THF (1.0 M)	96

Table 3. Effect of different bases on the conversion of 4'-bromoacetophenone **56** to acetophenone **58** in the conditions stated in the scheme above. Yields were determined by ^1H NMR spectroscopic analysis of the crude reaction mixture using CH_2Br_2 as an internal standard.

Scoping studies

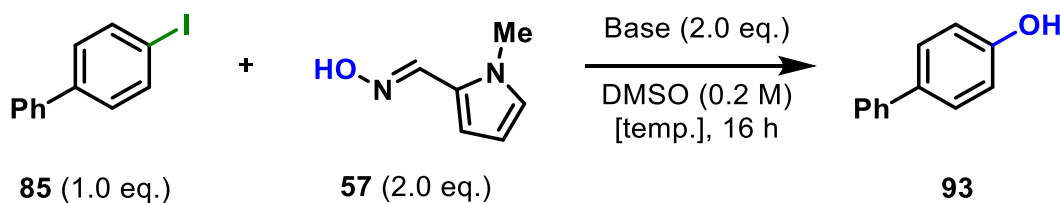
To fully explore the limitations of this hydroxylation protocol, a wider range of substrates were examined in collaboration with other group members, Patrycja Ubysz and Will Owens-Ward. Due to the collaborative nature of these studies, only a brief summary of these results are outlined in (**Scheme 23**). In general, aryl halides bearing electron-withdrawing groups (EWG), such as carbonyls **56, 73-75**, nitriles **76-78**, nitro groups **79-82** and trifluoromethyl groups **83-84** could be converted into the corresponding phenols in high yields. Interestingly, amongst these substrates there did not appear to be a significant difference in yield between substrates that only differed in the nucleofuge. Conversely, substrates which did not contain an EWG were generally unsuccessful. For example, no reaction was observed using electronically unactivated aryl iodides (**85 and 87**), heteroaryl halides (**89 and 90**) or electron-rich aryl iodides (**91 and 92**).



Scheme 23. Overview of isolated yields of substrates examined. NMR yields were determined by ^1H NMR spectroscopic analysis of the crude reaction mixture using CH_2Br_2 as an internal standard.* - indicates reactions completed by other group members

To improve upon the apparent limitations of this reaction protocol, further optimisation studies were conducted using 4-iodobiphenyl **85** (Table 4). Pleasingly, it was found that simply increasing the temperature of the reaction to 80 °C could promote the formation of the phenol **93** (Entry 1). Increasing the temperature again to 100 °C further improved the yield of phenol **93** to

33% (Entry 2). Finally, changing the base to sodium *tert*-butoxide enabled phenol **93** to be formed in 47% yield.

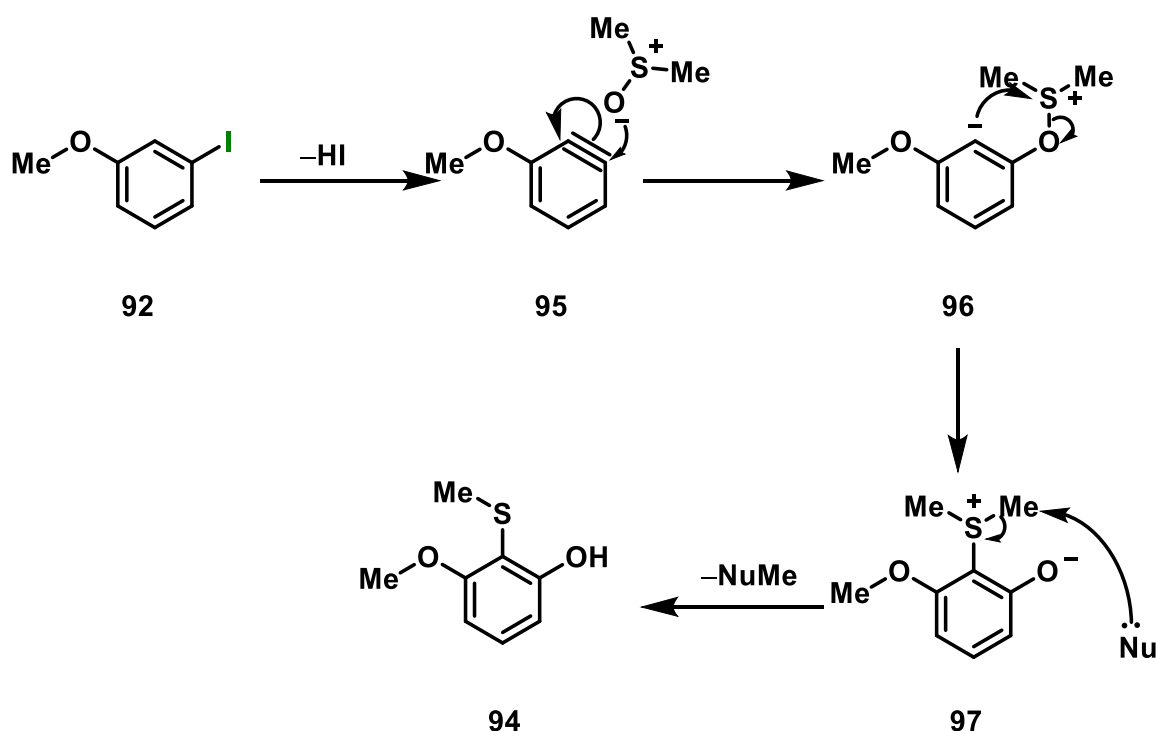


Entry	Base	Temp. / °C	Isolated yield / %
1	KO <i>t</i> -Bu	80	17
2	KO <i>t</i> -Bu	100	33
3	NaO <i>t</i> -Bu	100	47

Table 4. Effect on changing temperature and base on the conversion of 4-iodobiphenyl to a phenol.

Thus, using these more forcing conditions (100 °C, ^tBuONa) the reactivity of other previously challenging substrates was re-examined (**Scheme 24**). Under these conditions, both 4-iodo and 4-fluorobiphenyl **85** and **86** were converted into the phenol product in 34% and 76% isolated yield, respectively. Similarly, 1-iodonaphthalene **87** was now able to react at these elevated temperatures and form the phenol product in 54% yield. The same reaction conditions were also effective with 1-fluoronaphthalene **88**, which afforded the product in 84% yield. Next, bromoquinoline derivative **89** was similarly effective, giving a yield of phenol of 73%. Whereas another electron-rich aryl halide, 3-iodopyridine **90**, gave no conversion to a phenol. No conversion was also observed in another electron rich system, 4-iodoanisole **91**. The high temperatures required to drive these reactions could have been indicative of an S_NAr mechanism occurring.

would then split the S-O bond of the DMSO to generate **97**, when a methyl group was lost, probably from attack by a nucleophile, **94** would be formed.



Scheme 26. Mechanism of the formation of 3-methoxy-2-(methylthio)phenol from 3-iodoanisole via reaction of DMSO with benzyne intermediate. Mechanism for benzyne formation is uncertain.

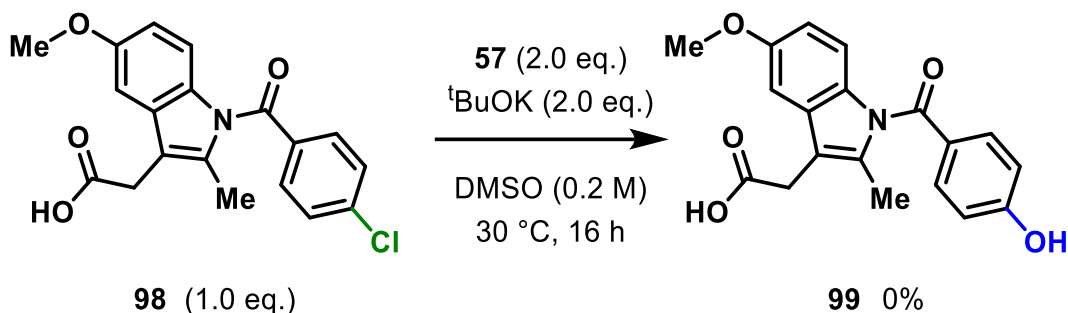
It is unclear why the reaction of this substrate may have led to a benzyne intermediate. It must have been a phenomenon unique to **92** out of all the substrates, as a mixture of regioisomers was not isolated for any of the other substrates. Which would have been observed, should a benzyne intermediate have been forming in these conditions for other substrates.

Hydroxylation of aryl halide drug molecules

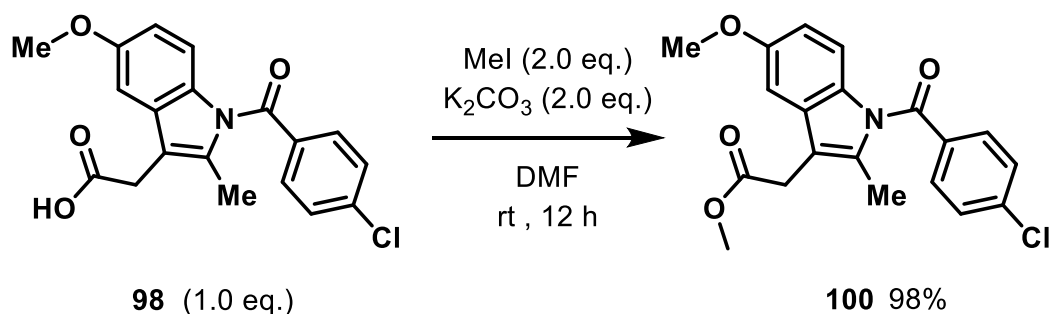
Considering the number of phenolic species that are present in pharmaceutical drugs, the compatibility of this hydroxylation protocol with more advanced synthetic intermediates was studied.

First, indomethacin **98**, and anti-inflammatory agent and an aryl halide drug derivative,^[74] was reacted under with oxime **57** and potassium *tert*-butoxide at 30 °C, but no product was detected (**Scheme 27**). It was rationalised that the most likely cause of this failure was the carboxylic acid group protonating the reactive oxime anion. Thus, indomethacin **98** was methylated with iodomethane to remove this acidic proton (**Scheme 28**). However, the methylated derivative **100**

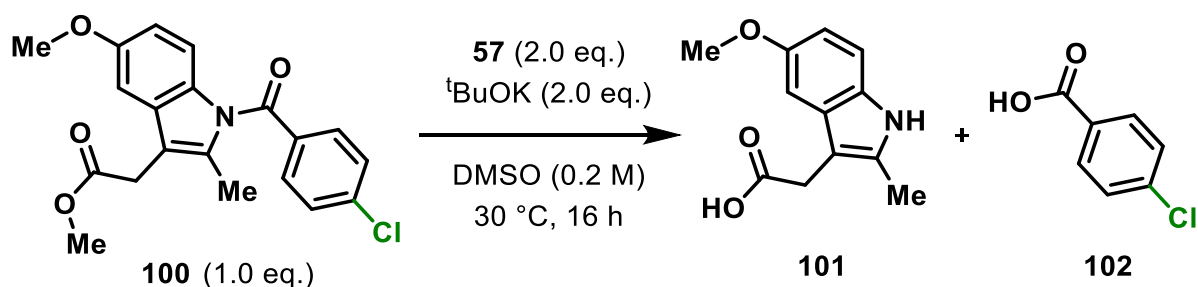
did not react to form the desired product, instead the main products of the reaction were 4-chlorobenzoic acid **101** and indole **102** (as evidenced by ¹H NMR and ESI-MS), which were presumably formed by the cleavage of the amide bond (**Scheme 29**).



Scheme 27. Reaction conditions for the attempted hydroxylation of indomethacin.



Scheme 28. Reaction protocol for the methylation of indomethacin.

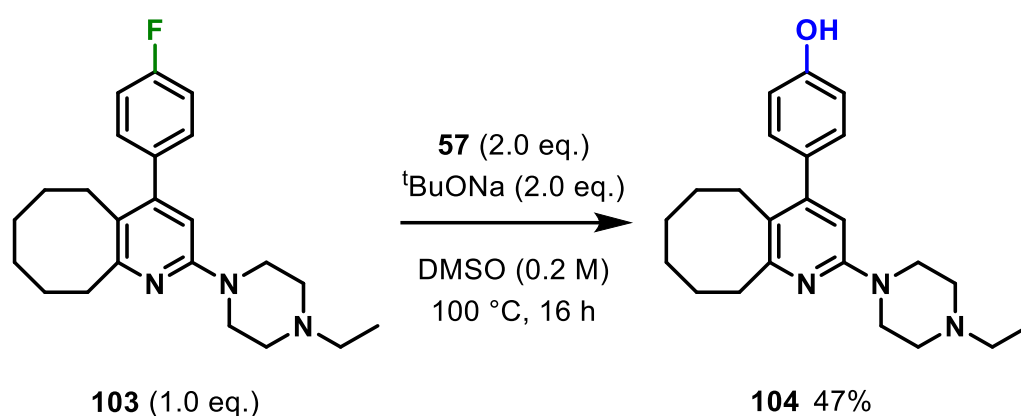


Scheme 29. Conditions for the attempted hydroxylation of methylated indomethacin.

The reaction was attempted at room temperature with photo stimulation in a light-box however the same cleavage of the C-N bond was observed. Suggesting this specific linkage was very intolerant to the other reagents.

Next, the reactivity of the antipsychotic agent blonanserin **103** was examined.^[75] Considering the successful reaction of 4-fluorobiphenyl **86** at higher reaction temperatures (100 °C, NaOt-Bu), these conditions were applied to **103**, which afforded phenol **104** in 47% yield (**Scheme 30**). The

structure of phenol **104** was also unambiguously confirmed by X-ray crystallography (**Figure 11**).



Scheme 30. Reaction protocol for the hydroxylation of blonanserine.

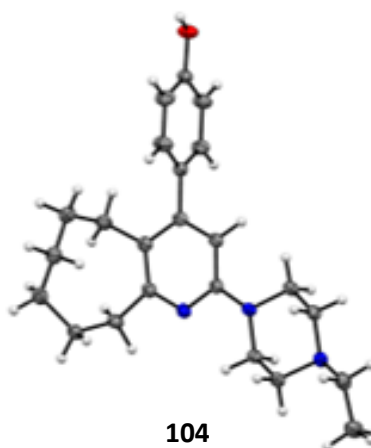
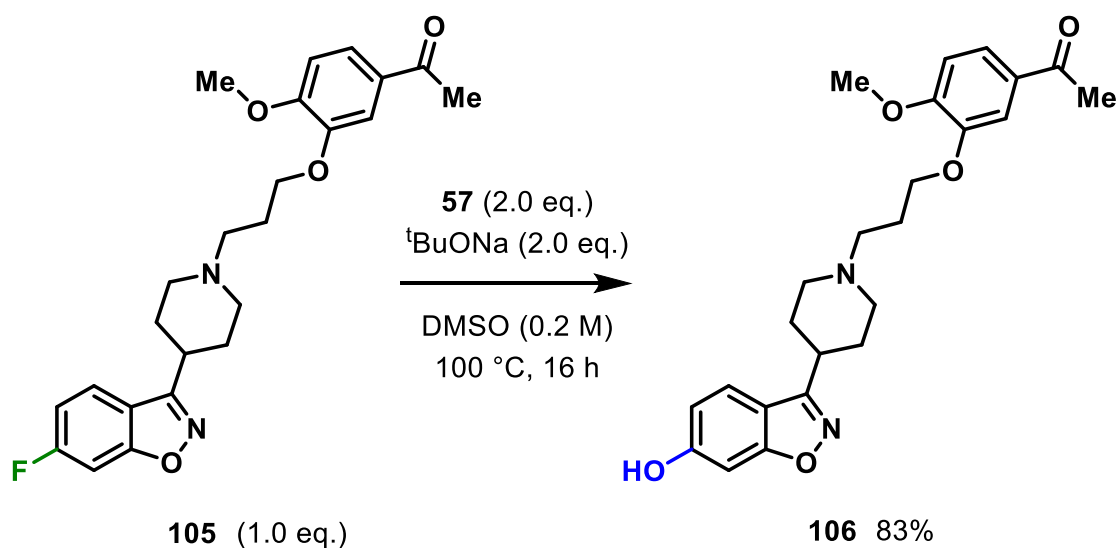


Figure 11. X-ray crystal structure of hydroxylated-blanserine.

Iloperidone **105** (schizophrenia treatment)^[76] was also converted into phenol **106** in 83% using these reaction conditions (**Scheme 31**).



Scheme 31. Reaction protocol for the hydroxylation of iloperidone.

It was then important to understand if these molecules were particularly suitable for conversion to phenols, or whether the conditions had been important to the success of the reactions. Therefore, blonanserine and iloperidone were attempted again, but at 60 °C with potassium *tert*-butoxide instead. They both worked but with reduced yields of 15% and 20% respectively, suggesting that both factors were true; the drug molecules were particularly suitable for the reaction and the conditions were vital for getting high yields.

Mechanistic studies

Considering the trends in reactivity that had been observed a $S_N\text{Ar}$ -type reaction mechanism seemed highly plausible for many of the substrates described. However not all the trends were supportive of a polar $S_N\text{Ar}$ mechanism. For example, *meta*-positioned EWGs do not facilitate $S_N\text{Ar}$ reactions as they cannot effectively stabilise the negative charge built-up through the addition of the nucleophile. Additionally, for many substrates examined there was no clear difference in reactivity between the different halogen nucleofuges.

To investigate whether these reactions were radical in nature, a number of substrates were reacted in the presence of radical scavengers or oxidising agents (**Figure 12**). With the assumption being that if the mechanism was dependent on the formation of radical species, the addition of these molecules would inhibit the reaction. Thus, TEMPO **107** and galvinoxyl **108** were selected as additives as they are both persistent radicals that have been frequently used to inhibit radical reactions.^[77]

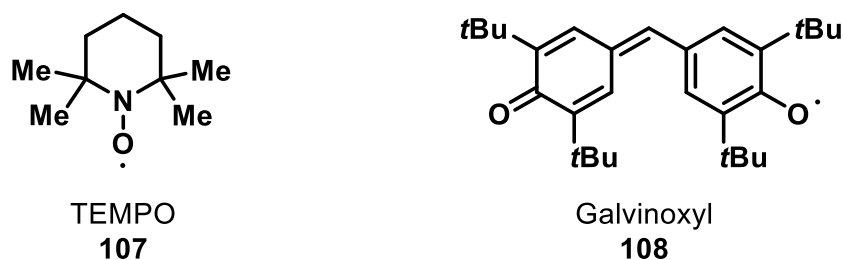
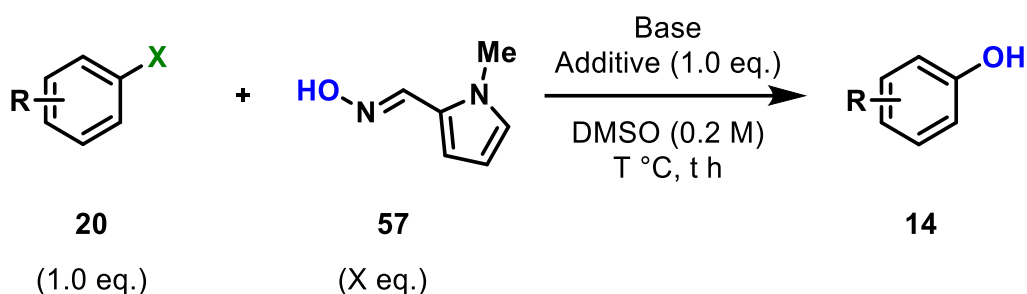


Figure 12. Structures of various radical inhibitors used

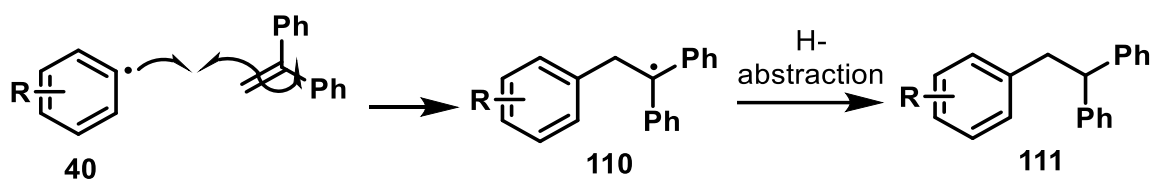
The reactivity of 4-iodo and 4-fluorobiphenyl **85** and **86** was examined in the presence of these additives (**Table 5**). Interestingly, there was a clear reduction in yield with the addition of these inhibitors. In particular, galvinoxyl was highly effective at inhibiting these reactions, potentially due to it having greater solubility in DMSO in comparison to TEMPO.^[78] From this data it was very likely that the mechanism of these reactions was radical in nature. However, no TEMPO or galvinoxyl trapped products could be detected in the crude reaction mixture by HRMS. It was anticipated that if an $S_{RN}1$ mechanism was operative, aryl radicals would rapidly couple with these additives to form products that could be detected by HRMS.



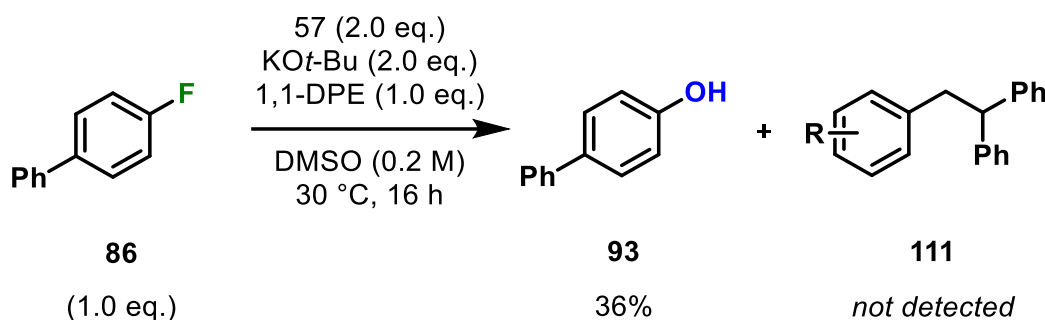
Additive		
None	57%	80%
TEMPO	13%	47%
galvinoxyl	6%	17%

Table 5. Effect on conversion in hydroxylation reactions in the presence of 1.0 eq. of radical scavengers or oxidising agents. Yields quoted are NMR yields of crude material using CH_2Br_2 internal standard. Conditions of reactions - 2.0 eq. **57**, $t\text{BuONa}$ 2.0 eq., 100 °C, 16 h.

Additional radical trapping studies were conducted using 1,1-diphenylethene (1,1-DPE) **109** an additive with 4-fluorobiphenyl **86** (**Scheme 33**), as again aryl radicals might rapidly add to this alkene to form **110**, which could then be detected by HRMS (**Scheme 32**). However, whilst the yield of phenol **14** was clearly reduced, no such species could be detected.



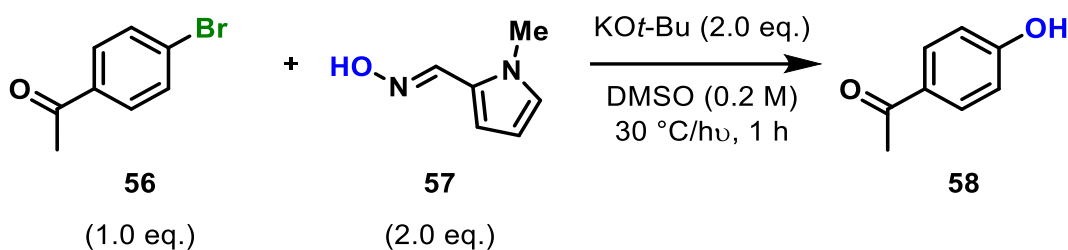
Scheme 32. Mechanism for the trapping of aryl radicals by 1,1-diphenylethene.



Scheme 33. Effect on conversion in hydroxylation reactions in the presence of 1.0 eq. of 1,1-DPE. Yields quoted are NMR yields of crude material using CH_2Br_2 internal standard. Detection of trapped material was monitored via ESI⁺-MS. Conditions were 2.0 eq. of oxime, 2.0 eq. of ^tBuOK, 30 °C for 16 h.

Having failed to detect an informative trapped product, investigations into the potential method of initiation were conducted. There was strong evidence throughout these studies that CTCs were forming as strongly coloured reaction mixtures were formed when the oxime anion and aryl substrates were mixed together in DMSO. In theory, the photochemical excitation of such a CTC should facilitate electron transfer, which would accelerate an $\text{S}_{\text{RN}}1$ reaction.

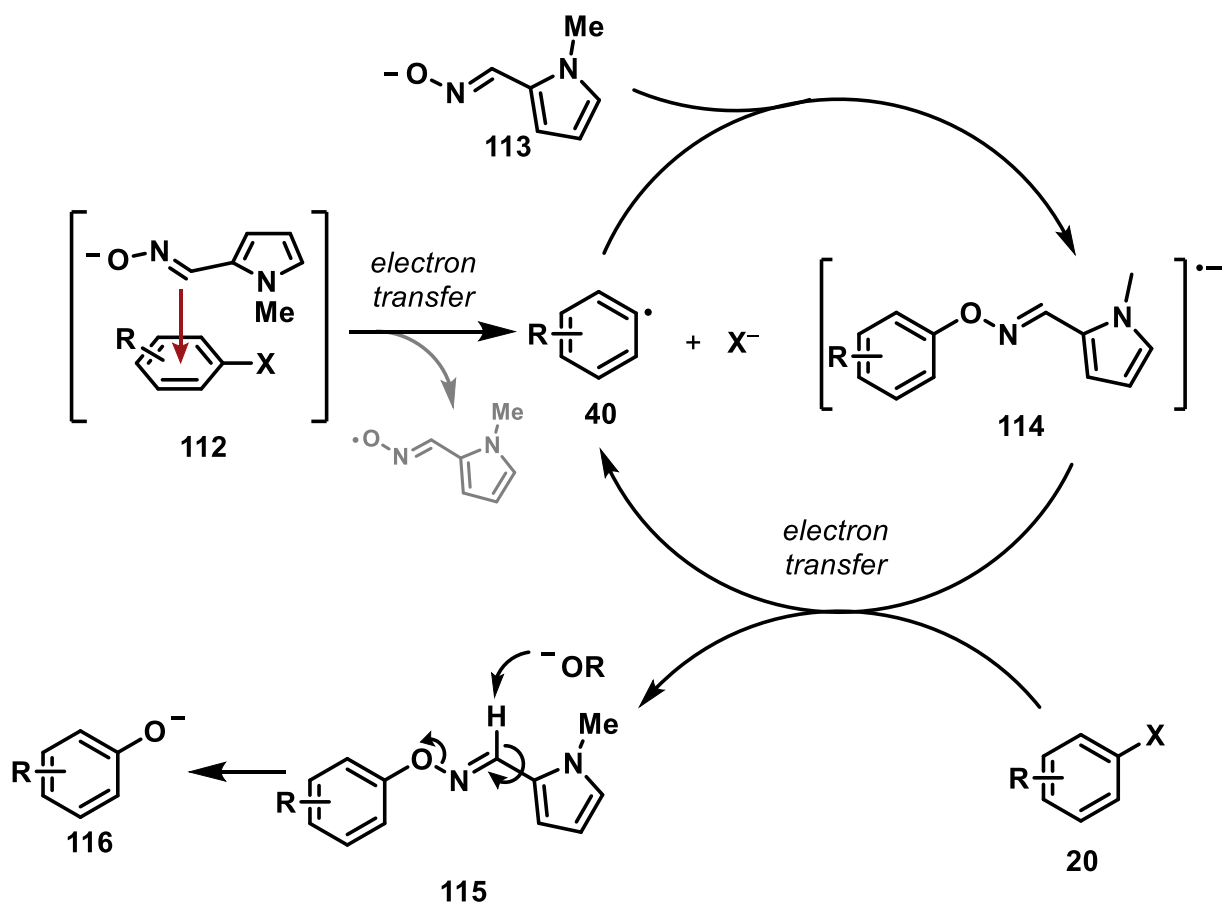
Thus, the effect of light on the conversion of 4'-bromoacetophenone **56** into phenol **58** was studied (**Table 6**). After one hour under the standard reaction conditions, phenol **58** was formed in 44% yield (Entry 1). Conversely, when the reaction vial was wrapped in foil to remove the effect of ambient light, there was a slight reduction in the yield of phenol **58** (38%, entry 2). This suggested that the reaction might proceed thermally but is accelerated by light. In support of this, a significantly increased yield was observed (65%) when the reaction mixture was irradiated with 455 nm light (Entry 4). These results provided further evidence that these transformations were radical in nature and likely initiated by thermal or photochemical activation of a CTC.



Entry	Conditions	Yield / %
1	30 °C, ambient light	44
2	30 °C, in darkness	38
3	rt, irradiation with 18 W 455 nm LEDs	65

Table 6. Effect on conversion in hydroxylation reactions of 4'-bromoacetophenone in different lighting conditions. Yields were determined by ^1H NMR spectroscopic analysis of the crude reaction mixture using CH_2Br_2 as an internal standard.

It is very likely that the exact mechanism for these reactions will change on a case-by-case basis, especially when higher reaction temperatures are used. However, considering all of the observations in this chapter and the other results disclosed in a recent publication of this work, a general $\text{S}_{\text{RN}}1$ mechanism may be proposed (**Scheme 34**).^[79] An aryl radical **40** may be formed through the thermal or photochemical activation of a CTC **112**. The aryl radical may then couple with oxime anion **113** to form an *O*-aryl oxime radical-anion intermediate **114**. Electron transfer from this reducing radical-anion to another equivalent of the aryl halide **20** would then regenerate an aryl radical **40** and form a neutral *O*-aryl oxime intermediate **115**. This neutral intermediate may then undergo an elimination reaction to form the phenolate product **116**.



Scheme 34. Proposed general mechanism for the hydroxylation of aryl halides through an $S_{RN}1$ radical chain.

Summary

A general and operationally simple reaction protocol for the hydroxylation of aryl halides was developed. Although at 30 °C only aryl halides that contained EWGs were able to react, this limitation could be circumvented by employing higher reaction temperatures. The functional group tolerance of this protocol was demonstrated through the hydroxylation of complex drug molecules. Mechanistic studies had been conducted which support the proposed $S_{RN}1$ mechanism.

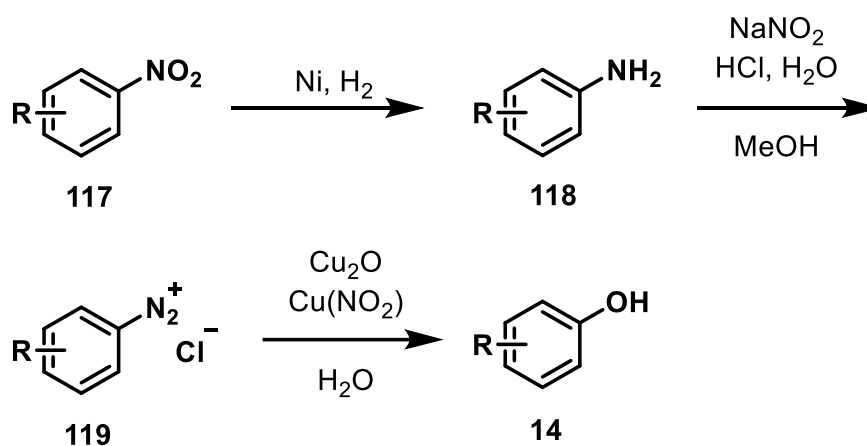
The work described in this Chapter was the subject of a recent publication.^[79]

Chapter 3. Denitrative Hydroxylation of Nitroarenes

Introduction

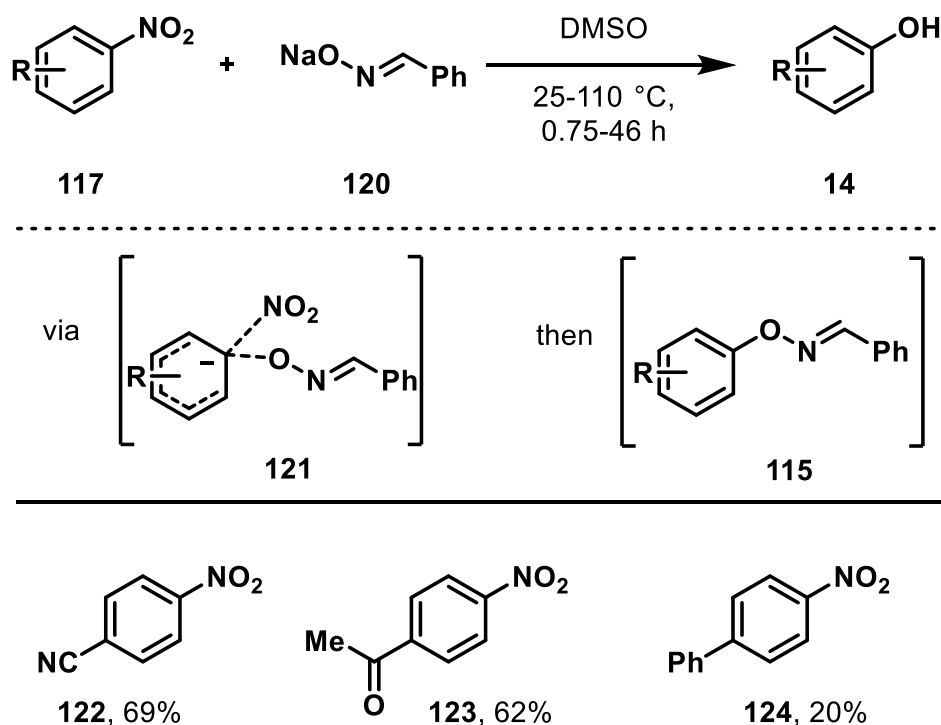
In comparison to aryl halide hydroxylation, general methods for the conversion of nitroarenes into phenols are rare. Whilst the denitrative substitution of nitroarenes is possible with very

electron-deficient substrates and hydroxides, these methods are far from general (2 examples reported to date).^[80,81] Therefore, arguably the most common method for the conversion of a nitroarene into a phenol is through the following three step process (**Scheme 35**): i) reduction of the nitroarene **117** to form an aniline **118** (e.g. via hydrogenation using a nickel catalyst);^[82] ii) conversion of the aniline **118** into a diazonium salt **119** (typically using sodium nitrite and hydrochloric acid)^[83]; iii) a Sandmeyer reaction can then be performed to hydroxylate the diazonium salt **119** (using copper oxide, copper nitrate and water).^[84] Finding an alternative synthetic method that can convert a nitroarene into a phenol in a single step would be a very attractive route. It would allow for a more straightforward synthesis and potentially improve the yield of phenol produced. Additionally, it would remove the need to synthesise the hazardous diazonium salt intermediate.



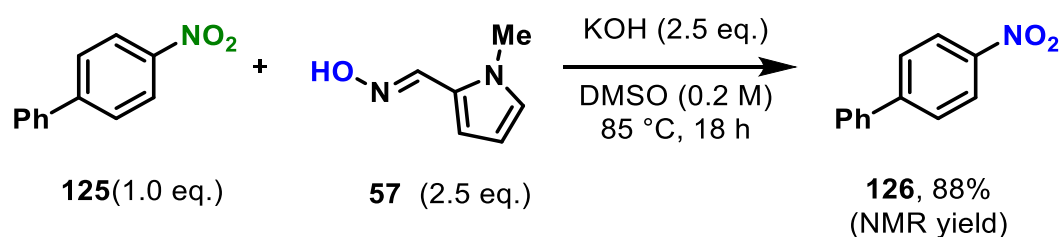
Scheme 35. Conversion of nitroarenes into phenols via diazonium salts. First step, reduction of nitro group to aniline using Ni-catalysed hydrogenation. Second step, formation of diazonium salt by using acidified sodium nitrite. Final step, Sandmeyer coupling to form phenol using cuprate complexes, driven by the release of nitrogen gas.

Alternatively, in 1974 Knudsen and Snyder showed that it may be possible to achieve a more direct approach using benzaldoxime anion **120** as a hydroxide surrogate (**Scheme 36**).^[85] A limited number of nitroarenes **117** were converted into phenols **14** in 20–94% yield. These reactions were proposed to proceed via an $S_{\text{N}}\text{Ar}$ mechanism involving the formation of a Meisenheimer complex **121** and the base-mediated elimination of an O-aryl intermediate **115**.



Scheme 36. Conversion of nitroarenes into phenols by using benzaldoxime as a nucleophile.

Considering the similarity of this approach to the work described in Chapter 2, the use of oxime **57** to promote and potentially generalise this transformation was targeted. Promising preliminary studies in this area revealed that phenol **126** could be formed in excellent yield (88% NMR yield, calculated by method using CH_2Br_2 internal standard) by reacting 4-nitrobiphenyl **125** with oxime **57** and potassium hydroxide in DMSO at 85 °C for 18 h (**Scheme 37**). Investigations to gain insight into the nature of the reaction mechanism were also targeted.

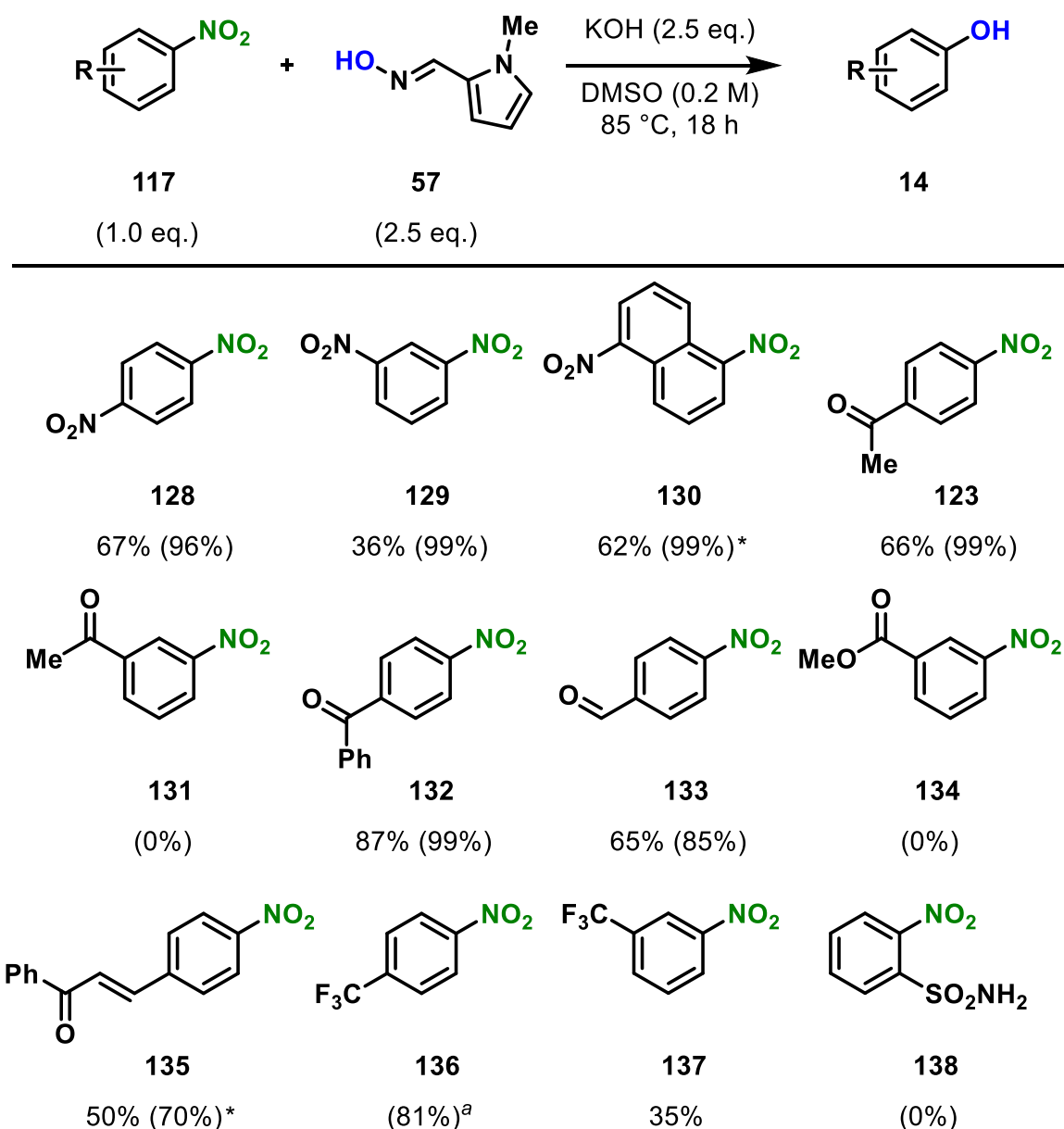


Scheme 37. Reaction scheme for the initial conditions used for converting 4-nitrobiphenyl to 4-phenylphenol.

Initial Scope

Building on this preliminary result, the reactivity of the other biphenyl nitroarene isomers **125**–**127** was examined (**Scheme 38**). Pleasingly, the phenol products **14** could all be isolated in 35–54% yield. However, it should be noted that whilst the yields determined by ^1H NMR

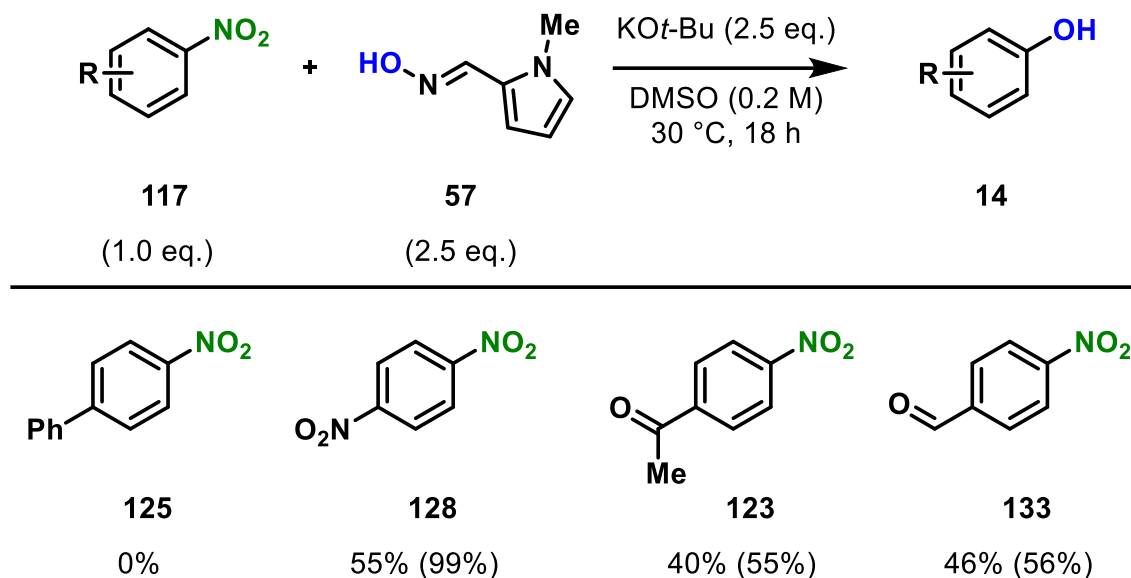
enough, or because the positioning in the *ortho*-position hindered any beneficial effect the group may have had.



Scheme 39. Yields hydroxylation of nitro substrates with an EWG substituent by oxime. Values quoted in brackets are yields that were determined by ^1H NMR spectroscopic analysis of the crude reaction mixture using CH_2Br_2 as an internal standard. ^a – reactions where NMR yield was obtained from ^{19}F NMR with 1-fluoronaphthalene as internal standard. * - indicates reactions completed by other group members

For comparison, the reactivity of a small selection of these substrates was also studied under the conditions employed in Chapter 2 (30 °C and using potassium *tert*-butoxide as the base) (**Scheme 40**). Interestingly, in contrast to 4-nitrophenyl **125**, the more electron-deficient nitroarenes

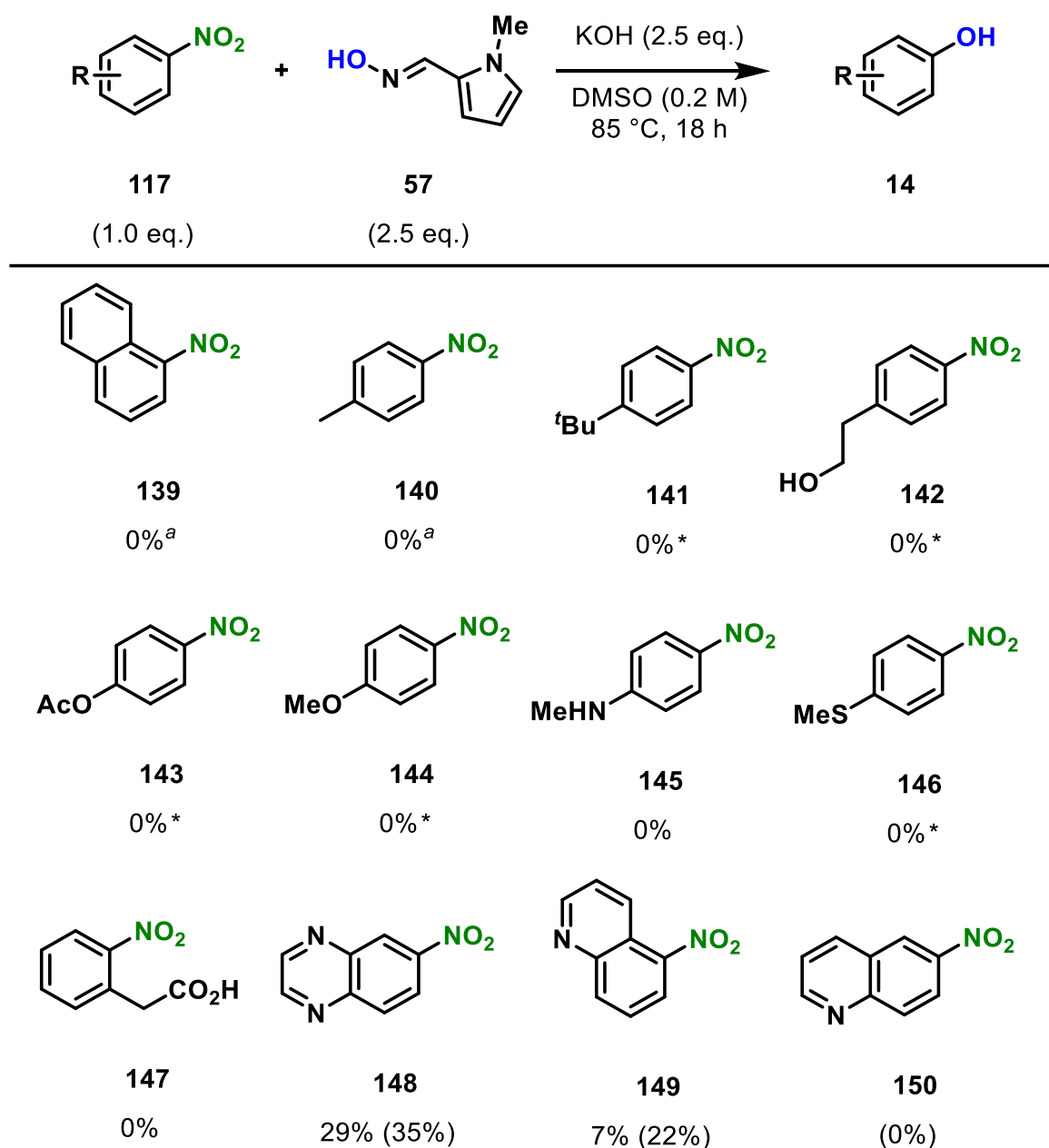
could also be converted into the corresponding phenols under milder reaction conditions, albeit in reduced yields.



Scheme 40. Isolated yields of crude material for reactions completed at 30 °C. Figures in brackets are yields that were determined by ^1H NMR spectroscopic analysis of the crude reaction mixture using CH_2Br_2 as an internal standard.

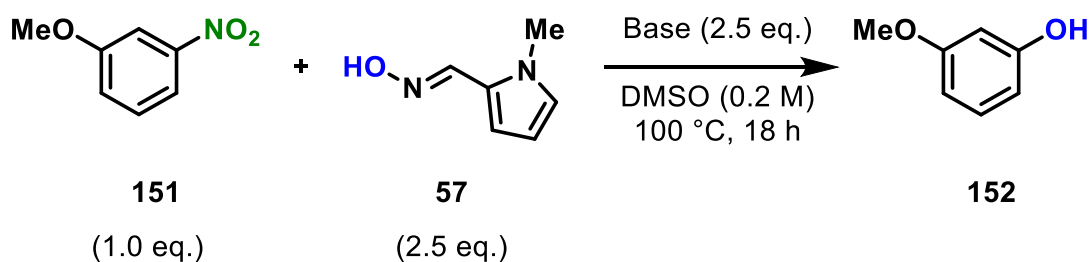
In addition to these, substrates lacking an EWG or including an EDG were also attempted (**Scheme 41**). Unlike the halide reactions 1-nitronaphthalene **139** did not hydroxylate, although an elevated temperature may have given better results. In addition to those, the substrates containing only simple alkyl substituents **140-141** also gave no conversion to the hydroxyl product. Additionally, 2-hydroxy-1-(4-nitro)phenyl ethane **142** gave no conversion. The expected product of 4-acetoxynitrobenzene **143** was also not observed, although this could have been due to cleavage of the acetate ester leading to a different product forming. It was also difficult to determine if the EDG nature of the substituent lowered the reactivity of the substrate, or if the ester linkage was incompatible. Since all of the other substrates that contained EDGs **144-146** also did not show any conversion, it could have been assumed the former reason was the most likely. The carboxylic acid 2-(2-nitro)phenylacetic acid **147** also gave no conversion. However, this could have been because deprotonation of the carboxylic acid group could have interfered with the reactivity of the species. Heteroaromatic substrates such as 5-nitroquinoline **148** were able to successfully react to form the desired product. Interestingly, 6-nitroquinoline **149**

was able to form a small amount of product, whereas 5-nitroquinoline **150** didn't form any product.



Scheme 41. Yields hydroxylation of nitro substrates with an EDG or neutral substituent by oxime. Yields were determined by ¹H NMR spectroscopic analysis of the crude reaction mixture using CH₂Br₂ as an internal standard. * - indicates reactions completed by other group members

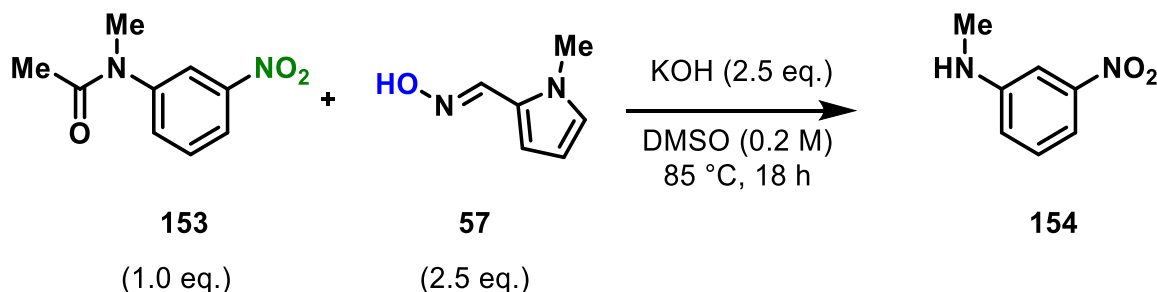
Attempts to force 3-nitroanisole **151** to react were also briefly explored. In addition to raising the temperature the base was switched to a sodium base, given that the aryl halide work had indicated sodium bases were more effective at higher temperatures (**Table 7**). Neither the reaction with sodium hydroxide or sodium *tert*-butoxide yielded any product.



Base	Yield / %
NaOH	0
^t BuONa	0

Table 7. NMR yields of the reaction scheme above with differing bases. Yields were determined by ^1H NMR spectroscopic analysis of the crude reaction mixture using CH_2Br_2 as an internal standard.

The final reaction attempted was on *N*-methyl-3-nitroacetanilide **153** (Scheme 42). Rather than the desired phenol forming, the reaction instead led to the cleavage of the amide linkage to yield the amine **154**.



Scheme 42. Reaction scheme for the cleavage of the amide bond in *N*-methyl-3-nitroacetanilide.

Mechanistic studies

It appeared that this denitrative hydroxylation reaction protocol followed similar trends to that observed with aryl halides in Chapter 2. Thus, the possibility of another radical-based mechanism seemed likely. However, it should be noted that it has been strongly debated whether nitroarenes are compatible substrates with the previously proposed $\text{S}_{\text{RN}}1$ mechanism as the cleavage of the radical-anion $\text{C}(\text{sp}^2)\text{-NO}_2$ bond is thermodynamically unfavourable.^[86]

Radical inhibition studies were achieved using radical traps TEMPO and galvinoxyl and persulfate oxidising agents (Figure 13). With the assumption being that if the mechanism was

dependent on the formation of radical species, the addition of these molecules would quench the reaction.

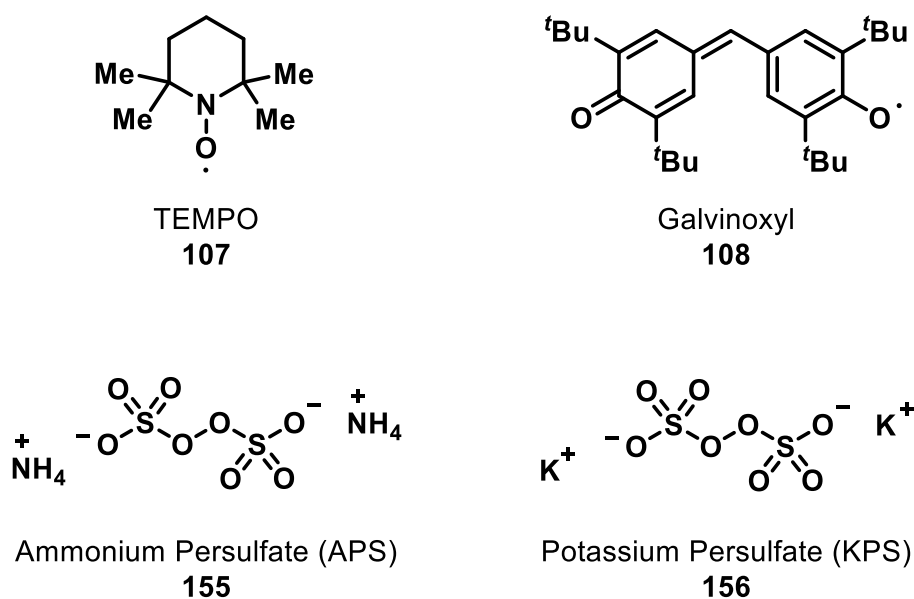
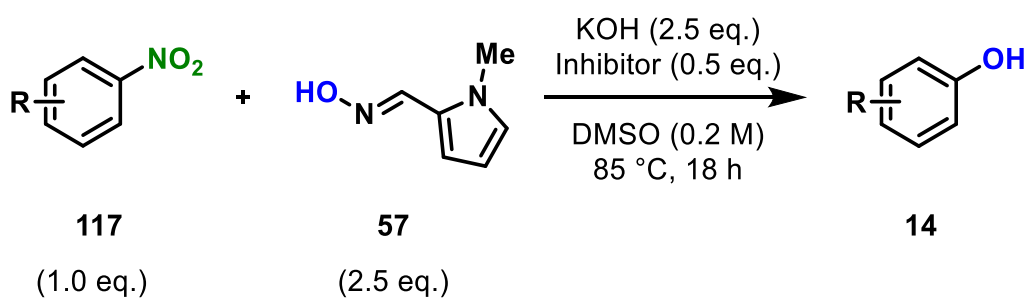


Figure 13. Structures of various radical inhibitors used

TEMPO and galvinoxyl were selected as additives as they are both persistent radicals that have been frequently used as radical trapping reagents in literature. Persulfate salts are known to act as electron traps,^[87] therefore it was believed they could also act as electron acceptors and inhibit a radical reaction.

Radical inhibition studies were conducted on successful substrates from the previous substrate scope, by adding of 0.5 equivalents of the shown inhibitors under the same reaction conditions (Table 8). The data showed a significant drop in yield between the reactions that contained no additives and those that did. This indicated that these reagents did quench the reaction, suggesting the present of reactive radical species were part of the reaction mechanism, however no trapped species were detected by HRMS to support this.



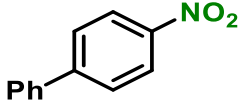
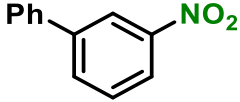
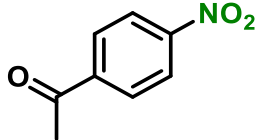
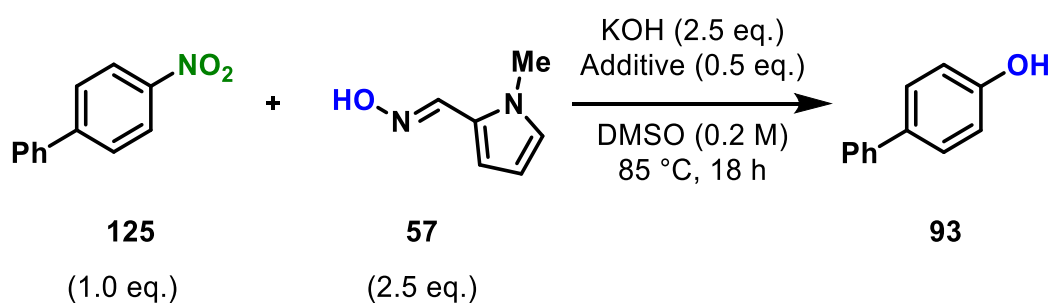
Inhibitor			
None	88%	99%	99%
TEMPO	66%	57%	30%
galvinoxyl	63%	54%	28%
APS	4%	1%	13%
KPS ^a	26%	21%	33%

Table 8. Effect on conversion in hydroxylation reactions in the presence of 0.5 eq. of radical scavengers or oxidising agents. Yields were determined by ¹H NMR spectroscopic analysis of the crude reaction mixture using CH₂Br₂ as an internal standard. ^a – indicates only 0.2 eq. of additive was used.

Further inhibition studies were conducted using 4-nitrophenyl **125** and alkene additives (cyclohexene, 1,4-cyclohexadiene and 1,1-DPE) in an attempt to trap any intermediate radical species (**Table 9**). Note: 1,4-cyclohexadiene may also intercept aryl radicals by reacting as a H-atom donor (**Scheme 43**). Clear inhibition was observed in all cases but no trapped intermediates could be detected by HRMS or ¹H NMR spectroscopic analysis of the crude reaction mixtures. Finally, when the same reaction was performed without degassing before heating the reaction mixture, an NMR yield of only 35% was obtained. This suggested that diatomic oxygen in the air was able to inhibit the reaction.

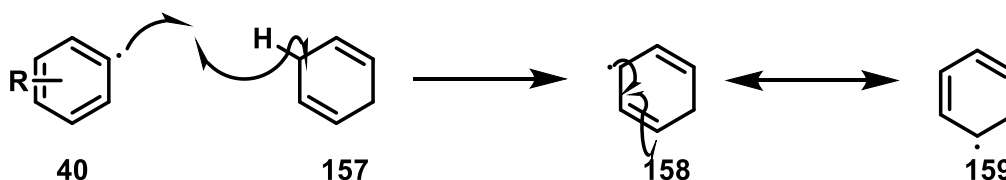


Additive	Yield / %
None	88
Cyclohexene	61
1,4-Cyclohexadiene	41
1,1-DPE	36

Without de-gassing

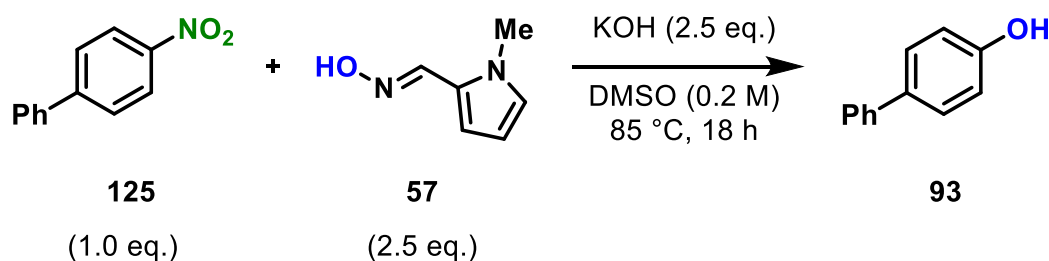
35

Table 9. Effect on conversion in hydroxylation reactions in the presence of 0.5 eq. of cyclohexenes. Yields were determined by ^1H NMR spectroscopic analysis of the crude reaction mixture using CH_2Br_2 as an internal standard.



Scheme 43. Mechanism for the quenching of aryl radicals by hydrogen abstraction from cyclohexenes.

As with the aryl halides in Chapter 2, strongly coloured reaction mixtures were observed when the oxime anion and nitroarene substrates were mixed together in DMSO (indicative of CTC formation). Therefore, the effect of light on the reaction of 4-nitrobiphenyl **125** was studied (**Table 10**). A significant reduction in the yield of phenol **93** was observed when the reaction was performed in the dark compared to when the reaction was exposed to ambient light from the laboratory (35% vs 88% yield, respectively).



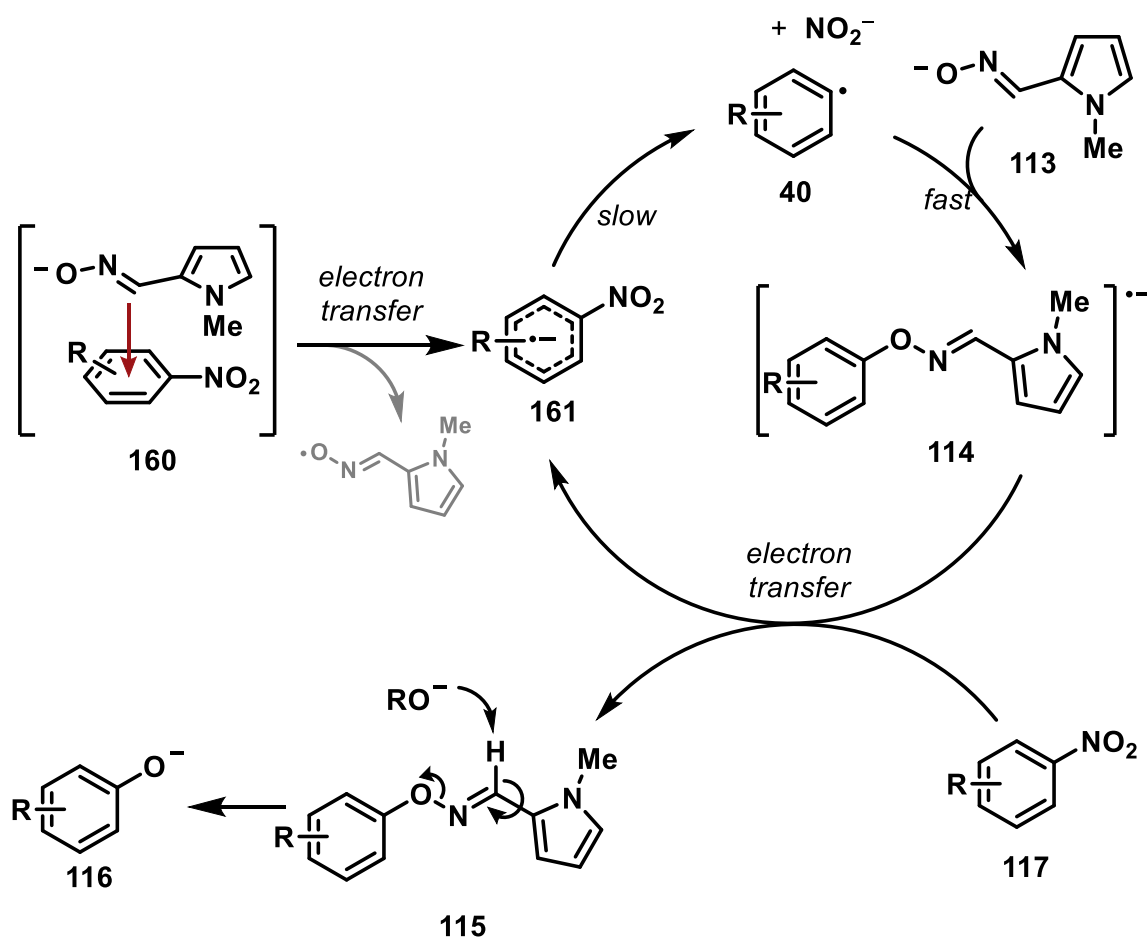
Conditions	Yield / %
Ambient light	88
Dark	35

Table 10. Effect on conversion in hydroxylation reactions of 4-nitrobiphenyl in different lighting conditions. Yields were determined by ^1H NMR spectroscopic analysis of the crude reaction mixture using CH_2Br_2 as an internal standard.

All of the above experiments strongly suggested that the mechanism of this nitroarene hydroxylation reaction was radical in nature. There are a number of mechanistic possibilities that

have been proposed for related denitrative substitution reactions, but it is difficult to propose a single mechanism with the current experimental data.

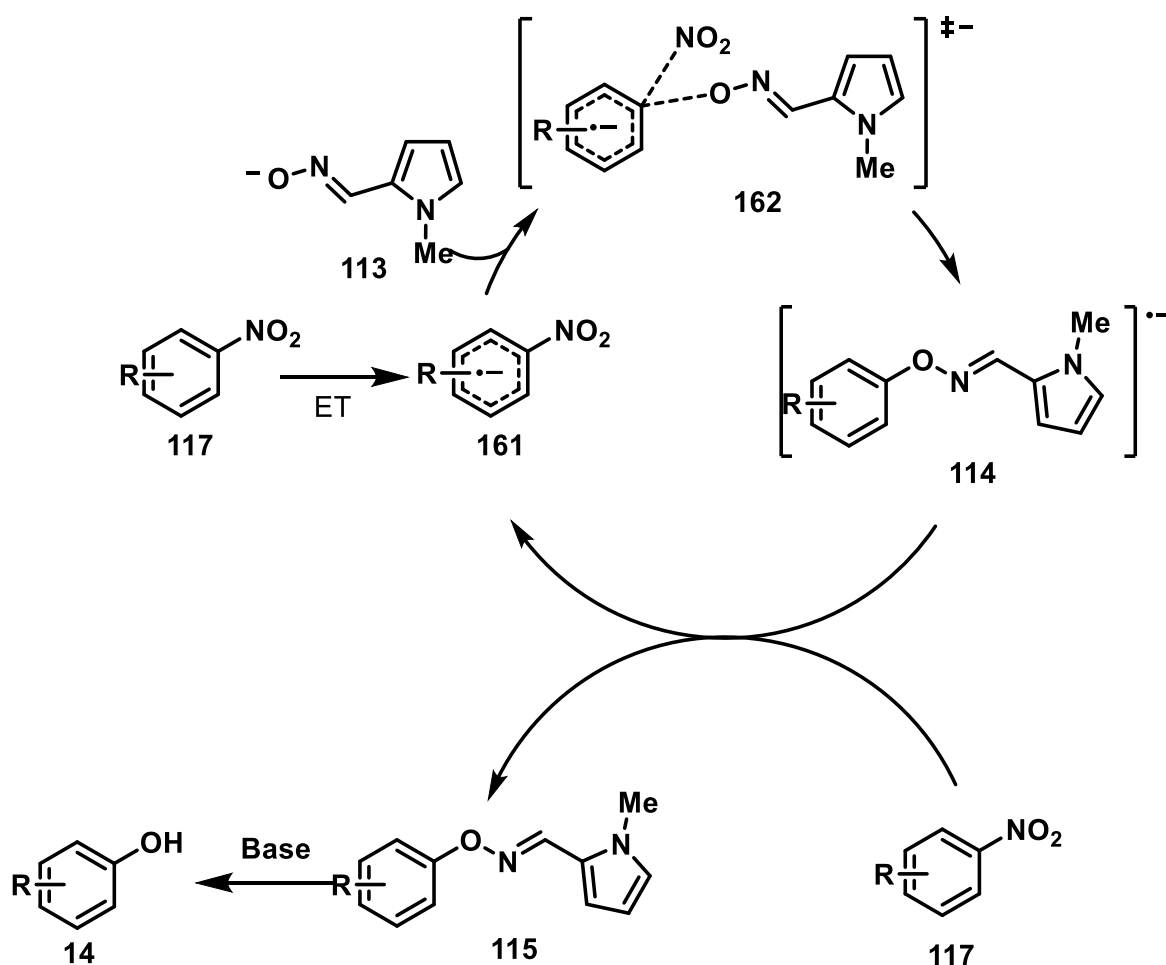
The first possibility is another radical chain $S_{RN}1$ mechanism (**Scheme 44**). In which, a radical anion **161** would be formed through the thermal or photochemical activation of a CTC **160**. The $C(sp^2)-NO_2$ bond of radical-anion **161** may then slowly cleave to afford aryl radical **40**. Aryl radical **40** could then couple with oxime anion **113** to form *O*-aryl oxime radical-anion intermediate **114**. Electron transfer from **114** to a nitroarene **117** would then regenerate radical anion **161** and form a neutral *O*-aryl oxime intermediate **115**, which would undergo a base-mediated elimination to form the phenolate product **116**.



Scheme 44. Possible $S_{RN}1$ mechanism for the hydroxylation of nitroarenes.

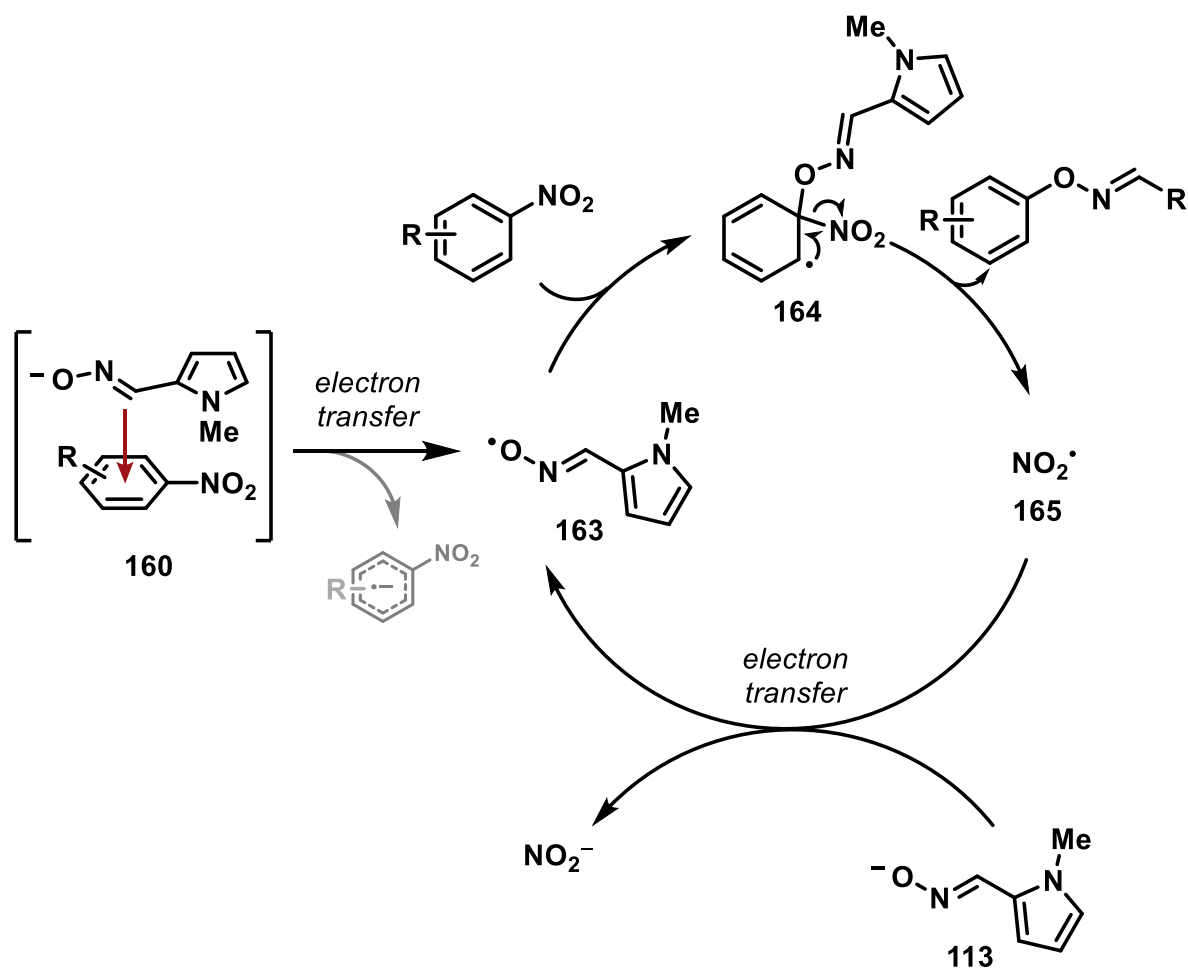
Another possibility is the controversial $S_{RN}2$ mechanism, which has been proposed for slow cleaving radical-anion species (**Scheme 45**).^[88] This mechanism is very similar to the $S_{RN}1$ mechanism, but the key difference in the $S_{RN}2$ mechanism is that the oxime anion would react directly with radical-anion intermediate **161** to displace the nitro group in a single concerted step.

However, this mechanism is generally considered very unlikely based on the strong coulombic repulsion between the two negatively charge species.^[86]



Scheme 45. Possible $S_{RN}2$ mechanism for the hydroxylation of nitroarenes.

More recently it has been proposed that oxygen-centred radicals may be able to directly substitute nitroarenes via homolytic aromatic *ipso* substitution.^[89] Here, the oxime radical generated through the thermal or photochemical activation of a CTC **160** would be the key reactant (**Scheme 46**). Oxime radical **163** could then add to the nitroarene at the *ipso* position to form radical intermediate **164**, which would rapidly rearomatise to form neutral *O*-aryl oxime **115** by ejecting the NO_2^\bullet radical **165**. Electron transfer from oxime anion **113** to **165** would then form nitrite anion and regenerate oxime radical **163**.



Scheme 46. Proposed homolytic aromatic *ipso* substitution mechanism for the hydroxylation of nitroarenes.

Further studies are required to determine if any of these potential reaction mechanisms are operative. For example, computational analysis, EPR spectroscopy or additional radical trapping experiments could all provide important clues about the identity of the mechanism.

The identification of the mechanism as $\text{S}_{\text{RN}}1$, raised a significant question over why the only substrates to hydroxylate included EWGs. The lower yields of EWG *meta*-substituted species was attributed to the orbital coefficients of those species. In *meta*-substituted aryl halides, the orbital coefficients of the π^* -orbital would have been very low on the C-X carbon atom (**Figure 14**).^[90] Therefore there could only have been very poor overlap between the π^* -orbital of the aromatic ring and the σ^* -orbital of the C-X bond. Electron transfer to this orbital would have therefore been very slow, and hence the rate of aryl radical formation would have been slow. This effect was most clearly observed in the acetophenone species. Since carbonyls are very strongly electron-withdrawing, it could have been inferred that the orbital coefficient of the nucleofuge

carbon was close to zero. Although why the effect was not observed to the same extent in *meta*-nitro substituted species was uncertain, given they have even greater electron-withdrawing capacity.^[91] This could also be used to explain why *para*-EWG substrates were able to react so well, since the orbital coefficient on that carbon would have been higher.

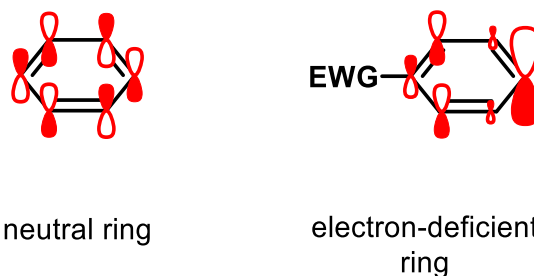


Figure 14. Difference in orbital coefficients of the π^* -orbital between neutral benzene ring and benzene ring with electron-withdrawing groups.

Summary

A general and operationally simple reaction protocol for the hydroxylation of aryl halides was developed. Although at 30 °C only aryl halides that contained EWGs were able to react, this limitation could be circumvented by employing higher reaction temperatures. The functional group tolerance of this protocol was demonstrated through the hydroxylation of complex drug molecules. Mechanistic studies had been conducted which support the proposed $S_{RN}1$ mechanism.

Chapter 4. Experimental

General Information

Except where stated, all reagents and anhydrous solvents were purchased from commercial sources and used without further purification.

NMR spectra were recorded on a Bruker AVIII300NB, JEOL ECX400, JEOL ECS400, or Bruker AVIIIHD500 spectrometer. All spectral data was acquired at the stated temperature. Chemical shifts (δ) are quoted in parts per million (ppm). The following residual solvent signals were used as references for ^1H and ^{13}C NMR spectra: δ_{H} 7.26 and δ_{C} 77.0 for CDCl_3 , and δ_{H} 2.50 ppm, δ_{C} 39.52 ppm for DMSO-d_6 . Coupling constants (J) are reported in Hertz (Hz) to the nearest 0.1 Hz. The multiplicity abbreviations used are: s singlet, d doublet, t triplet, q quartet, m multiplet.

Infrared (IR) spectra were recorded on a PerkinElmer UATR 2 spectrometer as a thin film dispersed from CH_2Cl_2 or CDCl_3 . The wave numbers (ν) of recorded IR-signals are quoted in cm^{-1} .

High-resolution mass-spectra were obtained by the University of York Mass Spectrometry Service, using electrospray ionisation (ESI) on a Bruker Daltonics, Micro-tof spectrometer.

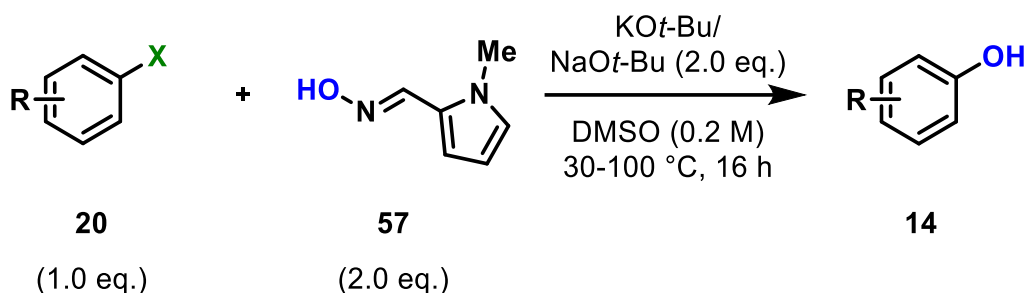
Thin layer chromatography was carried out on Merck silica gel 60F₂₅₄ pre-coated aluminium foil sheets and were visualised using UV light (254 nm) and stained with basic aqueous potassium permanganate. Column chromatography was carried out using Fluka silica gel (SiO_2), 35–70 μm , 60 Å under a light positive pressure, eluting with the specified solvent system.

No melting point data for these compounds was obtained as the majority of the target molecules had well documented spectroscopic data in the literature, which was believed to be a sufficient basis for accurate conformation of the identity of synthesised molecules.

All photochemical reactions were conducted in a fan cooled EvoluChem PhotoRedOx Box reactor using commercial LEDs purchased from HepatoChem Inc.

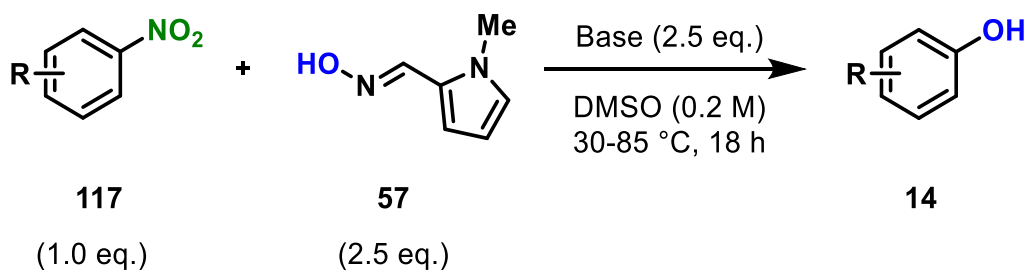
General Procedures

General Procedure A



To an oven-dried screwcap 8 mL reaction vial was charged base (2.0 eq.), oxime **57** (2.0 eq.), and the aryl halide substrate **20** (0.30 mmol, 1.0 eq.). To the solids was added a magnetic stir bar, anhydrous DMSO (1.5 mL). The vial was closed, and the reaction mixture was sparged with N₂ for 15 minutes, then sealed with parafilm. The reaction mixture was stirred and heated at the specified temperature in a metal heating block for the stated time. The mixture was then diluted with CH₂Cl₂ or EtOAc (20 mL), poured into a mixture of water (10 mL) and brine (5 mL), then acidified with 10% aq. HCl (~1 mL). The organic phase was collected, and the aqueous phase was extracted with CH₂Cl₂ or EtOAc (3 × 20 mL). The organics were combined, dried (MgSO₄), and concentrated under reduced pressure. The NMR yield of the reaction was determined at this point; CH₂Br₂ (1.0 eq.) was added to the crude mixture and the sample submitted for a ¹H NMR analysis. In the resulting spectrum, the signal for CH₂Br₂ (4.95 ppm) was integrated and set to 2H, allowing for a quantitative estimate of the yield of the reaction when the peaks corresponding to product were integrated in the spectrum. The crude product was then purified by column chromatography to afford the phenol product **14**.

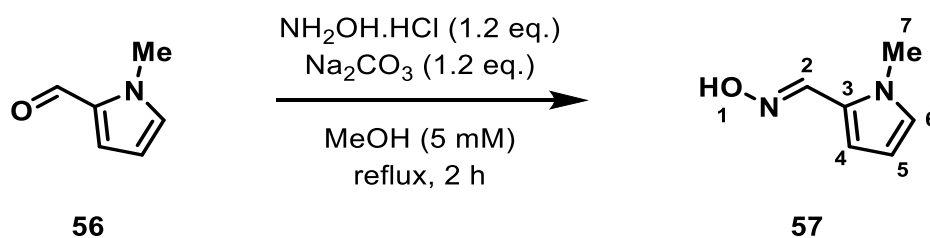
General Procedure B



To an oven-dried screwcap 8 mL reaction vial was charged base (2.0 eq.), oxime **57** (2.0 eq.), and the nitroarene substrate **117** (0.30 mmol, 1.0 eq.). To the solids was added a magnetic stir bar, anhydrous DMSO (1.5 mL). The vial was closed, and the reaction mixture was sparged with

N₂ for 15 minutes, then sealed with parafilm. The reaction mixture was stirred and heated at the specified temperature in a metal heating block for the stated time. The mixture was then diluted with CH₂Cl₂ or EtOAc (20 mL), poured into a mixture of water (10 mL) and brine (5 mL), then acidified with 10% aq. HCl (~1 mL). The organic phase was collected, and the aqueous phase was extracted with CH₂Cl₂ or EtOAc (3 × 20 mL). The organics were combined, dried (MgSO₄), and concentrated under reduced pressure. The NMR yield of the reaction was determined at this point; CH₂Br₂ (1.0 eq.) was added to the crude mixture and the sample submitted for a ¹H NMR analysis. In the resulting spectrum, the signal for CH₂Br₂ (4.95 ppm) was integrated and set to 2H, allowing for a quantitative estimate of the yield of the reaction when the peaks corresponding to product were integrated in the spectrum. The crude product was then purified by column chromatography to afford the phenol product **14**.

N-methyl-2-pyrrole carboxaldehyde oxime (**57**)



To a stirred solution of NH₂OH·HCl (1.67 g, 24.0 mmol) and Na₂CO₃ (2.54 g, 24.0 mmol) in MeOH (100 mL) was added *N*-methyl-2-pyrrolecarboxaldehyde (2.15 mL, 20.0 mmol). The mixture was then heated to reflux and stirred for 2 hours. The reaction was allowed to cool to room temperature and MeOH was removed under reduced pressure. The residue was dissolved in EtOAc (50 mL) and H₂O (50 mL). The organic phase was separated and the aqueous phase was extracted with EtOAc (2 × 50 mL). The organics were combined, washed with brine (20 mL), dried (MgSO₄), and concentrated under reduced pressure. The crude product was dissolved in a minimum amount of CH₂Cl₂ and purified by column chromatography (30% EtOAc + 3% Et₃N in hexane) to afford the title compound **57** (2.12 g, 17.1 mmol, 86%) as a white solid (AJG-01-073).

R_f 0.45 (30% EtOAc in hexane);

ATR-FTIR (thin film) ν_{max}/cm⁻¹ 3312, 1619, 1482, 1416, 1309, 1057, 948, 817, 730;

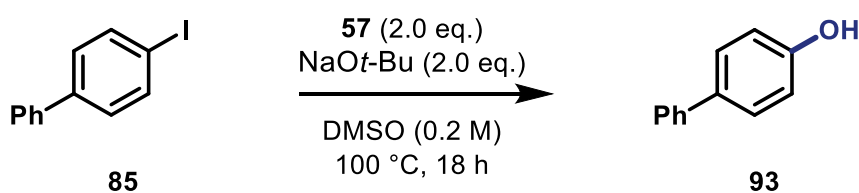
¹H NMR (300 MHz, DMSO-*d*₆) δ_H 10.71 (s, 1H, H-2), 8.03 (s, 1H, H-1), 6.85 (dd, J = 2.6, 1.8 Hz, 1H, H-4/5/6), 6.32 (dd, J = 3.7, 1.8 Hz, 1H, H-4/5/6), 6.02 (dd, J = 3.7, 2.6 Hz, 1H, H-4/5/6), 3.73 (s, 3H, H-7);

^{13}C NMR (101 MHz, DMSO- d_6) δ_{C} 141.5 (CH, C-2), 126.5 (CH, C-4/5/6), 125.6 (C, C-3), 112.4 (CH, C-4/5/6), 107.8 (CH, C-4/5/6), 35.9 (CH₃, C-7).

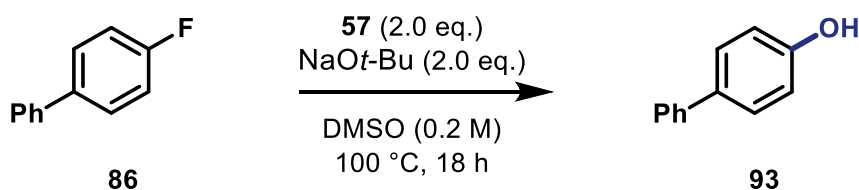
HRMS (ESI⁺) m/z calcd. for C₆H₉N₂O (M + H)⁺ 125.0709, found 125.0712.

Spectroscopic data matched those reported in the literature.^[66]

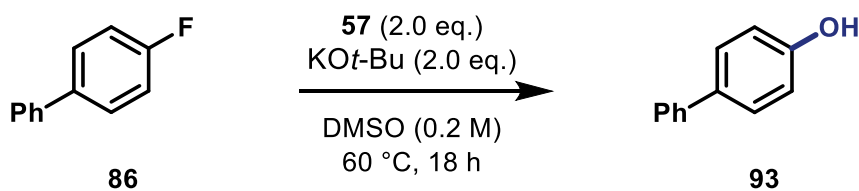
4-Phenylphenol (**93**)



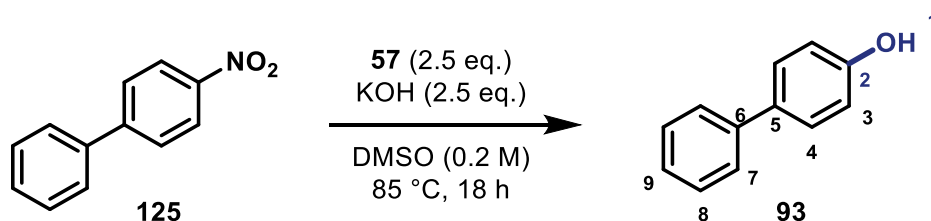
Synthesized using **General Procedure A** with sodium *tert*-butoxide (57.7 mg, 0.60 mmol, 2.0 eq.), oxime **57** (74.5 mg, 0.60 mmol, 2.0 eq.), 4-iodobiphenyl **85** (84.0 mg, 0.30 mmol, 1.0 eq.) in DMSO (1.5 mL). The reaction was heated at 100 °C and stirred for 18 h. The crude product was dissolved in a minimum amount of CH₂Cl₂, dried onto silica gel and purified by column chromatography (90% CH₂Cl₂ in hexane) to afford 4-phenylphenol **93** (17.3 mg, 0.10 mmol, 34%) as an off-white solid (AJG-01-055).



Synthesized using **General Procedure A** with sodium *tert*-butoxide (57.7 mg, 0.60 mmol, 2.0 eq.), oxime **57** (74.5 mg, 0.60 mmol, 2.0 eq.), 4-fluorobiphenyl **86** (51.7 mg, 0.30 mmol, 1.0 eq.) in DMSO (1.5 mL). The reaction was heated at 100 °C and stirred for 18 h. The crude product was dissolved in a minimum amount of CH₂Cl₂, dried onto silica gel and purified by column chromatography (90% CH₂Cl₂ in hexane) to afford 4-phenylphenol **93** (38.6 mg, 0.21 mmol, 76%) as an off-white solid (AJG-01-056).



Synthesized using **General Procedure A** with potassium *tert*-butoxide (67.3 mg, 0.60 mmol, 2.0 eq.), oxime **57** (74.5 mg, 0.60 mmol, 2.0 eq.), 4-fluorobiphenyl **86** (51.7 mg, 0.30 mmol, 1.0 eq.) in DMSO (1.5 mL). The reaction was heated at 60 °C and stirred for 18 h. The crude product was dissolved in a minimum amount of CH₂Cl₂, dried onto silica gel and purified by column chromatography (90% CH₂Cl₂ in hexane) to afford 4-phenylphenol **93** (24.7 mg, 0.15 mmol, 48%) as an off-white solid (AJG-01-085).



Synthesized using **General Procedure B** with potassium hydroxide (42.1 mg, 0.75 mmol, 2.5 eq.), oxime **57** (93.1 mg, 0.75 mmol, 2.5 eq.), 4-nitrobiphenyl **125** (59.8 mg, 0.30 mmol, 1.0 eq.) in DMSO (1.5 mL). The reaction was heated at 85 °C and stirred for 18 h. The crude product was dissolved in a minimum amount of CH₂Cl₂, dried onto silica gel and purified by column chromatography (90% CH₂Cl₂ in hexane) to afford 4-phenylphenol **93** (27.8 mg, 0.16 mmol, 54%) as an off-white solid (AJG-01-004).

R_f 0.30 (80% DCM in hexane);

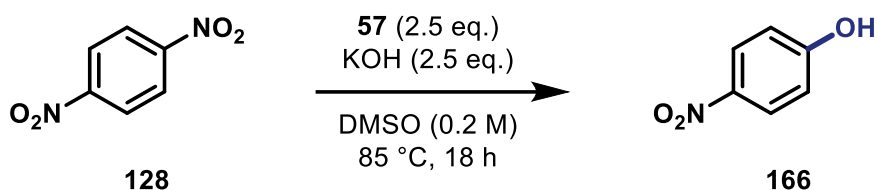
ATR-FTIR (thin film) $\nu_{\text{max}}/\text{cm}^{-1}$ 392, 1524, 1490, 1264, 833, 757, 688;

¹H NMR (400 MHz, CDCl₃) δ_{H} 7.54 (d, $J = 7.3$ Hz, 2H, H-7), 7.48 (d, $J = 8.7$ Hz, 2H, H-4), 7.42 (dd, $J = 7.3, 7.3$ Hz, 2H, H-8), 7.31 (t, $J = 7.3$ Hz, 1H, H-9), 6.91 (d, $J = 8.7$ Hz, 2H, H-3), 4.77 (br s, 1H, H-1);

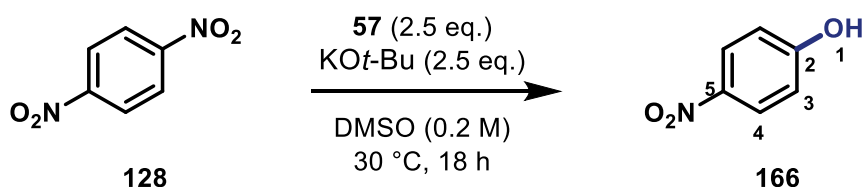
¹³C NMR (75 MHz, CDCl₃) δ_{C} 155.2 (C, C-5/6), 140.9 (C, C-5/6), 134.2 (C, C-2), 128.9 (CH, C-4), 128.5 (CH, C-8), 126.9 (CH, C-9), 115.8 (CH, C-3);

HRMS (ESI⁻) m/z calcd. for C₁₂H₉O (M - H)⁻ 169.0659, found 169.0657 (-0.8 ppm error).

Spectroscopic data matched those reported in the literature.^[92]

4-Nitrophenol (**166**)

Synthesized using **General Procedure B** with potassium hydroxide (42.1 mg, 0.75 mmol, 2.5 eq.), oxime **57** (93.1 mg, 0.75 mmol, 2.5 eq.), 1,4-dinitrobenzene **128** (50.4 mg, 0.30 mmol, 1.0 eq.) in DMSO (1.5 mL). The reaction was heated at 85 °C and stirred for 18 h. The crude product was dissolved in a minimum amount of CH₂Cl₂, dried onto silica gel and purified by column chromatography (10% EtOAc in hexane) to afford 4-nitrophenol **166** (28.1 mg, 0.20 mmol, 67%) as a dark orange solid (AJG-01-014).



Synthesized using **General Procedure B** with potassium *tert*-butoxide (84.2 mg, 0.75 mmol, 2.5 eq.), oxime **57** (93.1 mg, 0.75 mmol, 2.5 eq.), 1,4-dinitrobenzene **128** (50.4 mg, 0.30 mmol, 1.0 eq.) in DMSO (1.5 mL). The reaction was heated at 30 °C and stirred for 18 h. The crude product was dissolved in a minimum amount of CH₂Cl₂, dried onto silica gel and purified by column chromatography (10% EtOAc in hexane) to afford 4-nitrophenol **166** (22.8 mg, 0.16 mmol, 55%) as a dark orange solid (AJG-01-044).

R_f 0.30 (40% EtOAc in hexane);

ATR-FTIR (thin film) $\nu_{\text{max}}/\text{cm}^{-1}$ 3364, 1613, 1595, 1499, 1334, 1297, 1203, 1177, 1114, 845, 753, 693, 630;

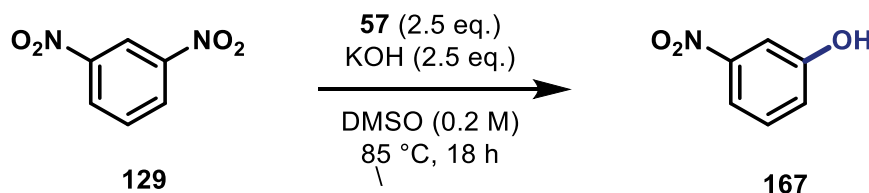
¹H NMR (400 MHz, CDCl₃) δ_{H} 8.18 (d, $J = 9.1$ Hz, 2H, H-4), 6.91 (d, $J = 9.1$ Hz, 2H, H-3), 5.58 (br s, 1H, H-1);

¹³C NMR (75 MHz, CDCl₃) δ_{C} 161.9 (C, C-5), 141.6 (C, C-2), 125.5 (CH, C-4), 115.9 (CH, C-3);

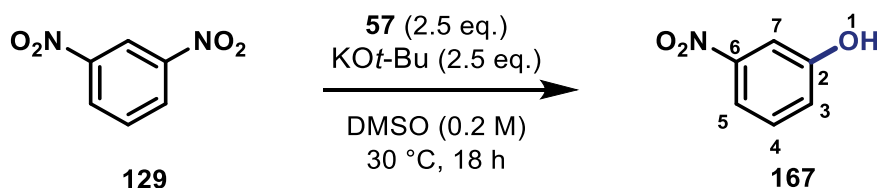
HRMS (ESI⁻) m/z calcd. for C₆H₄NO₃ (M - H)⁻ 138.0197, found 138.0193 (-2.7 ppm error).

Spectroscopic data matched those reported in the literature.^[37]

3-Nitrophenol (**167**)



Synthesized using **General Procedure B** with potassium hydroxide (42.1 mg, 0.75 mmol, 2.5 eq.), oxime **57** (93.1 mg, 0.75 mmol, 2.5 eq.), 1,3-dinitrobenzene **129** (50.4 mg, 0.30 mmol, 1.0 eq.) in DMSO (1.5 mL). The reaction was heated at 85 °C and stirred for 18 h. The crude product was dissolved in a minimum amount of CH₂Cl₂, dried onto silica gel and purified by column chromatography (25% EtOAc in hexane) to afford 3-nitrophenol **167** (15.2 mg, 0.11 mmol, 36%) as a dark orange solid (AJG-01-015).



Synthesized using **General Procedure B** with potassium *tert*-butoxide (84.2 mg, 0.75 mmol, 2.5 eq.), oxime **57** (93.1 mg, 0.75 mmol, 2.5 eq.), 1,3-dinitrobenzene **129** (50.4 mg, 0.30 mmol, 1.0 eq.) in DMSO (1.5 mL). The reaction was heated at 30 °C and stirred for 18 h. The crude product was dissolved in a minimum amount of CH₂Cl₂, dried onto silica gel and purified by column chromatography (10% EtOAc in hexane) to afford 3-nitrophenol **167** (27.3 mg, 0.20 mmol, 65%) as an orange solid (AJG-01-045).

R_f 0.30 (30% EtOAc in hexane);

ATR-FTIR (thin film) $\nu_{\text{max}}/\text{cm}^{-1}$ 3393, 2938, 1521, 1352, 1301, 1214, 818, 796, 745, 673;

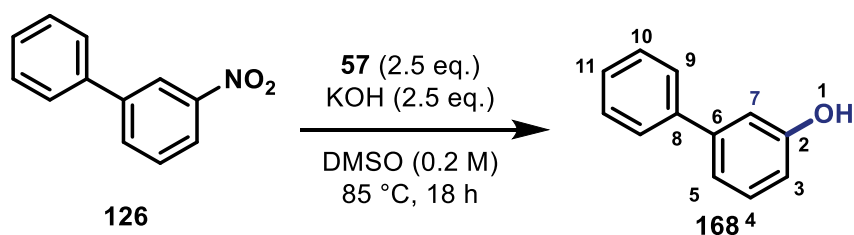
¹H NMR (300 MHz, CDCl₃) δ_{H} 7.81 (dd, $J = 8.2, 2.2$ Hz, 1H, H-5), 7.70 (t, $J = 2.2$ Hz, 1H, H-7), 7.40 (t, $J = 8.1$ Hz, 1H, H-4), 7.19 (dd, $J = 8.2, 2.2$ Hz, 1H, H-3), 5.83 (br s, 1H, H-1);

¹³C NMR (75 MHz, CDCl₃) δ_{C} 156.5 (C, C-6), 149.3 (C, C-2), 130.4 (CH, C-5), 122.2 (CH, C-7), 116.0 (CH, C-4), 110.7 (CH, C-3);

HRMS (ESI⁻) m/z calcd. for C₆H₄NO₃ (M - H)⁻ 138.0197, found 138.0198 (-0.7 ppm error).

Spectroscopic data matched those reported in the literature.^[93]

3-Phenylphenol (**168**)



Synthesized using **General Procedure B** with potassium hydroxide (42.1 mg, 0.75 mmol, 2.5 eq.), oxime **57** (93.1 mg, 0.75 mmol, 2.5 eq.), 3-nitrobiphenyl **126** (59.8 mg, 0.30 mmol, 1.0 eq.) in DMSO (1.5 mL). The reaction was heated at 85 °C and stirred for 18 h. The crude product was dissolved in a minimum amount of CH₂Cl₂, dried onto silica gel and purified by column chromatography (80% CH₂Cl₂ in hexane) to afford 3-phenylphenol **168** (18.1 mg, 0.11 mmol, 35%) as an off-white solid (AJG-01-097).

R_f 0.25 (CH₂Cl₂);

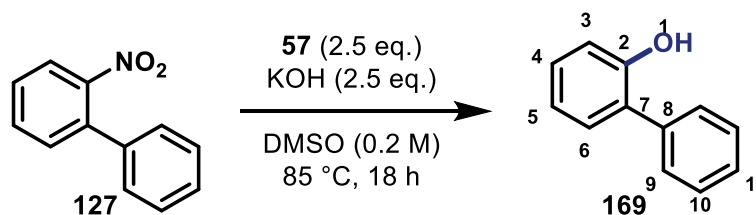
ATR-FTIR (thin film) $\nu_{\text{max}}/\text{cm}^{-1}$ 3362, 1970, 1596, 1476, 1430, 1301, 1199, 883, 757, 697;

¹H NMR (400 MHz, CDCl₃) δ_{H} 7.58 – 7.55 (m, 2H), 7.45 – 7.40 (m, 2H), 7.36 – 7.28 (m, 2H), 7.18 – 7.14 (m, 1H), 7.06 – 7.04 (m, 1H), 6.83 – 6.79 (m, 1H), 4.76 (br s, 1H, H-1);

¹³C NMR (101 MHz, CDCl₃) δ_{C} 155.9 (C, C-8), 143.1 (C, C-6), 140.8 (C, C-1), 130.1 (CH), 128.9 (CH), 127.6 (CH), 127.3 (CH), 119.9 (CH), 114.3 (CH), 114.2 (CH);

HRMS (ESI⁻) m/z calcd. for C₁₂H₉O (M - H)⁻ 169.0659, found 169.0660 (-0.4 ppm error).

Spectroscopic data matched those reported in the literature.^[94]

2-Phenylphenol (**169**)

Synthesized using **General Procedure B** with potassium hydroxide (42.1 mg, 0.75 mmol, 2.5 eq.), oxime **57** (93.1 mg, 0.75 mmol, 2.5 eq.), 2-nitrobiphenyl **127** (59.8 mg, 0.30 mmol, 1.0 eq.) in DMSO (1.5 mL). The reaction was heated at 85 °C and stirred for 18 h. The crude product was dissolved in a minimum amount of CH₂Cl₂, dried onto silica gel and purified by column chromatography (60% CH₂Cl₂ in hexane) to afford 2-phenylphenol **169** (20.7 mg, 0.12 mmol, 41%) as an off-white solid (AJG-01-095).

R_f 0.35 (80% DCM in hexane);

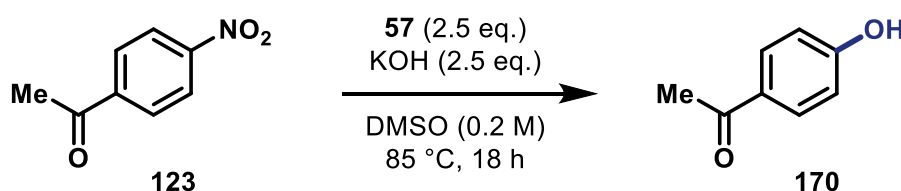
ATR-FTIR (thin film) $\nu_{\text{max}}/\text{cm}^{-1}$ 3533, 1968, 1585, 1479, 1435, 1271, 1180, 830, 753, 700;

¹H NMR (400 MHz, CDCl₃) δ_{H} 7.54 – 7.46 (m, 4H), 7.44 – 7.37 (m, 1H), 7.30 – 7.22 (m, 2H), 7.03 – 6.97 (m, 2H), 5.18 (br s, 1H, H-1);

¹³C NMR (101 MHz, CDCl₃) δ_{C} 152.5 (C, C-8), 137.2 (C, C-2), 130.4 (CH), 129.4 (CH), 129.3 (CH), 129.2 (CH), 128.2 (C, C-7), 128.0 (CH), 121.0 (CH), 115.9 (CH);

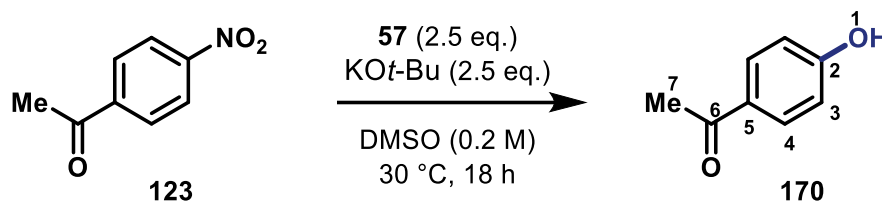
HRMS (ESI⁻) m/z calcd. for C₁₂H₉O (M – H)⁻ 169.0659, found 169.0648 (6.4 ppm error).

Spectroscopic data matched those reported in the literature.^[95]

4'-Hydroxyacetophenone (**170**)

Synthesized using **General Procedure B** with potassium hydroxide (42.1 mg, 0.75 mmol, 2.5 eq.), oxime **57** (93.1 mg, 0.75 mmol, 2.5 eq.), 4-nitroacetophenone **123** (49.6 mg, 0.30 mmol, 1.0 eq.) in DMSO (1.5 mL). The reaction was heated at 85 °C and stirred for 18 h. The crude product

was dissolved in a minimum amount of CH_2Cl_2 , dried onto silica gel and purified by column chromatography (5% EtOAc in hexane) to afford 4'-hydroxyacetophenone **170** (27.1 mg, 0.20 mmol, 66%) as a dark orange solid (AJG-01-022).



Synthesized using **General Procedure B** with potassium *tert*-butoxide (84.2 mg, 0.75 mmol, 2.5 eq.), oxime **57** (93.1 mg, 0.75 mmol, 2.5 eq.), 4-nitroacetophenone **123** (49.6 mg, 0.30 mmol, 1.0 eq.) in DMSO (1.5 mL). The reaction was heated at 30 °C and stirred for 18 h. The crude product was dissolved in a minimum amount of CH_2Cl_2 , dried onto silica gel and purified by column chromatography (20% EtOAc in hexane) to afford 4'-hydroxyacetophenone **170** (16.3 mg, 0.12 mmol, 40%) as a dark orange solid (AJG-01-046).

R_f 0.25 (40% EtOAc in hexane);

ATR-FTIR (thin film) $\nu_{\text{max}}/\text{cm}^{-1}$ 3310, 1663, 1602, 1576, 1357, 1279, 1221, 1167, 848, 567;

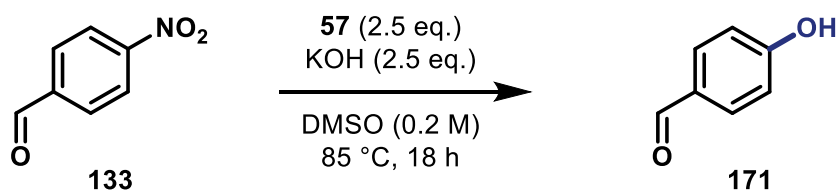
$^1\text{H NMR}$ (400 MHz, CDCl_3) δ_{H} 7.91 (d, $J = 8.7$ Hz, 2H, H-4), 6.89 (d, $J = 8.7$ Hz, 2H, H-3), 2.56 (s, 3H, H-7);

$^{13}\text{C NMR}$ (101 MHz, CDCl_3) δ_{C} 198.7 (C, C-6), 161.4 (C, C-5), 131.4 (CH, C-4), 129.7 (C, C-2), 115.7 (CH, C-2), 26.5 (CH_3 , C-7);

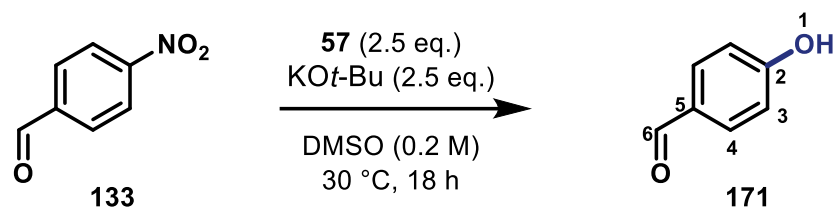
HRMS (ESI $^-$) m/z calcd. for $\text{C}_8\text{H}_7\text{O}_2$ ($\text{M} - \text{H}$) $^-$ 135.0452, found 135.0456 (-3.6 ppm error).

Spectroscopic data matched those reported in the literature.^[95]

4-Hydroxybenzaldehyde (171)



Synthesized using **General Procedure B** with potassium hydroxide (42.1 mg, 0.75 mmol, 2.5 eq.), oxime **57** (93.1 mg, 0.75 mmol, 2.5 eq.), 4-nitrobenzaldehyde **133** (45.3 mg, 0.30 mmol, 1.0 eq.) in DMSO (1.5 mL). The reaction was heated at 85 °C and stirred for 18 h. The crude product was dissolved in a minimum amount of CH₂Cl₂, dried onto silica gel and purified by column chromatography (10% EtOAc in hexane) to afford 4-hydroxybenzaldehyde **171** (23.7 mg, 0.19 mmol, 65%) as a red solid (AJG-01-023).



Synthesized using **General Procedure B** with potassium *tert*-butoxide (84.2 mg, 0.75 mmol, 2.5 eq.), oxime **57** (93.1 mg, 0.75 mmol, 2.5 eq.), 4-nitrobenzaldehyde **133** (45.3 mg, 0.30 mmol, 1.0 eq.) in DMSO (1.5 mL). The reaction was heated at 30 °C and stirred for 18 h. The crude product was dissolved in a minimum amount of CH₂Cl₂, dried onto silica gel and purified by column chromatography (20% EtOAc in hexane) to afford 4-hydroxybenzaldehyde **171** (16.8 mg, 0.14 mmol, 46%) as an orange solid (AJG-01-047).

R_f 0.3 (40% EtOAc in hexane);

ATR-FTIR (thin film) $\nu_{\max}/\text{cm}^{-1}$ 3185, 1670, 1600, 1580, 1515, 1454, 1285, 1218, 1159, 834, 604;

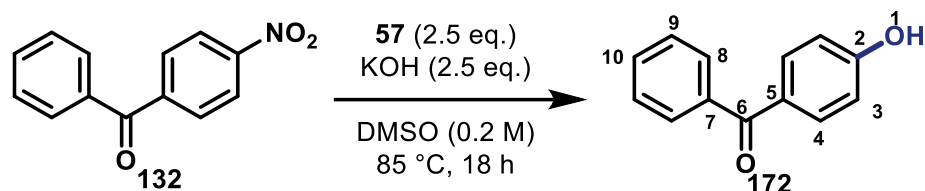
¹H NMR (400 MHz, CDCl₃) δ_{H} 9.88 (s, 1H, H-6), 7.83 (d, $J = 8.5$ Hz, 2H, H-4), 6.96 (d, $J = 8.5$ Hz, 2H, H-3), 5.58 (br s, 1H, H-1);

¹³C NMR (101 MHz, CDCl₃) δ_{C} 191.5 (CH, C-6), 161.8 (C, C-5), 132.7 (CH, C-4), 130.0 (C, C-2), 116.2 (CH, C-3);

HRMS (ESI⁻) m/z calcd. for C₇H₅O₂ (M - H)⁻ 121.0295, found 121.0295 (0.0 ppm error).

Spectroscopic data matched those reported in the literature.^[93]

4'-Hydroxybenzophenone (172)



Synthesized using **General Procedure B** with potassium hydroxide (42.1 mg, 0.75 mmol, 2.5 eq.), oxime **57** (93.1 mg, 0.75 mmol, 2.5 eq.), 4-nitrobenzophenone **132** (68.2 mg, 0.30 mmol, 1.0 eq.) in DMSO (1.5 mL). The reaction was heated at 85 °C and stirred for 18 h. The crude product was dissolved in a minimum amount of CH₂Cl₂, dried onto silica gel and purified by column chromatography (20% EtOAc in hexane) to afford 4'-hydroxybenzophenone **172** (51.5 mg, 0.26 mmol, 87%) as a dark orange solid (AJG-01-069).

R_f 0.4 (30% EtOAc in hexane);

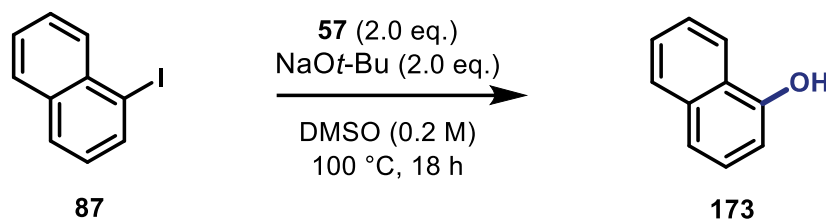
ATR-FTIR (thin film) $\nu_{\text{max}}/\text{cm}^{-1}$ 3273, 1634, 1601, 1511, 1445, 1320, 1282, 1151, 924, 699, 607;

¹H NMR (400 MHz, CDCl₃) δ_{H} 7.80 (d, $J = 8.6$ Hz, 2H, H-4), 7.76 (d, $J = 7.6$ Hz, 2H, H-8), 7.57 (t, $J = 7.6$ Hz, 1H, H-10), 7.47 (dd, $J = 7.6, 7.6$ Hz, 2H H-9), 6.92 (d, $J = 8.6$ Hz, 2H, H-3), 5.76 (br s, 1H, H-1).

¹³C NMR (101 MHz, CDCl₃) δ_{C} 196.6 (C, C-6), 160.5 (C, C-7), 138.2 (C, C-5), 135.9 (C, C-2), 133.2 (CH, C-4), 132.3 (CH, C-8), 130.0 (CH, C-10), 128.4 (CH, C-9), 115.4 (CH, C-3);

HRMS (ESI⁺) m/z calcd. for C₁₃H₁₁O₂ (M + H)⁺ 199.0754, found 199.0759 (-2.4 ppm error).

Spectroscopic data matched those reported in the literature.^[96]

1-Naphthol (**173**)

Synthesized using **General Procedure A** with sodium *tert*-butoxide (57.7 mg, 0.60 mmol, 2.0 eq.), oxime **57** (74.5 mg, 0.60 mmol, 2.0 eq.), 1-iodonaphthalene **87** (76.2 mg, 0.30 mmol, 1.0 eq.) in DMSO (1.5 mL). The reaction was heated at 100 °C and stirred for 18 h. The crude product was dissolved in a minimum amount of CH₂Cl₂, dried onto silica gel and purified by column chromatography (10% EtOAc in hexane) to afford 1-naphthol **173** (23.2 mg, 0.16 mmol, 54%) as a beige solid (AJG-01-062).



Synthesized using **General Procedure A** with sodium *tert*-butoxide (57.7 mg, 0.60 mmol, 2.0 eq.), oxime **57** (74.5 mg, 0.60 mmol, 2.0 eq.), 1-fluoronaphthalene **88** (43.8 mg, 0.30 mmol, 1.0 eq.) in DMSO (1.5 mL). The reaction was heated at 100 °C and stirred for 18 h. The crude product was dissolved in a minimum amount of CH₂Cl₂, dried onto silica gel and purified by column chromatography (10% EtOAc in hexane) to afford 1-naphthol **173** (36.3 mg, 0.25 mmol, 84%) as a pale lilac solid (AJG-01-063).

R_f 0.35 (20% EtOAc in hexane);

ATR-FTIR (thin film) $\nu_{\text{max}}/\text{cm}^{-1}$ 3245, 1579, 1516, 1459, 1386, 1278, 1084, 1044, 1020, 879, 795, 772, 573, 480;

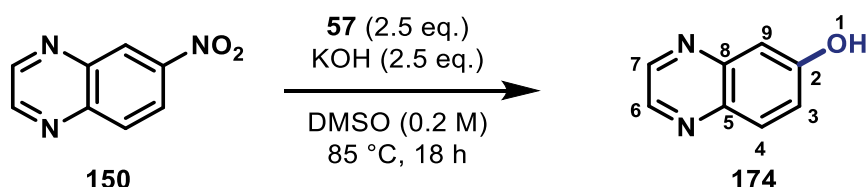
¹H NMR (400 MHz, DMSO-*d*₆) δ_{H} 10.11 (br s, 1H, H-1), 8.11 (dd, $J = 7.8, 1.7$ Hz, 1H, H-10), 7.80 (dd, $J = 7.7, 1.6$ Hz, 1H, H-5), 7.49 – 7.39 (m, 2H), 7.36 – 7.25 (m, 2H), 6.86 (dd, $J = 7.1, 1.4$ Hz, 1H, H-3);

¹³C NMR (101 MHz, DMSO-*d*₆) δ_{C} 153.2 (C, C-6), 134.4 (C, C-11), 127.2 (CH, C-10), 126.5 (CH, C-5), 126.1 (CH), 124.6 (CH), 121.9 (CH), 118.3 (CH), 108.1 (CH, C-3);

HRMS (ESI⁻) m/z calcd. for C₁₀H₇O (M - H)⁻ 143.0502, found 143.0500 (1.3 ppm error).

Spectroscopic data matched those reported in the literature.^[97]

6-Hydroxyquinoxaline (174)



Synthesized using **General Procedure B** with potassium hydroxide (42.1 mg, 0.75 mmol, 2.5 eq.), oxime **57** (93.1 mg, 0.75 mmol, 2.5 eq.), 6-nitroquinoxaline **150** (52.5 mg, 0.30 mmol, 1.0 eq.) in DMSO (1.5 mL). The reaction was heated at 85 °C and stirred for 18 h. The crude product was dissolved in a minimum amount of CH₂Cl₂, dried onto silica gel and purified by column chromatography (3% MeOH in DCM) to afford 6-hydroxyquinoxaline **174** (12.7 mg, 0.09 mmol, 29%) as an off-white solid (AJG-02-001).

R_f 0.25 (3% MeOH in DCM);

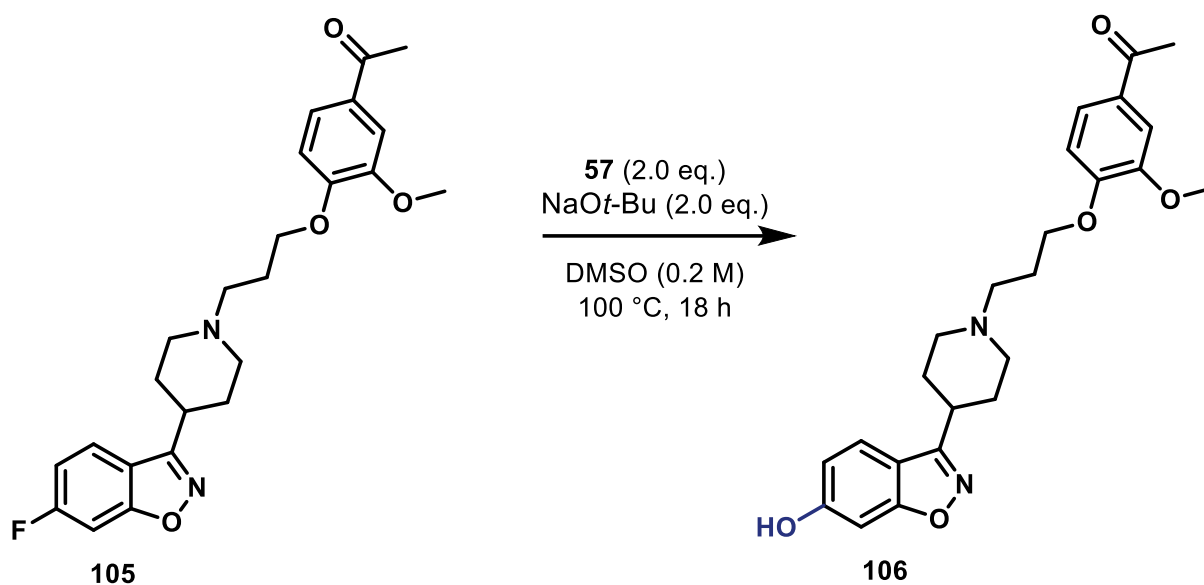
ATR-FTIR (thin film) $\nu_{\text{max}}/\text{cm}^{-1}$ 2931, 1617, 1548, 1510, 1382, 1304, 1227, 1156, 1027, 873;

¹H NMR (400 MHz, DMSO-*d*₆) δ_{H} 10.54 (br s, 1H, H-1), 8.78 (d, $J = 1.9$ Hz, 1H, H-6/7), 8.69 (d, $J = 1.9$ Hz, 1H, H-6/7), 7.93 (d, $J = 8.9$ Hz, 1H, H-4), 7.41 (dd, $J = 8.9, 2.8$ Hz, 1H, H-3), 7.26 (d, $J = 2.8$ Hz, 1H, H-9);

¹³C NMR (101 MHz, DMSO-*d*₆) δ_{C} 159.3 (C, C-5/8), 145.9 (CH, C-6/7), 144.6 (C, C-5/8), 142.7 (CH, C-6/7), 138.1 (C, C-2), 131.0 (CH, C-4), 123.4 (CH, C-3), 110.0 (CH, C-9);

HRMS (ESI⁻) m/z calcd. for C₈H₅N₂O (M - H)⁻ 145.0407, found 145.0402 (3.6 ppm error).

Spectroscopic data matched those reported in the literature.^[55]

Phenol (**106**) (Iloperidone SM)

Synthesized using **General Procedure A** with sodium *tert*-butoxide (46.1 mg, 0.48 mmol, 2.0 eq.), oxime **57** (59.6 mg, 0.48 mmol, 2.0 eq.), Iloperidone **105** (104.3 mg, 0.24 mmol, 1.0 eq.) in DMSO (1.2 mL). The reaction was heated at 100 °C and stirred for 18 h. The crude product was dissolved in a minimum amount of CH₂Cl₂, dried onto silica gel and purified by column chromatography (3% MeOH in DCM) to afford phenol **106** (84.9 mg, 0.20 mmol, 83%) as a pale-yellow solid (AJG-02-009).

R_f 0.3 (10% MeOH in DCM);

ATR-FTIR (thin film) $\nu_{\max}/\text{cm}^{-1}$ 2943, 1671, 1595, 1510, 1418, 1270, 1221, 1148, 1031, 827, 735;

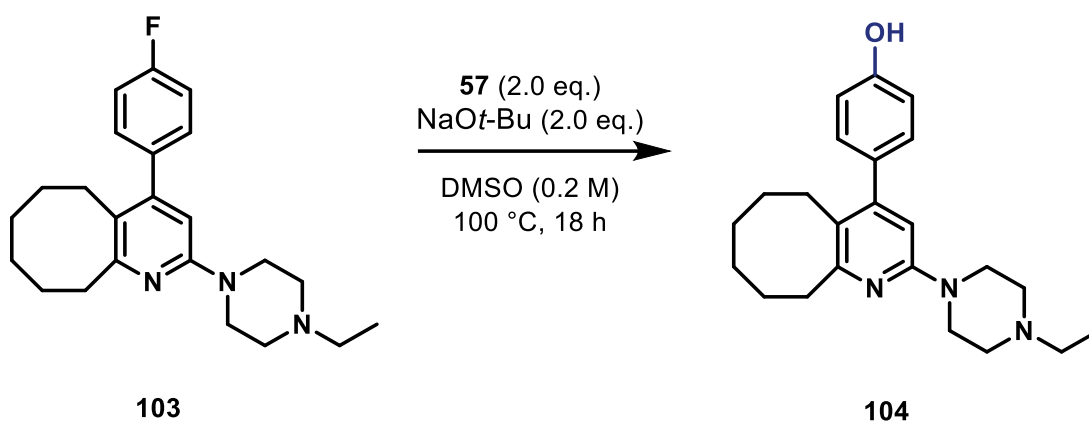
¹H NMR (400 MHz, DMSO-d₆) δ_{H} 10.36 (br s, 1H), 7.68 (d, $J = 8.7$ Hz, 1H), 7.61 (dd, $J = 8.5$, 2.0 Hz, 1H), 7.44 (d, $J = 2.0$ Hz, 1H), 7.07 (d, $J = 8.5$ Hz, 1H), 6.92 (d, $J = 2.0$ Hz, 1H), 6.83 (dd, $J = 8.7$, 2.0 Hz, 1H), 4.11 (t, $J = 6.4$ Hz, 2H), 3.82 (s, 3H), 3.10 – 2.96 (m, 3H), 2.58 – 2.50 (m, 5H), 2.18 (t, $J = 11.5$ Hz, 2H), 2.03 – 1.79 (m, 6H);

¹³C NMR (101 MHz, DMSO-d₆) δ_{C} 196.4 (C), 164.3 (C), 160.8 (C), 160.2 (C), 152.4 (C), 148.7 (C), 129.8 (C), 123.2 (CH), 122.6 (CH), 113.8 (CH), 112.7 (CH), 111.7 (C), 110.4 (CH), 94.7 (CH), 66.8 (CH₂), 55.6 (CH₃), 54.5 (CH₂), 53.0 (CH₂), 33.4 (CH), 30.0 (CH₂), 26.4 (CH₃), 26.0 (CH₂);

HRMS (ESI⁺) m/z calcd. for C₂₄H₂₉N₂O₅ (M + H)⁺ 425.2071, found 425.2073 (−1.0 ppm error).

No spectroscopic data reported in the literature.

Phenol (104) (Blonanserin SM)



Synthesized using **General Procedure A** with sodium *tert*-butoxide (11.5 mg, 0.12 mmol, 2.0 eq.), oxime **57** (14.9 mg, 0.12 mmol, 2.0 eq.), Blonanserin **103** (20.6 mg, 0.06 mmol, 1.0 eq.) in DMSO (0.3 mL). The reaction was heated at 100 °C and stirred for 18 h. The crude product was dissolved in a minimum amount of CH₂Cl₂, dried onto silica gel and purified by column chromatography (5% MeOH in DCM) to afford phenol **104** (10.2 mg, 0.03 mmol, 47%) as a pale-yellow solid (AJG-02-010).

R_f 0.35 (15% MeOH in DCM);

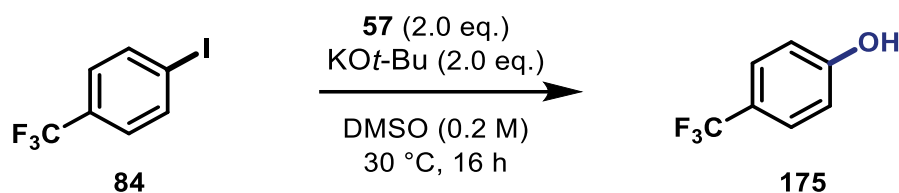
ATR-FTIR (thin film) $\nu_{\text{max}}/\text{cm}^{-1}$ 2922, 2850, 1588, 1543, 1514, 1448, 1270, 1243, 1168, 998, 832;

¹H NMR (400 MHz, DMSO-*d*₆) δ_{H} 9.53 (br s, 1H), 7.05 (d, *J* = 8.5 Hz, 2H), 6.80 (d, *J* = 8.5 Hz, 2H), 6.34 (s, 1H), 3.62 – 3.34 (m, 5H), 2.85 – 2.72 (m, 2H), 2.63 – 2.50 (m, 4H), 1.72 – 1.61 (m, 2H), 1.42 – 1.19 (m, 9H), 1.05 (t, *J* = 7.1 Hz, 3H);

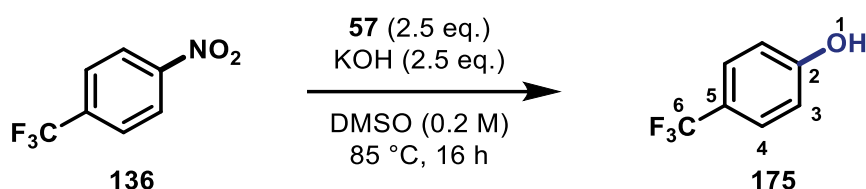
¹³C NMR Not obtained, due to difficulties with solubility in DMSO-*d*₆.

HRMS (ESI⁺) *m/z* calcd. for C₂₃H₃₂N₃O (M + H)⁺ 366.2540, found 366.2544 (−0.4 ppm error).

No spectroscopic data reported in the literature.

4-Hydroxybenzotrifluoride (**175**)

Synthesized using **General Procedure A** with potassium *tert*-butoxide (67.3 mg, 0.6 mmol, 2.0 eq.), oxime **57** (74.5 mg, 0.6 mmol, 2.0 eq.), 4-iodobenzotrifluoride **84** (81.6 mg, 0.30 mmol, 1.0 eq.) in DMSO (1.5 mL). The reaction was heated at 30 °C and stirred for 16 h. The crude product was dissolved in a minimum amount of CH₂Cl₂, dried onto silica gel and purified by column chromatography (60% DCM in hexane) to afford 4-hydroxybenzotrifluoride **175** (8.1 mg, 0.05 mmol, 17%) as an off-white solid (AJG-02-027).



Synthesized using **General Procedure B** with potassium hydroxide (42.1 mg, 0.75 mmol, 2.5 eq.), oxime **57** (93.1 mg, 0.75 mmol, 2.5 eq.), 4-nitrobenzotrifluoride **136** (57.3 mg, 0.30 mmol, 1.0 eq.) in DMSO (1.5 mL). The reaction was heated at 85 °C and stirred for 16 h. The crude product was dissolved in a minimum amount of CH₂Cl₂, dried onto silica gel and purified by column chromatography (60% DCM in hexane) to afford 4-hydroxybenzotrifluoride **175** (1.2 mg, 0.01 mmol, 2%) as an off-white solid (AJG-02-029).

R_f 0.20 (75% DCM in hexane);

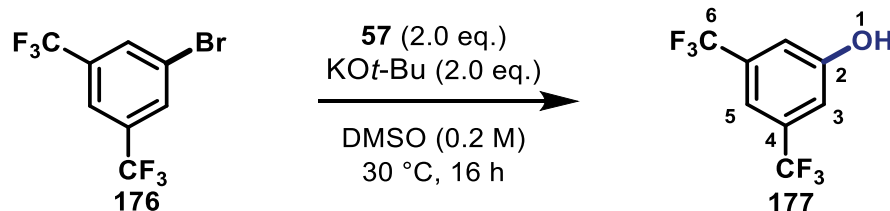
ATR-FTIR (thin film) $\nu_{\max}/\text{cm}^{-1}$ 3674, 2922, 2852, 1463, 1324, 1122, 1065, 840, 816, 754;

¹H NMR (400 MHz, CDCl₃) δ_{H} 7.50 (d, $J = 8.4$ Hz, 2H, H-4), 6.91 (d, $J = 8.4$ Hz, 2H, H-3), 6.21 (br s, 1H, H-1);

¹⁸F NMR (282 MHz, CDCl₃) δ_{F} -61.5 (s, 3F, F-6);

HRMS (ESI⁻) m/z calcd. for C₇H₄F₃O (M - H)⁻ 161.0220, found 161.018 (1.2 ppm error).

Spectroscopic data matched those reported in the literature.^[95]

3,5-Bis(trifluoromethyl)phenol (**177**)

Synthesized using **General Procedure A** with potassium *tert*-butoxide (67.3 mg, 0.6 mmol, 2.0 eq.), oxime **57** (74.5 mg, 0.6 mmol, 2.0 eq.), 3,5-bis(trifluoromethyl)bromobenzene **176** (87.9 mg, 0.30 mmol, 1.0 eq.) in DMSO (1.5 mL). The reaction was heated at 30 °C and stirred for 16 h. The crude product was dissolved in a minimum amount of CH₂Cl₂, dried onto silica gel and purified by column chromatography (60% DCM in hexane) to afford 3,5-bis(trifluoromethyl)phenol **177** (6.6 mg, 0.03 mmol, 10%) as an off-white solid (AJG-02-028).

R_f 0.20 (75% DCM in hexane);

ATR-FTIR (thin film) $\nu_{\max}/\text{cm}^{-1}$ 3276, 2922, 2852, 1710, 1614, 1464, 1391, 1279, 1176, 1136, 946, 846, 683;

¹H NMR (400 MHz, CDCl₃) δ_{H} 7.43 (s, 1H, H-5), 7.26 (s, 2H, H-3), 6.02 (br s, 1H, H-1);

¹⁸F NMR (282 MHz, CDCl₃) δ_{F} -63.2 (s, 6F, F-6);

HRMS (ESI⁻) m/z calcd. for C₈H₄F₆O (M - H)⁻ 229.0094, found 229.0093 (-1.5 ppm error).

Spectroscopic data matched those reported in the literature.^[98]

References

- [1] N. le Dang, T. B. Hughes, G. P. Miller, S. J. Swamidass, *Chemical Research in Toxicology* **2017**, *30*, 1046-1059, DOI 10.1021/acs.chemrestox.6b00336.
- [2] J. R. Vane, R. M. Botting, *Inflammation Research* **1995**, *44*, 1-10, DOI 10.1007/BF01630479.
- [3] G. G. Graham, M. J. Davies, R. O. Day, A. Mohamudally, K. F. Scott, *Inflammopharmacology* **2013**, *21*, 201-232, DOI 10.1007/s10787-013-0172-x.
- [4] F. C. Churchill, L. C. Patchen, C. C. Campbell, I. K. Schwartz, P. Nguyen-Dinh, C. M. Dickinson, *Life Sciences* **1985**, *36*, 53-62, DOI 10.1016/0024-3205(85)90285-1.
- [5] M. K. Mahajan, V. Uttamsingh, J. S. Daniels, L. S. Gan, B. W. LeDuc, D. A. Williams, *Drug Metabolism and Disposition* **2011**, *39*, 693-702, DOI 10.1124/dmd.110.036004.
- [6] E. F. Minet, G. Daniela, C. Meredith, E. D. Massey, *Xenobiotica* **2012**, *42*, 429-411, DOI 10.3109/00498254.2011.637582.
- [7] A. Vandesteene, V. Trempont, E. Engelman, T. Deloof, M. Focroul, A. Schoutens, M. De Rood, *Anaesthesia* **1988**, *43*, 1365-2044, DOI 10.1111/j.1365-2044.1988.tb09067.x.
- [8] J. E. Beal, R. Olson, L. Laubenstein, J. O. Morales, P. Bellman, B. Yangco, L. Lefkowitz, T. F. Plasse, K. v. Shepard, *Journal of Pain and Symptom Management* **1995**, *10*, 89-97, DOI 10.1016/0885-3924(94)00117-4.
- [9] B. Testa, A. Pedretti, G. Vistoli, *Drug Discovery Today* **2012**, *17*, 549-560, DOI 10.1016/j.drudis.2012.01.017.
- [10] S. Rohn, H. M. Rawel, J. Kroll, *Journal of Agricultural and Food Chemistry* **2002**, *50*, 3566-3571, DOI 10.1021/jf011714b.
- [11] S. Rohn, H. M. Rawel, N. Pietruschinski, J. Kroll, *Journal of the Science of Food and Agriculture* **2001**, *81*, 977-980, DOI 10.1002/jsfa.977.
- [12] F. G. Smith, J. C. Walker, W. J. Hooker, *American Journal of Botany* **1946**, *33*, 1537-2197, DOI 10.1002/j.1537-2197.1946.tb10384.x.
- [13] J. Lister, *British Medical Journal* **1867**, *2*, 246-248, DOI 10.1136/bmj.2.351.246.
- [14] J. L. Thompson, M. Hinton, *British Poultry Science* **1997**, *38*, 59-65, DOI 10.1080/00071669708417941.
- [15] R. Selvin, H. L. Hsu, P. Aneesh, S. H. Chen, L. H. Hung, *Reaction Kinetics, Mechanisms and Catalysis* **2010**, *100*, 197-204, DOI 10.1007/s11144-010-0165-3.
- [16] J. P. Lange, A. J. M. Breed, *Catalysis Communications* **2002**, *3*, 25-28, DOI 10.1016/S1566-7367(01)00071-1.
- [17] J. H. Yang, G. Sun, Y. Gao, H. Zhao, P. Tang, J. Tan, A. H. Lu, D. Ma, *Energy and Environmental Science* **2013**, *6*, 793-798, DOI 10.1039/c3ee23623d.

- [18] J. L. Motz, H. Heinichen, W. F. Hölderich, *Journal of Molecular Catalysis A: Chemical* **1998**, *136*, 175-184, DOI 10.1016/S1381-1169(98)00048-X.
- [19] P. Gogoi, P. Bezboruah, J. Gogoi, R. C. Boruah, *European Journal of Organic Chemistry* **2013**, 1871-1882, DOI 10.1002/ejoc.201301228.
- [20] J. F. Bunnett, *Quarterly Reviews, Chemical Society* **1958**, *12*, 1-16, DOI 10.1039/qr9581200001.
- [21] C. N. Neumann, J. M. Hooker, T. Ritter, *Nature* **2016**, *534*, 369-373, DOI 10.1038/nature17667.
- [22] M. Liljenberg, T. Brinck, B. Herschend, T. Rein, S. Tomasi, M. Svensson, *Journal of Organic Chemistry* **2012**, *77*, 3262-3269, DOI 10.1021/jo202569n.
- [23] S. Rohrbach, A. J. Smith, J. H. Pang, D. L. Poole, T. Tuttle, S. Chiba, J. A. Murphy, *Angewandte Chemie - International Edition* **2019**, *58*, 16368-16388, DOI 10.1002/anie.201902216.
- [24] X. Zhang, G. P. Lu, C. Cai, *Green Chemistry* **2016**, *18*, 5580-5585, DOI 10.1039/c6gc01742h.
- [25] E. Vitaku, D. T. Smith, J. T. Njardarson, *Journal of Medicinal Chemistry* **2014**, *57*, 10257-10274, DOI 10.1021/jm501100b.
- [26] M. Baumann, I. R. Baxendale, *Beilstein Journal of Organic Chemistry* **2013**, *9*, 2265-2319, DOI 10.3762/bjoc.9.265.
- [27] M. Imoto, Y. Matsui, M. Takeda, A. Tamaki, H. Taniguchi, K. Mizuno, H. Ikeda, *Journal of Organic Chemistry* **2011**, *76*, 1901-1922, DOI 10.1021/jo2007219.
- [28] W. J. Hale, E. C. Britton, *Industrial and Engineering Chemistry* **1928**, *20*, 114, DOI 10.1021/ie50218a006.
- [29] E. Stridfeldt, E. Lindstedt, M. Reitti, J. Blid, P. O. Norrby, B. Olofsson, *Chemistry - A European Journal* **2017**, *23*, 13249-13258, DOI 10.1002/chem.201703057.
- [30] S. W. Goldstein, A. Bill, J. Dhuguru, O. Ghoneim, *Journal of Chemical Education* **2017**, *94*, 1388-1390, DOI 10.1021/acs.jchemed.6b00680.
- [31] M. R. Crampton, V. Gold, *Journal of the Chemical Society (Resumed)* **1964**, 4293-4295, DOI 10.1039/jr9640004293.
- [32] A. J. J. Lennox, *Angewandte Chemie - International Edition* **2018**, *57*, 14686-14688, DOI 10.1002/anie.201809606.
- [33] S. Rohrbach, J. A. Murphy, T. Tuttle, *Journal of the American Chemical Society* **2020**, *142*, 14871-14876, DOI 10.1021/jacs.0c01975.
- [34] J. Hicks, P. Vasko, A. Heilmann, J. M. Goicoechea, S. Aldridge, *Angewandte Chemie - International Edition* **2020**, *59*, 20376-20380, DOI 10.1002/anie.202008557.
- [35] K. W. Anderson, T. Ikawa, R. E. Tundel, S. L. Buchwald, *Journal of the American Chemical Society* **2006**, *128*, 10694-10695, DOI 10.1021/ja0639719.

- [36] J. Chen, T. Yuan, W. Hao, M. Cai, *Catalysis Communications* **2011**, *12*, 1463-1465, DOI 10.1016/j.catcom.2011.06.002.
- [37] P. S. Fier, K. M. Maloney, *Organic Letters* **2017**, *19*, 3033-3036, DOI 10.1021/acs.orglett.7b01403.
- [38] G. A. Russell, F. Ros, J. Hershberger, H. Tashtoush, *Journal of Organic Chemistry* **1982**, *47*, 1480-1483, DOI 10.1021/jo00347a021.
- [39] M. P. Moon, J. F. Wolfe, *Journal of Organic Chemistry* **1979**, *44*, 4081-4085, DOI 10.1021/jo01337a013.
- [40] J. F. Bunnett, *Accounts of Chemical Research* **1978**, *11*, 5761-5765, DOI 10.1021/ar50131a003.
- [41] J. K. Kim, J. F. Bunnett, *Journal of the American Chemical Society* **1970**, *92*, 2806-2813, DOI 10.1021/ja00728a037.
- [42] A. Levy, D. Meyerstein, M. Ottolenghi, *Journal of Physical Chemistry* **1971**, *75*, 3350-3354, DOI 10.1021/j100690a025.
- [43] M. C. R. Symons, *Pure and Applied Chemistry* **1981**, *53*, 223-238, DOI 10.1351/pac198153010223.
- [44] F. A. Beland, S. O. Farwell, P. R. Callis, R. D. Geer, *Journal of Electroanalytical Chemistry* **1977**, *78*, 145-159, DOI 10.1016/S0022-0728(77)80430-0.
- [45] D. B. Denney, D. Z. Denney, *Tetrahedron* **1991**, *47*, 10117-10165, DOI 10.1016/S0040-4020(01)82312-7.
- [46] Q. Q. Zhou, Y. Q. Zou, L. Q. Lu, W. J. Xiao, *Angewandte Chemie - International Edition* **2019**, *58*, 1586-1604, DOI 10.1002/anie.201803102.
- [47] A. I. Ilovaisky, V. M. Merkulova, M. N. Elinson, G. I. Nikishin, *Russian Chemical Reviews* **2012**, *81*, 1427-1439, DOI 10.1070/rc2012v081n05abeh004244.
- [48] F. Yu, R. Mao, M. Yu, X. Gu, Y. Wang, *Journal of Organic Chemistry* **2019**, *84*, 9946-9956, DOI 10.1021/acs.joc.9b01113.
- [49] E. Shirakawa, T. Hayashi, *Chemistry Letters* **2012**, *41*, DOI 10.1246/cl.2012.130.
- [50] M. D. Thum, S. Wolf, D. E. Falvey, *Journal of Physical Chemistry A* **2020**, *124*, 4211-4222, DOI 10.1021/acs.jpca.0c02678.
- [51] I. M. Khan, M. Islam, S. Shakya, K. Alam, N. Alam, M. Shahid, *Bioorganic Chemistry* **2020**, *99*, 103779, DOI 10.1016/j.bioorg.2020.103779.
- [52] C. J. Bender, *Chemical Society Reviews* **1986**, *15*, 475-502, DOI 10.1039/CS9861500475.
- [53] I. M. Khan, A. Ahmad, *Spectrochimica Acta - Part A: Molecular and Biomolecular Spectroscopy* **2009**, *73*, 4405-4414, DOI 10.1016/j.saa.2009.05.009.
- [54] R. S. Mulliken, *Journal of the American Chemical Society* **1952**, *74*, 18117-18127, DOI 10.1021/ja01123a067.

- [55] Y. H. Nguyen, B. J. Lampkin, A. Venkatesh, A. Ellern, A. J. Rossini, B. Vanveller, *Journal of Organic Chemistry* **2018**, *83*, 9850-9857, DOI 10.1021/acs.joc.8b01331.
- [56] G. C. Vogel, R. S. Drago, *Journal of Chemical Education* **1996**, *73*, 18495-18501, DOI 10.1021/ed073p701.
- [57] S. v. Rosokha, J. K. Kochi, *Accounts of Chemical Research* **2008**, *41*, 461-653, DOI 10.1021/ar700256a.
- [58] M. A. Fox, J. Younathan, G. E. Fryxell, *Journal of Organic Chemistry* **1983**, *48*, 9681-9687, DOI 10.1021/jo00166a038.
- [59] S. Senaweera, J. D. Weaver, *Chemical Communications* **2017**, *53*, 7545-7548, DOI 10.1039/c7cc03996d.
- [60] R. A. Rossi, A. B. Pierini, A. B. Penenory, *ChemInform* **2010**, *28*, DOI 10.1002/chin.199708305.
- [61] C. Amatore, J. Pinson, J. M. Savéant, A. Thiébault, *Journal of the American Chemical Society* **1981**, *103*, 6933, DOI 10.1021/ja00413a028.
- [62] R. G. Scamehorn, J. M. Hardacre, J. M. Lukanich, L. R. Sharpe, *Journal of Organic Chemistry* **1984**, *49*, 17818-17826, DOI 10.1021/jo00199a027.
- [63] E. Shirakawa, Y. Hayashi, K. Itoh, R. Watabe, N. Uchiyama, W. Konagaya, S. Masui, T. Hayashi, *Angewandte Chemie* **2012**, *124*, 218-221, DOI 10.1002/ange.201106086.
- [64] B. E. Haines, O. Wiest, *Journal of Organic Chemistry* **2014**, *79*, 2771-2774, DOI 10.1021/jo500222d.
- [65] S. M. Barolo, S. E. Martín, R. A. Rossi, *Arkivoc* **2012**, *2012*, 98-106, DOI 10.3998/ark.5550190.0013.809.
- [66] J. K. Augustine, R. Kumar, A. Bombrun, A. B. Mandal, *Tetrahedron Letters* **2011**, *52*, 1074-1077, DOI 10.1016/j.tetlet.2010.12.090.
- [67] S. H. Yun, K. H. Yeon, H. H. Won, N. C. Ho, *Biotechnology Letters* **2004**, *26*, 1581-1584, DOI 10.1023/B:BILE.0000045656.00138.93.
- [68] M. N. LeMaster, S. S. Chauhan, M. P. Wick, D. L. Clark, E. M. England, *Meat Science* **2019**, *156*, 222-230, DOI 10.1016/j.meatsci.2019.05.019.
- [69] D. Li, F. Shi, S. Guo, Y. Deng, *Tetrahedron Letters* **2005**, *46*, 671-674.
- [70] A. E. Rosamilia, F. Aricò, P. Tundo, *Journal of Physical Chemistry B* **2008**, *112*, 14525-14529, DOI 10.1021/jp804814e.
- [71] I. Thomé, A. Nijs, C. Bolm, *Chemical Society Reviews* **2012**, *41*, 979-987, DOI 10.1039/c2cs15249e.
- [72] R. G. Scamehorn, J. F. Bunnett, *Journal of Organic Chemistry* **1977**, *42*, 13501-13506, DOI 10.1021/jo00428a039.
- [73] J. Morey, A. Costa, P. M. Deyá, G. Suñer, J. M. Saá, *Journal of Organic Chemistry* **1990**, *55*, 3902-3909, DOI 10.1021/jo00299a038.

- [74] S. Lucas, *Headache* **2016**, *56*, 436-446, DOI 10.1111/head.12769.
- [75] T. Yoshizawa, H. Yamada, K. Horiuchi, M. Nakahara, M. Tani, Y. Takayama, A. Iwanami, N. Kato, M. Hachisu, T. Yamamoto, M. Mimura, Y. Nakano, *Journal of the Showa Medical Association* **2016**, *76*, 468-478.
- [76] N. v. Dargani, A. K. Malhotra, *Expert Opinion on Drug Safety* **2014**, *13*, 241-246, DOI 10.1517/14740338.2014.854770.
- [77] M. Scherübl, C. G. Daniliuc, A. Studer, *Angewandte Chemie - International Edition* **2021**, *60*, 711-715, DOI 10.1002/anie.202012654.
- [78] L. L. Lumata, M. E. Merritt, C. R. Malloy, A. D. Sherry, J. van Tol, L. Song, Z. Kovacs, *Journal of Magnetic Resonance* **2013**, *227*, 14-19, DOI 10.1016/j.jmr.2012.11.006.
- [79] A. J. Greener, P. Ubysz, W. Owens-Ward, G. Smith, I. Ocaña, A. C. Whitwood, V. Chechik, M. J. James, *Chemical Science* **2021**, *12*, 14641-14646, DOI 10.1039/d1sc04748e.
- [80] J. R. Beck, *Tetrahedron* **1978**, *34*, 2157-2068, DOI 10.1016/0040-4020(78)89004-8.
- [81] R. C. Kerber, M. M. Kestner, B. N. Newton, H. W. Pinnick, R. G. Smith, P. A. Wade, N. Kornblum, L. Cheng, *Journal of Organic Chemistry* **1976**, *41*, 4858-4860, DOI 10.1021/jo00871a016.
- [82] M. Orlandi, D. Brenna, R. Harms, S. Jost, M. Benaglia, *Organic Process Research and Development* **2018**, *22*, 430-445, DOI 10.1021/acs.oprd.6b00205.
- [83] C. J. Zhao, D. Xue, Z. H. Jia, C. Wang, J. Xiao, *Synlett* **2014**, *25*, 1577-1584, DOI 10.1055/s-0033-1339118.
- [84] T. Cohen, A. G. Dietz, J. R. Miser, *Journal of Organic Chemistry* **1977**, *42*, 776-789, DOI 10.1021/jo00432a003.
- [85] R. D. Knudsen, H. R. Snyder, *Journal of Organic Chemistry* **1974**, *39*, 881-885, DOI 10.1021/jo00937a007.
- [86] J. M. Savéant, *Tetrahedron* **1994**, *50*, 10117-10165, DOI 10.1016/S0040-4020(01)81748-8.
- [87] H. Sun, F. Guo, J. Pan, W. Huang, K. Wang, W. Shi, *Chemical Engineering Journal* **2021**, *406*, 126844, DOI 10.1016/j.cej.2020.126844.
- [88] H. Zipse, *Journal of the American Chemical Society* **1994**, *116*, 10773-10774, DOI 10.1021/ja00102a048.
- [89] J. G. Traynham, *Chemical Reviews* **1979**, *79*, 76-82, DOI 10.1021/cr60320a002.
- [90] A. B. Pierini, J. S. Duca, D. M. A. Vera, *Journal of the Chemical Society. Perkin Transactions 2* **1999**, 1003-1010, DOI 10.1039/a809210i.
- [91] Y. Takahata, D. P. Chong, in *International Journal of Quantum Chemistry*, **2005**, *103*, 509-515.

- [92] S. D. Schimler, M. S. Sanford, *Synlett* **2016**, *27*, 2279-2284, DOI 10.1055/s-0035-1562529.
- [93] H. L. Qi, D. S. Chen, J. S. Ye, J. M. Huang, *Journal of Organic Chemistry* **2013**, *78*, 7482-7487, DOI 10.1021/jo400981f.
- [94] M. L. N. Rao, S. Meka, *Tetrahedron Letters* **2020**, *61*, 151512, DOI 10.1016/j.tetlet.2019.151512.
- [95] C. Zhu, R. Wang, J. R. Falck, *Organic Letters* **2012**, *14*, 3494-3497, DOI 10.1021/ol301463c.
- [96] P. Lei, G. Meng, Y. Ling, J. An, S. P. Nolan, M. Szostak, *Organic Letters* **2017**, *19*, 6510-6513, DOI 10.1021/acs.orglett.7b03191.
- [97] C. W. Cheung, S. L. Buchwald, *Journal of Organic Chemistry* **2014**, *79*, 8470-8474, DOI 10.1021/jo500662s.
- [98] K. I. Burton, I. Elser, A. E. Waked, T. Wagener, R. J. Andrews, F. Glorius, D. W. Stephan, *Chemistry - A European Journal* **2021**, *27*, 11730-11737, DOI 10.1002/chem.202101534.